Therapeutic Efficacy of the Small Molecule GS-5734 against Ebola virus in Rhesus Monkeys

Travis K. Warren[1], Robert Jordan[2], Michael K. Lo[3], Adrian S. Ray[2], Richard L. Mackman[2], Veronica Soloveva[1], Dustin Siegel[2], Michel Perron[2], Roy Bannister[2], Hon C. Hui[2], Nate Larson[2], Robert Strickley[2], Jay Wells[1], Kelly S. Stuthman[1], Sean A. Van Tongeren[1], Nicole L. Garza[1], Ginger Donnelly[1], Amy C. Shurtleff[1], Cary J. Retterer[1], Dima Gharaibeh[1], Rouzbeh Zamani[1], Tara Kenny[1], Brett P. Eaton[1], Elizabeth Grimes[1], Lisa S. Welch[1,5], Laura Gomba[1], Catherine L. Wilhelmsen[1], Donald K. Nichols[1], Jonathan E. Nuss[1], Edward Doerffler[2], Sean Neville[2], Ernest Carra[2], Michael O. Clarke[2], Lijun Zhang[2], Willard Lew[2], Bruce Ross[2], Queenie Wang[2], Kwon Chun[2], Lydia Wolfe[2], Darius Babusis[2], Yeojin Park[2], Kirsten M. Stray[2], Iva Trancheva[2], Joy Y. Feng[2], Ona Baraskaus[2], Yili Xu[2], Pamela Wong[2], Molly R. Braun[4], Mike Flint[3], Laura K. McMullan[3], Shan-Shan Chen[2], Rachel Fearns[4], Swami Swaminathan[2], Douglas L. Mayers[1,6], Christina F. Spiropoulou[3], William A. Lee[2], Stuart T. Nichol[3], Tomas Cihlar[2], and Sina Bavari[1]

[1]United States Army Medical Research Institute of Infectious Diseases (USAMRIID), Fort Detrick, Maryland, USA.

[2]Gilead Sciences, Inc. Foster City, California, USA.

[3]Centers for Disease Control and Prevention, Atlanta, Georgia, USA.

[4]Boston University School of Medicine, Boston, Massachusetts, USA.

[5]Currently of Medivector, Inc., Boston, Massachusetts, USA.

[6]Currently of Cocrystal Pharma, Inc. Atlanta, Georgia, USA.

Disclaimers:

Opinions, interpretations, conclusions, and recommendations are those of the authors and are not necessarily endorsed by the U.S. Army or the Centers for Disease Control and Prevention, U.S. Department of Health and Human Services. Research was conducted under an IACUC approved protocol in compliance with the Animal Welfare Act, PHS Policy, and other Federal statutes and regulations relating to animals and experiments involving animals. The facility where this research was conducted is accredited by the Association for Assessment and Accreditation of Laboratory Animal Care, International and adheres to principles stated in the Guide for the Care and Use of Laboratory Animals, National Research Council, 2011.

Abstract

The ongoing 2013-15 Ebola virus outbreak in West Africa – unprecedented in the number of cases and fatalities, the geographic distribution, and the number of nations affected – has highlighted the critical need for safe, effective, and readily available antiviral agents for treatment and prevention of acute Ebola virus (EBOV) disease (EVD) or sequelae[1]. No antiviral therapeutics have yet received regulatory approval or demonstrated clinical efficacy. Here we describe the discovery of a novel anti-EBOV small molecule antiviral, GS-5734, a monophosphoramidate prodrug of an adenosine analog. GS-5734 exhibits potent antiviral activity against multiple variants of EBOV in cell-based assays. The pharmacologically active nucleoside triphosphate (NTP) is efficiently formed in multiple human cell types incubated with GS-5734 in vitro, and the NTP acts as an alternate substrate and RNA-chain terminator in

primer-extension assays utilizing a surrogate respiratory syncytial virus RNA polymerase. Intravenous administration of GS-5734 to nonhuman primates resulted in high and persistent NTP levels in peripheral blood mononuclear cells and distribution to sanctuary sites for viral replication including testes, eye, and brain. In a rhesus monkey model of EVD, once daily administration of 10 mg/kg GS-5734 for 12 days resulted in profound suppression of EBOV replication and protected 100% of EBOV-infected animals against lethal disease, ameliorating clinical disease signs and pathophysiological markers, even when treatments were initiated three days after virus exposure when systemic viral RNA was detected in multiple treated animals. These results provide the first substantive, post-exposure protection by a small molecule antiviral compound against EBOV in nonhuman primates. Additionally, the broad-spectrum antiviral activity of GS-5734 in vitro against other pathogenic RNA viruses − including filoviruses, arenaviruses, and coronaviruses − suggests the potential for expanded indications. GS-5734 is amenable to large-scale manufacturing, and clinical studies investigating the safety and pharmacokinetics of GS-5734 in humans are ongoing.

Main Text

Ebola virus disease (EVD) or Ebola hemorrhagic fever, is a rare and often fatal disease caused by infection with Ebola virus (EBOV). The current outbreak in West Africa, which is thought to have started in December 2013, is the largest and most complex Ebola virus outbreak since EBOV was identified as the etiological agent of EVD. With over 28,000 confirmed, suspected, or probable EVD cases and over 11,000 reported deaths, there have been more cases and deaths in the current outbreak than in all others combined[1]. Moreover, with over 500

confirmed deaths in health care workers, the medical infrastructures of Guinea, Sierra Leone, and Liberia have been seriously impacted[1]. Additionally, EVD-related sequelae – e.g. joint and muscle pain, headache, ophthalmic problems, and other symptoms – and instances of viral persistence and recrudescence in individuals who survived the acute disease are now being documented[2-4].

EBOV is a single-stranded, negative-sense, non-segmented RNA virus from the *Filoviridae* family, and other representatives of this family – namely Marburg virus, Sudan virus, and Bundibugyo virus – have caused outbreaks associated with high case fatality rates[5].

While multiple clinical trials have been initiated during the ongoing outbreak to test the efficacy of various experimental small molecules and biologics for treatment of EBOV infection[6], there currently are no therapeutic agents for which the clinical efficacy and safety have been established in the treatment of acute EVD or its sequelae. Broad spectrum nucleoside/tide antivirals such as favipiravir or brincidofovir have shown varying degrees of antiviral activity in cell culture and/or animal models of EBOV infection[7,8,9]. Favipiravir has been tested in an open-label clinical efficacy study in patients with symptomatic EVD conducted in Guinea; however, the efficacy analysis relies on historical mortality data and thus may not provide a clear conclusion about the compound's clinical efficacy in the setting of developed EVD[10]. A brincidofovir efficacy trial initiated in Liberia was not completed[11]. In addition, the nucleoside analog BCX4430 has shown in vivo therapeutic efficacy in models of MARV infection, but evidence of therapeutic efficacy against EBOV has not been reported[12,13]. Finally, other therapeutic modalities such as a mixture of neutralizing antibodies (namely ZMapp, ZMab, and MB003) and small interfering RNA complexed with lipid nanoparticles (LNP-siRNA) have shown promising therapeutic efficacy in nonhuman primate models of EVD[14-16]. While clinical

testing of ZMapp is in progress, a West African trial with a LNP-siRNA (TKM-100802) was terminated when interim analysis of the data indicated that additional enrollment is unlikely to result in therapeutic benefit[17]. Therefore, it is important to continue searching for novel anti-EBOV compounds that can be safely administered to patients with EVD. The availability of broadly effective antiviral(s) with a favorable benefit/risk profile would address a serious unmet medical need for the treatment of EBOV infection.

A 1′-cyano substituted adenine C-nucleoside ribose analogue (Nuc) has been found to be an inhibitor of viral RNA-dependent RNA polymerases (RdRp) and has demonstrated antiviral activity toward a number of RNA viruses[18]. Structurally, the 1′-cyano group provides potency and selectivity for viral polymerases, while the C-linked pyrrolo[2,1-*f*][1,2,4]triazin-4-amine base is stable to deglycosylation. The mechanism of action of Nuc requires intracellular anabolism to the active triphosphate metabolite (NTP), which interferes with viral RNA synthesis through incorporation into viral RNA and termination of its synthesis. Because of slow first phosphorylation kinetics, modification of parent nucleosides with monophosphate promoieties can greatly enhance intracellular NTP concentrations[19]. Accordingly, a range of phosphoramidate prodrugs were prepared and screened to bypass the rate-limiting phosphorylation of the Nuc, resulting in the identification of GS-5734, the single *Sp* isomer of the 2-ethylbutyl L-alaninate phosphosphoramidate (Supplementary Information). A pharmacologically active NTP is formed from GS-5734 through a multistep intracellular activation pathway (Fig. 1a; Extended Data Fig. 1a). In human monocyte-derived macrophages, incubation with GS-5734 rapidly loads cells with high levels of NTP that persist following removal of GS-5734 from media (Extended Data Fig. 1b), resulting in up to 30-fold higher levels compared to incubation with Nuc (Fig. 1b). GS-5734 is active against a broad range of

filoviruses including Marburg virus and several variants of EBOV (Fig. 1c). The compound inhibits EBOV replication in multiple relevant human cell types including primary macrophages, human endothelial cells, as well as Huh-7, HeLa, and HFF-1 human cell lines with EC_{50} values ranging from 0.06 to 0.14 μM (Table 1). The parent Nuc was less active with EC_{50} values ranging from 0.77 to >20 μM. Notably, treatment with GS-5734 of liver Huh-7 cells infected with the EBOV-Makona variant isolated during the West African outbreak resulted in profound dose-dependent reductions in viral RNA production and infectious virus yield (Extended Data Fig. 2). In addition, GS-5734 and the Nuc inhibited replication of other human RNA viral pathogens including respiratory syncytial virus (RSV), Junin virus (JUNV), Lassa fever virus (LASV) and Middle East respiratory syndrome virus (MERS), with EC_{50} values ranging from 0.02 to 1.65 μM (Table 1). Prior studies have reported activity of the Nuc against flaviviruses (hepatitis C virus, yellow fever virus, dengue virus type 2), parainfluenza type 3, and severe acute respiratory syndrome (SARS) associated coronavirus but little or no activity against West Nile virus, influenza A or Coxsackie A[18,20]. GS-5734 was not active against alphaviruses such as Chikungunya virus (CHIK) and Venezuelan equine encephalitis virus (VEEV) or retroviruses such as human immunodeficiency virus type 1 (HIV-1) (Table 1). Importantly, the antiviral activity of GS-5734 was selective as demonstrated by low cytotoxicity in a wide range of human primary cells and cell lines (Extended Data Table 1).

Isolation and expression of Ebola RdRp has been elusive, but the computational analysis of the catalytic palm subdomain demonstrated high sequence and structure homology with respiratory syncytial virus (RSV) RdRp[21] (Fig. 1d and Extended Data Fig. 3). Consistent with the proposed mechanism of action, NTP inhibited RSV RdRp-catalyzed RNA synthesis (Fig. 1e) by incorporating into the nascent viral RNA transcript and causing its premature termination

(Fig. 1f). In contrast, NTP did not inhibit the human RNA or DNA polymerases at concentrations up to 200 μM (Fig. 1e). These data suggest that GS-5734 selectively inhibits the EBOV replication by targeting its RdRp and inhibiting viral RNA synthesis following the efficient intracellular conversion to the active NTP metabolite.

Rodent test systems were not considered suitable for GS-5734 in vivo efficacy evaluations because high serum esterase activity, present in many rodent species, degrade the GS-5734 pro-moiety and adversely impacts its pharmacokinetic profile[22]. Rhesus monkeys do not express high levels of serum esterase and in vitro experiments established that rhesus lymphoid cells efficiently activated GS-5734, although NTP levels were somewhat reduced relative to the same cell types isolated from human (Extended Data Fig. 1c). In rhesus monkeys, intramuscular inoculation with clinically derived wild-type Ebola virus produces a fulminant disease with pathophysiological responses that closely resemble those observed in human EVD cases[23,24]. In this model, systemic viral RNA is detectable by PCR within 2 to 4 days of virus exposure, with rapidly increasing levels, often with multiple $\log_{10}$-fold increases observed over 24 h. Febrile responses are common, and blood markers associated with liver damage and renal impairment, and coagulopathy are often profoundly altered up to the time of death, which typically occurs 6 to 9 days following virus exposure. Because of their close phylogenetic relationship to humans, the similarity of disease manifestations, and their susceptibility to unadapted, clinically derived virus isolates, the nonhuman primate disease models are considered model systems well suited for evaluating the efficacy of antiviral interventions, when trials in infected humans are not feasible.

In preparation for in vivo efficacy studies, GS-5734 pharmacokinetics, metabolism, and distribution were examined in monkeys (cynomolgus and rhesus macaques). Upon intravenous

administration of a 10 mg/kg dose in rhesus monkeys, GS-5734 exhibits a short plasma half-life ($t_{1/2}$ = 0.39 h), with concentrations decreasing to undetectable levels (<0.1 μM) within 2 h (Fig. 2a). Elimination in plasma is followed by the sequential appearance of transient levels of the key intracellular intermediate alanine metabolite (Ala-Met) and more persistent levels of Nuc. GS-5734 is rapidly distributed into peripheral blood mononuclear cells (PBMCs), and efficient conversion to active NTP is apparent within 2 h of dose administration. In PBMCs, NTP represents the predominant metabolite and is persistent with a $t_{1/2}$ = 14 h (Fig. 2a). Importantly, the intracellular concentrations of NTP exceed levels required for >50% virus inhibition for 24 h (Fig. 2a; Extended Data Fig. 1d). In cynomolgus macaques, intravenous administration of a 10 mg/kg dose of [^{14}C]GS-5734 demonstrated that [^{14}C]GS-5734-derived material distributed to testes, epididymis, eyes, and brain within 4 h of administration (Fig. 2b). In brain, levels were low relative to other tissues but were strongly persistent up to 168 h. Taken together, the pharmacokinetic analysis indicates that sustained intracellular NTP levels can be achieved with a once-daily dosing regimen of GS-5734 and that intravenous administration of GS-5734 efficiently delivers its metabolites to cells relevant to acute disease and to sanctuary sites where virus may persist.

To evaluate the in vivo efficacy of GS-5734 we conducted a two-part, adaptive-design study in EBOV-infected rhesus monkeys. The two parts were conducted sequentially, and a blinded, randomized experimental approach was employed for each part (Fig. 2c). All animals were exposed to a target dose of 1,000 plaque forming units (pfu) of EBOV-Kikwit by intramuscular injection. Clinical signs were monitored multiple times per day, and the primary endpoint was survival to day 28 following virus challenge (day of virus challenge was designated day 0). All GS-5734 treatments were administered by slow (approximately 1 min) bolus

intravenous injections once daily for 12 days with matching vehicle administration to maintain experimental blinding (Fig. 2c). In part 1, animals were administered vehicle (n = 3) or 3 mg/kg GS-5734 (n = 6/treatment group) beginning on day 0 (D0; 30-90 min following virus challenge) or Day 2 (D2). Regardless of the time of initiation, 3 mg/kg dose regimens conferred improved survival, 33% (2/6) in the 3 mg/kg D0 group and 66% (4/6) in the 3 mg/kg D2 group, and a favorable antiviral effect by reducing systemic viremia compared with the vehicle-control regimen (Fig. 2d–e). However, mortalities observed in both treatment groups suggest that drug exposure provided by the 3 mg/kg regimen was sub-optimal. Therefore, in part 2, GS-5734 was administered once at a loading dose of 10 mg/kg followed by once-daily 3 mg/kg doses beginning either 2 days (group designated "10/3 mg/kg D2") or 3 days (group designated "10/3 mg/kg D3") after virus exposure or 10 mg/kg doses were administered beginning 3 days after virus exposure (group designated "10/3 mg/kg D3") with n = 6/group. In all three treated groups, GS-5734 was administered for 12 consecutive days. All animals (12 of 12) in which GS-5734 treatments were initiated 3 days after virus exposure survived to the end of the in-life phase (Fig. 2d). However, the analysis of multiple endpoints show that antiviral effects were consistently greater in animals that were administered repeated 10 mg/kg GS-5734 doses (Fig. 2e). On Day 4, plasma viral RNA was significantly decreased ($P<0.05$), with geometric means reduced by 1.7 $\log_{10}$ or greater in all GS-5734-treated groups compared with the combined vehicle-treated groups (Fig. 2e, 2f; Extended Data Tables 2, 3), with profound reductions of plasma viral RNA observed in the 10 mg/kg group (Fig. 2e, 2f; Extended Data Table 3). On Days 5 and 7, when the geometric mean viral RNA concentration of the vehicle group exceeded 10^9 copies/mL, viral RNA was detected at levels less than the lower limit of quantitation (8×10^4 RNA copies/mL) in 4 of 6 animals in the 10 mg/kg D3 group. Three of these animals were free

of clinical disease signs for the duration of the study, and clinical signs in the remaining 3 animals in this group were mild and transient, contrasting the severity of EVD in the other GS-5734 treatment groups (Fig. 2g; Extended Data Fig. 4). Additionally, the 10 mg/kg D3 GS-5734 regimen was associated with amelioration of EVD-related markers of coagulopathy, including thrombocytopenia, elevation of circulating d-dimer and prolongations of thrombin time and activated partial thromboplastin time (Fig. 3a-d). Moreover, compared with vehicle treated animals, animals administered 10 mg/kg GS-5734 exhibited significantly reduced elevations of markers associated with liver damage, including ALT and AST; pancreatic insult, such as lipase; and renal function, including BUN and creatinine (Fig. 3e-i). Although greater survival was observed in the 10/3 mg/kg D3 group than in the 10/3 mg/kg D2 group, survival and viral RNA load in these two groups were not statistically distinguishable (Fig. 2e). Results in these groups likely represent natural variation associated with sub-optimal efficacy conferred by the 10/3 mg/kg GS-5734 regimen, as indicated by less pronounced effects on clinical signs of the EVD and systemic viral load compared with the 10 mg/kg regimen.

In summary, the novel nucleotide prodrug GS-5734 is a potent and selective inhibitor of EBOV in relevant permissive cell types. In a nonhuman primate model of clinical EVD, intravenous administration of GS-5734 results in a rapid accumulation and persistence of the active NTP form in the intracellular compartment. Pronounced antiviral effects, amelioration of EVD signs, and significant survival benefit in nonhuman primates was achieved despite treatment initiation on day 3, a time when viral RNA was already systemically distributed. These results represent the first case of substantive postexposure protection against EVD by a small-molecule antiviral compound in nonhuman primates and suggest that efficacy may be possible with even greater delays of GS-5734 treatment initiation. Intravenously administered

GS-5734 is currently being evaluated in single and multiple ascending dose studies in healthy human volunteers to assess its clinical safety and pharmacokinetics. These studies will help determine whether GS-5734 can provide therapeutic benefit in acute cases of EVD or instances in which sequelae related to viral recrudescence are identified. In addition, the broad-spectrum antiviral activity of GS-5734 and its amenability to large-scale manufacturing practices warrants further assessment of its therapeutic potential against other significant human viral pathogens for which no treatment is currently available.

REFERENCES

1 World Health Organization. *Ebola Situation Report - 21 October 2015.* http://apps.who.int/ebola/current-situation/ebola-situation-report-21-october-2015 (2015).

2 Nanyonga, M., Saidu, J., Ramsay, A., Shindo, N. & Bausch, D. G. Sequelae of Ebola Virus Disease, Kenema District, Sierra Leone. *Clinical infectious diseases : an official publication of the Infectious Diseases Society of America*, doi:10.1093/cid/civ795 (2015).

3 Varkey, J. B. *et al.* Persistence of Ebola virus in ocular fluid during convalescence. *N. Engl.J. Med.* **372**, 2423-2427 (2015).

4 Mate, S. E. *et al.* Molecular evidence of sexual transmission of Ebola virus. *N. Engl.J. Med.* doi:10.1056/NEJMoa1509773 (2015).

5 Kuhn, J. H. *Filoviruses: A Compendium of 40 Years of Epidemiological, Clinical, and Laboratory Studies.* (SpringWien, New York, 2008).

6 Kupferschmidt, K. & Cohen, J. Infectious diseases. Ebola drug trials lurch ahead. *Science* **347**, 701-702 (2015).

7 Smither, S. J. *et al.* Post-exposure efficacy of oral T-705 (Favipiravir) against inhalational Ebola virus infection in a mouse model. *Antiviral Res.* **104**, 153-155 (2014).

8 Oestereich, L. *et al.* Successful treatment of advanced Ebola virus infection with T-705 (favipiravir) in a small animal model. *Antiviral Res.***105**, 17-21 (2014).

9 Wong, G., Qiu, X., Olinger, G. G. & Kobinger, G. P. Post-exposure therapy of filovirus infections. *Trends Microbiol*. **22**, 456-463 (2014).

10 Sissoko, D. *et al.* Favipiravir in patients with Ebola virus disease: Early results of the JIKI trial in Guinea [Abstract 103-ALB]. *Conference of Reterviruses and Opportunistic Infections (CROI)* (Seattle, WA, 2015).

11 Chimerix, Inc. *Brincidofovir Will Not Be Considered in Further Clinical Trials in Ebola Virus Disease*. http://ir.chimerix.com/releasedetail.cfm?ReleaseID=893927 (2015).

12 Warren, T. K. *et al.* Protection against filovirus diseases by a novel broad-spectrum nucleoside analogue BCX4430. *Nature* **508**, 402-405 (2014).

13 BioCryst Pharmaceuticals, Inc. *BioCryst Announces Study Results for BCX4430 in a Non-Human Primate Model of Ebola Virus Infection*. http://investor.shareholder.com/biocryst/releasedetail.cfm?ReleaseID=888802 (2014).

14 Thi, E. P. *et al.* Lipid nanoparticle siRNA treatment of Ebola-virus-Makona-infected nonhuman primates. *Nature* **521**, 362-365 (2015).

15 Qiu, X. *et al.* Reversion of advanced Ebola virus disease in nonhuman primates with ZMapp. *Nature* **514**, 47-53 (2014).

16 Olinger, G. G., Jr. *et al.* Delayed treatment of Ebola virus infection with plant-derived monoclonal antibodies provides protection in rhesus macaques. *Proc Natl Acad Sci U S A* **109**, 18030-18035 (2012).

17 Tekmira Pharmaceuticals Corporation. *Tekmira Provides Update on TKM-Ebola-Guinea*. http://www.sec.gov/Archives/edgar/data/1447028/000117184315003522/newsrelease.htm (2015).

18 Cho, A. *et al.* Synthesis and antiviral activity of a series of 1'-substituted 4-aza-7,9-dideazaadenosine C-nucleosides. *Bioorg.Med. Chem. Lett.* **22**, 2705-2707 (2012).

19 Murakami, E. *et al.* The mechanism of action of beta-D-2'-deoxy-2'-fluoro-2'-C-methylcytidine involves a second metabolic pathway leading to beta-D-2'-deoxy-2'-fluoro-2'-C-methyluridine 5'-triphosphate, a potent inhibitor of the hepatitis C virus RNA-dependent RNA polymerase. *Antimicrob. Agents Chemother.* **52**, 458-464 (2008).

20 Mackman, R. L., Parrish, J. P., Ray, A. S. & Theodore, D. A. Methods and compounds for treating respiratory syncytial virus infections. *US Patent 2011045102*. Filed 22 Jul 2011.

21 Jacome, R., Becerra, A., Ponce de Leon, S. & Lazcano, A. Structural analysis of monomeric RNA-dependent polymerases: Evolutionary and therapeutic implications. *PloS One* **10**, e0139001, doi:10.1371/journal.pone.0139001 (2015).

22 Bahar, F. G., Ohura, K., Ogihara, T. & Imai, T. Species difference of esterase expression and hydrolase activity in plasma. *J. Pharm. Sci.* **101**, 3979-3988 (2012).

23 Hunt, L. *et al.* Clinical presentation, biochemical, and haematological parameters and their association with outcome in patients with Ebola virus disease: an observational cohort study. *Lancet Infect. Dis.* doi:10.1016/S1473-3099(15)00144-9 (2015).

24 Martins, K. *et al.* Characterization of clinical and immunological parameters during Ebola virus infection of rhesus macaques. *Viral Immunol.* **28**, 32-41 (2015).

Supplementary information is linked to the online version of the paper at www.nature.com/nature.

Acknowledgements T. Bocan, A. Duplantier, R. Panchal, and C. Kane of USAMRIID Therapeutic Development Center, provided scientific input. B. Norquist assisted with manuscript preparation. These studies were in part supported by The Joint Science and Technology Office for Chemical and Biological Defense (JSTO-CBD) of the Defense Threat Reduction Agency (DTRA) under plan #CB10218. C. Cooper of USAMRIID provided scientific input with human macrophage cultures for high-content image assessments. S. Tritsch and G. Gomba of USAMRIID assisted with GS-5734 dose preparations for efficacy studies. C. Rice of USAMRIID provided animal husbandry support services. X. Wei, W. Garner, and L. Zhong of Gilead Sciences provided additional support for statistical analyses. Also of Gilead Sciences, K. Wang, K. Brendza, T. Alfredson, and L. Serafini assisted with analytical methods, S. Bondy and R. Seemayer procured key raw materials, L. Heumann, R. Polniaszeck, E. Rueden, A. ChtChemelinine, K. Brak, and B. Hoang contributed to synthesis, Y. Zherebina helped with chiral separations. G. Lee supported the RSV antiviral assay, and G. Stepan, S. Ahmadyar, and H. Yu conducted part of the cytotoxicity testing. Work in the Fearns laboratory was supported by NIH R01AI113321.

Author Contributions: R.L.M., D.S., H.C.H., E.D., S.N., E.C., M.O.C., L.Z., W.L., B.S., Q.W., K.C., and L.W. were responsible for the synthesis, characterization, and scale-up of small molecules. T.K.W. designed and supervised activities associated with efficacy evaluations, and interpreted study results. J.W., K.S.S., N.L.G., G.D., S.A.V.T., and J.E.N. conducted in vivo efficacy studies and performed associated sample analyses. A.C. S., L.S.W., and L.G. coordinated efficacy study activities. M.K.L., M.F., L.K.M., designed and executed the initial in

317 vitro antiviral testing against EBOV and analyzed data. V. S., C.J.R., D.N.G., and T.K. and
318 B.P.E. designed and executed cell-based infection assays and analyzed these data. E.G.
319 conducted quantitative PCR analysis. D.K.N. and C.L.W. performed anatomic pathology
320 examinations and analyses of all nonhuman primate subjects. N.L., I.T. and R.S. developed and
321 tested drug formulations. A.S.R., D.B. Y.P., and K.M.S. designed and executed the PK and
322 metabolism studies and summarized results. M.P., O.B., M.R.B. and R.F. designed and
323 conducted biochemical enzymatic assays. K.M.S., J.F. and Y.X. conducted cell based assays for
324 cytotoxicity. P.W. conducted statistical analysis and S.S.C. oversaw the analysis. A.S.R., R.J.,
325 R.L.M., V.S., R.B., S.S., D.L.M., C.F.S., S.T.N., W.L., T.C., and S.B. designed experiments,
326 evaluated results, and provided project oversight. T.K.W., A.S.R., R.J., D.S., M.P., and T.C.
327 outlined and wrote the manuscript.

328

Author Information: Reprints and permissions information is available at www.nature.com/reprints. The authors from Gilead Sciences are employees of the company and may own company stock. Correspondence and requests for materials should be addressed to S. Bavari (sina.bavari.civ@mail.mil) and T. Cihlar (tomas.cihlar@gilead.com).

FIGURE LEGENDS

Figure 1. Metabolism and mechanism of antiviral activity of GS-5734. **a**, Chemical structures of GS-5734 with highlighted prodrug moiety and putative metabolic pathway to the pharmacologically active metabolite (NTP). **b**, NTP formation in human monocyte-derived macrophages following 72-h incubation with 1 μM GS-5734 (black) or Nuc (red). **c**, Antiviral activity of GS-5734 in HeLa cells against Ebola virus (EBOV-Makona, closed black symbols; EBOV-Kikwit, open symbols), Marburg virus (MARV, red), Bundibugyo virus (BDBV, orange), and Sudan virus (SUDV, blue). **d**, Amino acid sequence homology of EBOV (Zaire) and RSV (strain A2) RdRp pre-Motif A, Motif A, and Motif B regions. Asterisks depict amino acid residues predicted to contact NTP in the polymerase active site. **e**, Inhibition of transcription by RSV RdRp (blue), but not human RNA Pol II (black) or mitochondrial (mt) RNA (red) polymerases by NTP (10, 30, or 100 μM). **f**, RNA chain termination induced by the incorporation of NTP into RNA by purified RSV RdRp in a primer-extension assay .

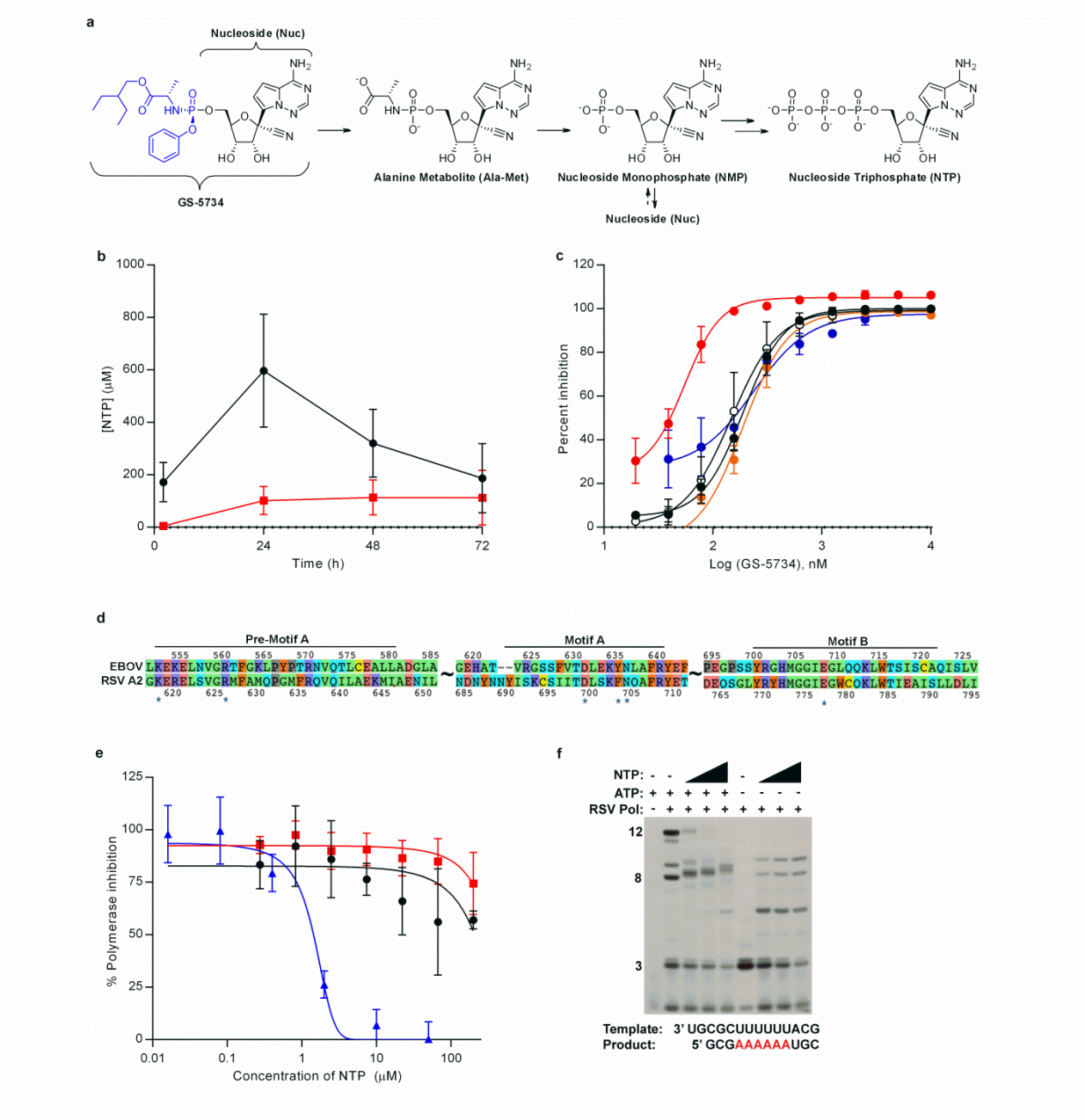
a
Nucleoside (Nuc)
GS-5734
Alanine Metabolite (Ala-Met)
Nucleoside Monophosphate (NMP)
Nucleoside Triphosphate (NTP)
Nucleoside (Nuc)
b
[NTP] (μM)
Time (h)
c
Percent inhibition
Log (GS-5734), nM
d
Pre-Motif A
Motif A
Motif B
EBOV
RSV A2
e
% Polymerase inhibition
Concentration of NTP (μM)
f
NTP:
ATP:
RSV Pol:
12
8
3
Template: 3' UGCGCUUUUUUACG
Product: 5' GCGAAAAAAUGC

347

Figure 2. GS-5734 pharmacokinetics and post-exposure protection against EBOV in rhesus monkeys. **a,** pharmacokinetic profile following intravenous (slow bolus) administration of 10 mg/kg GS-5734 to uninfected rhesus macaques (values represent mean and standard deviation for three monkeys). Plasma profile of GS-5734 (black), Ala-Met (red), and Nuc (blue). Intracellular concentration of NTP in PBMCs (green). **b,** Tissue distribution of [^{14}C]GS-5734 and metabolites to sanctuary sites of viral infection at 4 h (blue) and 168 h (red) following intravenous (slow bolus) administration of 10 mg/kg GS-5734 to uninfected cynomolgus macaques (values represent mean and standard deviation for three monkeys). **c,** Schematic of two-part blinded, randomized experimental design to evaluate GS-5734 efficacy against EBOV in rhesus monkeys. **d**, Kaplan-Meier survival curves. *P<0.05 for comparison of treatment versus vehicle by Log-Rank using Dunnet-Hsu adjustment. **e,** Group geometric mean of plasma viral RNA concentrations; LLOQ, lower limit of quantitation; LOD, lower limit of detection. **f,** Plasma viral RNA concentrations in individual animals treated with vehicle (blue) or 10 mg/kg GS-5734 (black). **g**, Group average daily clinical disease score. **d,e,g**, vehicle (black, open symbols), 3 mg/kg D0 (red), 3 mg/kg D2 (green), 10/3 mg/kg D2 (blue), 10/3 mg/kg D3(orange), 10 mg/kg D4 (black, closed symbols). Error bars omitted for clarity (**e,g**), and x-axes are truncated to emphasize responses during the acute disease phase (**f,g**).

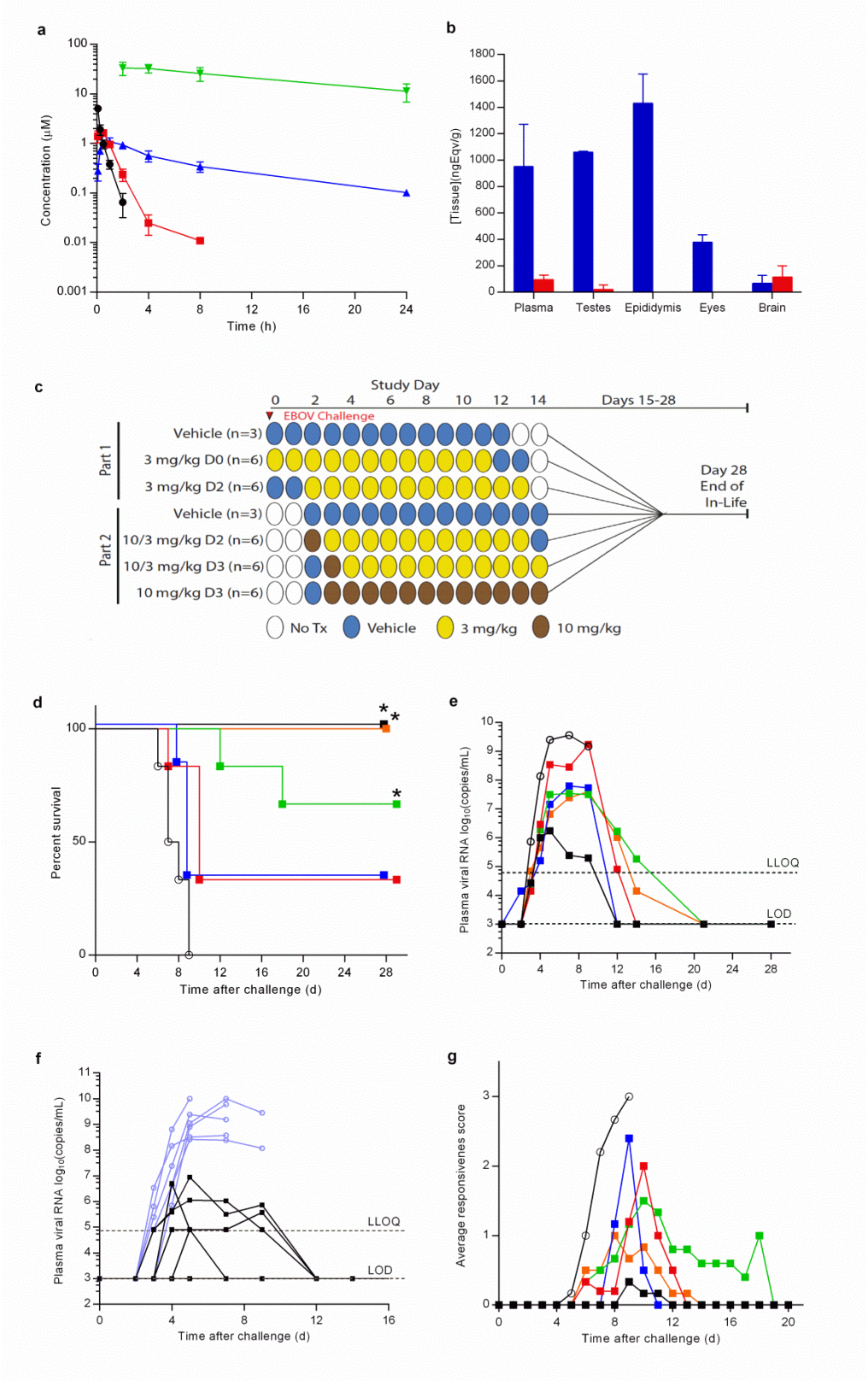
a
Concentration (μM)
Time (h)
b
[Tissue]ngEqv/g
Plasma
Testes
Epididymis
Eyes
Brain
c
Study Day
EBOV Challenge
Days 15-28
Part 1
Vehicle (n=3)
3 mg/kg D0 (n=6)
3 mg/kg D2 (n=6)
Part 2
Vehicle (n=3)
10/3 mg/kg D2 (n=6)
10/3 mg/kg D3 (n=6)
10 mg/kg D3 (n=6)
Day 28
End of
In-Life
No Tx
Vehicle
3 mg/kg
10 mg/kg
d
Percent survival
Time after challenge (d)
e
Plasma viral RNA log10(copies/mL)
LLOQ
LOD
Time after challenge (d)
f
Plasma viral RNA log10(copies/mL)
LLOQ
LOD
Time after challenge (d)
g
Average responsivenes score
Time after challenge (d)

365

366 **Figure 3.** Amelioration of EVD clinical pathology alterations by GS-5734 in rhesus monkeys.
367 Group mean values of platelets (**a**), d-dimer (**b**), thrombin time (**c**), activated partial
368 thromboplastin time (**d**), aspartate aminotransferase (AST, **e**), alanine aminotransferase (ALT, **f**),
369 lipase (**g**), blood urea nitrogen (BUN, **h**), and creatinine (**i**). Vehicle (black, open symbols), 3
370 mg/kg D0 (red), 3 mg/kg D2 (green), 10/3 mg/kg D2 (blue), 10/3 mg/kg D3(orange), 10 mg/kg
371 D3 (black, closed symbols). Error bars omitted for clarity, and x-axes are truncated to emphasize
372 responses during the acute disease phase. *$P<0.05$ for comparison of vehicle and 10 mg/kg D3
373 groups.

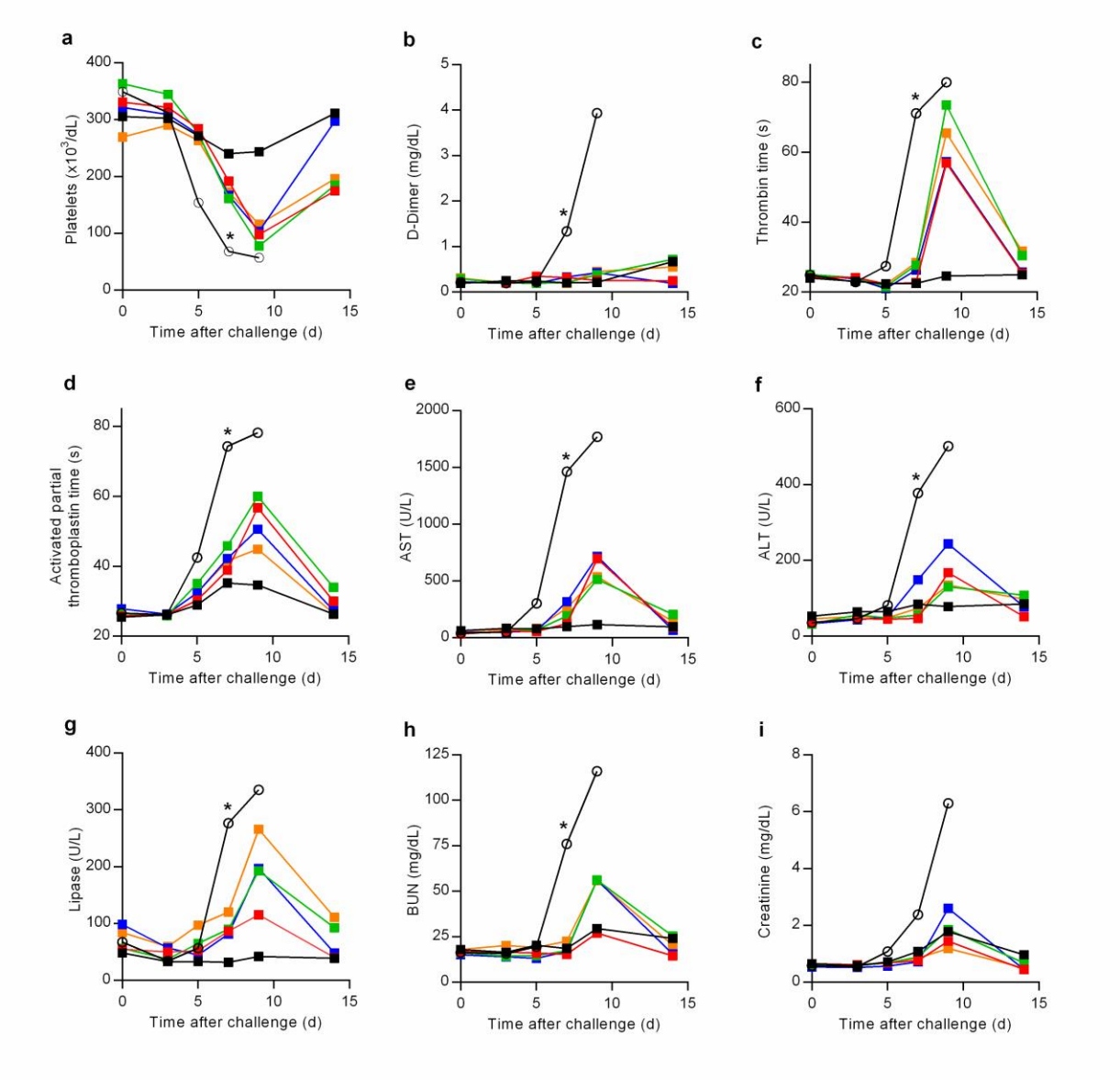
a
Platelets (x10^3/dL)
Time after challenge (d)
b
D-Dimer (mg/dL)
Time after challenge (d)
c
Thrombin time (s)
Time after challenge (d)
d
Activated partial thromboplastin time (s)
Time after challenge (d)
e
AST (U/L)
Time after challenge (d)
f
ALT (U/L)
Time after challenge (d)
g
Lipase (U/L)
Time after challenge (d)
h
BUN (mg/dL)
Time after challenge (d)
i
Creatinine (mg/dL)
Time after challenge (d)

374

375 **Table 1. Antiviral Activity of GS-5734 and Nuc**

	Antiviral activity; EC_{50} / EC_{90} [μM]	
	GS-5734	Nuc
EBOV		
Primary macrophages*	0.086 / 0.18	>20 / >20
HeLa cells†	0.14 / 0.41	>20 / >20
HFF-1*	0.13 / 0.26	>20 / >20
HMVEC-TERT cells†	0.06 / 0.22	0.77 / 3.12
Huh-7 cells†	0.07 / 0.22	1.49 / 6.04
Other human RNA viruses		
RSV‡	0.019 / 0.051	0.75 / 2.84
JUNV§	0.47 / 1.26	
LASV§	1.65 / 3.31	
MERS§	0.52 / 1.29	
CHIV§	>20 / >20	
VEEV§	>20 / >20	
HIV-1§	>20 / >20	

376 CC_{50} values for all compounds in primary human cells and human cell lines were greater than the highest
377 concentration tested (> 20 μM).
378 * Mean values from duplicated titrations conducted in differentiated macrophages or HFF-1 cells in a single
379 experiment (n = 1). Cells were infected with EBOV (Makona) for antiviral activity determination.

380 [†] Mean values from quadruplicate (HMVEC-TERT) or duplicate (Huh-7) titrations generated from a single experiment
381 (n = 1) or from multiple experiments (n = 6) for HeLa cells. Cells were infected with a replication competent
382 reporter virus (EBOV-GFP) or wild type EBOV strain Zaire (HeLa) for antiviral activity determination.
383 [‡] Mean values from two (GS-5734) or four (Nuc) independent experiments with each drug dilution tested in triplicate
384 against the respiratory syncytial virus (RSV).
385 [§] Mean values from duplicate titrations with each drug concentration tested in quadruplicate from a single experiment
386 (n = 1). Junin virus (JUNV), Lassa fever virus (LASV), Middle East respiratory syndrome coronavirus (MERS),
387 Chikungunya virus (CHIK), Venezuelan equine encephalitis virus (VEEV) and human immunodeficiency virus
388 type 1 (HIV-1).
389

METHODS

Small Molecules

GS-5734, Nuc, and NTP were synthesized at Gilead Sciences, Inc. and chemical identity, sample purity were established using NMR, HRMS, and HPLC analysis (Supplementary information). The radiolabeled analogue [^{14}C]GS-5734 (specific activity 58.0 mCi/mmol) was obtained from Moravek Biochemicals (Brea, CA) and was prepared in a similar manner described for GS-5734 using [^{14}C]trimethylsilylcyanide (Supplementary information).

Viruses

RSV A2 was purchased from Advanced Biotechnologies, Inc. EBOV (Kikwit and Makona variants), Sudan virus (SUDV, Gulu), Marburg virus (MARV, Ci67), Junin virus (JUNV, Romero), Lassa virus (LASV, Josiah), Middle East respiratory syndrome virus (MERS, Jordan N3), Chikungunya virus (CHIV, AF 15561), and Venezuelan equine encephalitis virus (VEEV, SH3) were all prepared and characterized at USAMRIID. EBOV containing a GFP reporter gene (EBOV-GFP), EBOV Makona (Liberia, 2014), and MARV containing a GFP reporter gene (MARV-GFP) were prepared and characterized at the Centers for Disease Control and Prevention (CDC)[25,26].

Cells

HEp-2 (CCL-23), PC-3 (CCL-1435), HeLa (CCL-2), U2OS (HTB-96), Vero (CCL-81), HFF-1 (SCRC-1041), and HepG2 (HB-8065) cell lines were purchased from the American Type Culture Collection. HEp-2 cells were cultured in Eagle's Minimum Essential Media (MEM) with GlutaMAX^{TM} supplemented with 10% fetal bovine serum (FBS) and 100 units/mL

411 penicillin and streptomycin. PC-3 cells were cultured in Kaighn's F12 media supplemented with
412 10% FBS and 100 units/mL penicillin and streptomycin. HeLa, U2OS, and Vero cells were
413 cultured in MEM supplemented with 10% FBS, 1% L-glutamine, 10 mM HEPES, 1% non-
414 essential amino acids, and 1% penicillin/streptomycin. HFF-1 cells were cultured in MEM
415 supplemented with 10% FBS and 0.5 mM sodium pyruvate. HepG2 cells were cultured in
416 Dulbecco's Modified Eagle Medium (DMEM) with GlutaMAX™ supplemented with 10% FBS,
417 100 units/mL penicillin and streptomycin, and 0.1 mM non-essential amino acids. The MT-4
418 cell line was obtained from the NIH AIDS Research and Reference Reagent Program and
419 cultured in RPMI-1640 medium supplemented with 10% FBS, 100 units/mL penicillin and
420 streptomycin, and 2 mM L-glutamine. The Huh-7 cell line was obtained from Dr. Charles M.
421 Rice at the Rockefeller University and cultured in DMEM supplemented with 10% FBS, 100
422 units/mL penicillin and streptomycin, and non-essential amino acids.

423 Primary human hepatocytes were purchased from Invitrogen and cultured in William's Medium
424 E medium containing cell maintenance supplement. Donor profiles were limited to 18- to 65-
425 year-old nonsmokers with limited alcohol consumption. Upon delivery, the cells were allowed
426 to recover for 24 h in complete medium with supplement provided by the vendor at 37 °C.
427 Human peripheral blood mononuclear cells (PBMCs) were isolated from human buffy coats
428 obtained from healthy volunteers (Stanford Medical School Blood Center, Palo Alto, CA) and
429 maintained in RPMI-1640 with GlutaMAX™ supplemented with 10% FBS, 100 units/mL
430 penicillin and streptomycin. Rhesus fresh whole blood was obtained from Valley Biosystems
431 (Sacramento, CA). PBMCs were isolated from whole blood by Ficoll-Hypaque density gradient
432 centrifugation. Briefly, blood was overlaid on 15 mL Ficoll-Paque™ (GE Healthcare Bio-
433 Sciences AB, Piscataway, NJ), and centrifuged at 500 × *g* for 20 minutes. The top layer

containing platelets and plasma was removed, and the middle layer containing PBMCs was transferred to a fresh tube, diluted with Tris Buffered Saline up to 50 mL, and centrifuged at 500 × *g* for 5 minutes. The supernatant was removed and the cell pellet was resuspended in 5 mL red blood cell lysis buffer (155 mM ammonium chloride, 10 mM potassium bicarbonate, 0.1 mM EDTA, pH 7.5). To generate stimulated PBMCs, freshly isolated quiescent PBMCs were seeded into a T-150 cm^2 tissue culture flask containing fresh medium supplemented with 10 units/mL of recombinant human interleukin-2 (IL-2) and 1 μg/mL phytohemagglutinin-P at a density of 2 × 10^6 cells/mL and incubated for 72 h at 37°C. Human macrophage cultures were isolated from PBMCs that were purified by Ficoll gradient centrifugation from 50 mL of blood from healthy human volunteers. PBMCs were cultured for 7 to 8 days in in RPMI cell culture media supplemented with 10% FBS, 5 to 50 ng/mL granulocyte-macrophage colony-stimulating factor (GM-CSF) and 50 μM β-mercaptoethanol (BME) to induce macrophage differentiation. The cryopreserved human primary renal proximal tubule epithelial cells were obtained from LifeLine Cell Technology and isolated from the tissue of human kidney. The cells were cultured at 90% confluency with RenaLife complete medium in a T75 flask for 3 to 4 days before seeding into 96-well assay plates. Immortalized human microvascular endothelial cells (HMVEC-TERT) were obtained from Dr. Rong Shao at the Pioneer Valley Life Sciences Institute[27]. HMVEC-TERT cells were cultured in endothelial basal media supplemented with 10% FBS, 5 μg of epithelial growth factor, 0.5 mg hydrocortisone, and gentamycin/amphotericin-B.

Enzymes

RNA POLII was purchased as part of the "HeLaScribe® Nuclear Extract *in vitro* Transcription System" kit from Promega. The recombinant human POLRMT and transcription factors mitochondrial transcription factors A (mtTFA or TFAM) and B2 (mtTFB2 or TFB2M) were

purchased from Enzymax. RSV ribonucleoprotein (RNP) complexes were prepared according to a method modified from Mason *et al*.[28].

Intracellular metabolism studies

The intracellular metabolism of GS-5734 was assessed in different cell types (HMVEC, HeLa, and primary human and rhesus PBMC, monocytes and monocyte derived macrophages) following 2-h pulse or 72-h continuous incubations with 10 μM GS-5734. For comparison, intracellular metabolism during a 72-h incubation with 10 μM of Nuc was completed in human monocyte derived macrophages. For pulse incubations, monocyte derived macrophages isolated from rhesus or human were incubated for 2 h in compound containing media followed by removal, washing with 37°C drug-free media, and incubated for an additional 22 h in media not containing GS-5734. Human monocyte derived macrophages, HeLa and HMVEC were grown to confluence (approximately 0.5, 0.2, and 1.2×10^6 cells/well, respectively) in 500 μL of media in 12 well tissue culture plates. Monocyte and PBMC were incubated in suspension (approximately 1×10^6 cells/mL) in 1 mL of media in micro centrifuge tubes.

For adherent cells (HMVEC, HeLa, and monocyte derived macrophages), media was removed at select time points from duplicate wells, cells washed twice with 2 mL of ice cold 0.9% normal saline. For non-adherent cells (monocytes and PBMC), duplicate incubation were centrifuged at 5,000 rpm for 30 seconds to remove media. The cell pellets were re-suspended with 500 μL cell culture media (RPMI with 10% FBS) and layered on top of a 500 μL oil layer (Nyosil M25; Nye Lubricants, Fairhaven, MA) in a microcentrifuge tube. Samples were then centrifuged at room temperature at 13,000 rpm for 45 seconds. The media layer was removed and the oil layer was washed twice with 500 μL water. The oil layer was then carefully removed using a Pasteur pipet

attached to vacuum. A volume of 0.5 mL of 70% methanol containing 100 nM of the analytical internal standard 2-chloro-adenosine-5´-triphosphate (Sigma-Aldrich, St. Louis, MO) was added to isolated cells. Samples were stored overnight at –20°C to facilitate extraction, centrifuged at 15,000 × *g* for 15 minutes and then supernatant was transferred to clean tubes for drying in a MiVac Duo concentrator (Genevac, Gardiner, NY). Dried samples were then reconstituted in mobile phase A containing 3 mM ammonium formate (pH5.0) with 10 mM dimethylhexylamine (DMH) in water for analysis by liquid chromatography coupled to triple quadrupole mass spectrometry (LC-MS/MS).

LC-MS/MS was done using low flow, ion pairing chromatography similar to methods described previously[29]. Briefly, analytes were separated using a 50 × 2 mm × 2.5 µm Luna C18(2) HST column (Phenomenex, Torrance, CA, USA) connected to a LC-20ADXR (Shimadzu, Columbia, MD) ternary pump system and HTS PAL autosampler (LEAP Technologies, Carrboro, NC). A multi-stage linear gradient from 10% to 50% acetonitrile in a mobile phase containing 3 mM ammonium formate (pH 5.0) with 10 mM dimethylhexylamine over 8 minutes at a flow rate of 150 µL/min was used to separate analytes. Detection was performed on anAPI 4000 (Applied Biosystems, Foster City, CA) MS/MS operating in positive ion and multiple reaction monitoring modes. Intracellular metabolites Ala-Met, Nuc, NMP, NDP and NTP were quantified using 7 point standard curves ranging from 0.274 to 200 pmol (approximately 0.5 to 400 µM) prepared in cell extract from untreated cells. Levels of adenosine nucleotides were also quantified to assure dephosphorylation had not taken place during sample collection and preparation. In order to calculate intracellular concentration of metabolites, the total number of cells per sample were counted using a Countess automated cell counter (Invitrogen, Carlsbad, CA).

EBOV Huh-7 and HMVEC antiviral assay

Antiviral assays were conducted in biosafety level-4 containment (BSL-4) at the CDC. EBOV antiviral assays were conducted in primary HMVEC-TERT and in Huh-7 cells. Ten concentrations of compound were diluted in 4-fold serial dilution increments in media, and 100 µL per well of each dilution was transferred in duplicate (Huh-7) or quadruplicate (HMVEC-TERT) onto 96-well assay plates containing cell monolayers. The plates were transferred to BSL-4 containment, and the appropriate dilution of virus stock was added to test plates containing cells and serially diluted compounds. Each plate included four wells of infected untreated cells and four wells of uninfected cells that served as 0% and 100% virus inhibition controls, respectively. After the infection, assay plates were incubated for 3 days (Huh-7) or 5 days (HMVEC-TERT) in a tissue culture incubator. Virus replication was measured by direct fluorescence using a Biotek HTSynergy plate reader. For virus yield assays, Huh-7 cells were infected with wild-type EBOV for 1 h at 0.1 pfu per cell. The virus inoculum was removed and replaced with 100 µL per well of media containing the appropriate dilution of compound. At 3 days post-infection, supernatants were collected, and the amount of virus was quantified by endpoint dilution assay. The endpoint dilution assay was conducted by preparing serial dilutions of the assay media and adding these dilutions to fresh Vero cell monolayers in 96-well plates to determine the tissue culture infectious dose that caused 50% cytopathic effects ($TCID_{50}$). To measure levels of viral RNA from infected cells, total RNA was extracted using the MagMAX™-96 Total RNA Isolation Kit and quantified using a quantitative reverse transcription polymerase chain reaction (qRT-PCR) assay with primers and probes specific for the EBOV nucleoprotein gene.

EBOV assay in HeLa and HFF-1 cells

Antiviral assays were conducted in BSL-4 at USAMRIID. HeLa or HFF-1 cells were seeded at 2,000 cells per well in 384-well plates. Ten serial dilutions of compound in triplicate were added directly to the cell cultures using the HP D300 digital dispenser (Hewlett Packard, Palo Alto, CA) in 2-fold dilution increments starting at 10 μM at 2 h prior to infection. The DMSO concentration in each well was normalized to 1% using an HP D300 digital dispenser. The assay plates were transferred to the BSL-4 suite and infected with EBOV-Kikwit at a multiplicity of infection of 0.5 pfu per cell for HeLa cells and with EBOV-Makona at a multiplicity of infection of 5 pfu per cell for HFF-1 cells. The assay plates were incubated in a tissue culture incubator for 48 h. Infection was terminated by fixing the samples in 10% formalin solution for an additional 48 h prior to immune-staining, as described in Table 2.

EBOV human macrophage infection assay

Antiviral assays were conducted in BSL-4 at USAMRIID. Primary human macrophage cells were seeded in a 96-well plate at 40,000 cells per well. Eight to ten serial dilutions of compound in triplicate were added directly to the cell cultures using an HP D300 digital dispenser in 3-fold dilution increments 2 h prior to infection. The concentration of DMSO was normalized to 1% in all wells. The plates were transferred into the BSL-4 suite, and the cells were infected with 1 pfu per cell of EBOV in 100 μL of media and incubated for 1 h. The inoculum was removed, and the media was replaced with fresh media containing diluted compounds. At 48 h post-infection, virus replication was quantified by immuno-staining as described in Table 2.

RSV A2 antiviral assay

For antiviral tests, compounds were 3-fold serially diluted in source plates from which 100 nL of diluted compound was transferred to a 384-well cell culture plate using an Echo acoustic transfer apparatus. HEp-2 cells at a density of 5×10^5 cells/mL were then infected by adding RSV A2 at a titer of $1 \times 10^{4.5}$ tissue culture infectious doses ($TCID_{50}$)/mL. Immediately following virus addition, 20 µL of the virus/cell mixture was added to the 384-well cell culture plates using a µFlow liquid dispenser and cultured for 4 days at 37°C. After incubation, the cells were allowed to equilibrate to 25°C for 30 minutes. The RSV-induced cytopathic effect was determined by adding 20 µL of CellTiter-Glo™ Viability Reagent. After a 10-minute incubation at 25°C, cell viability was determined by measuring luminescence using an Envision plate reader.

High content imaging assay detecting viral infection

Antiviral assays were conducted in 384-or 96-well plates in BSL-4 at USAMRIID using a high-content imaging system to quantify virus antigen production as a measure of virus infection. A "no virus" control and a "1% DMSO" control were included to determine the 0% and 100% virus infection, respectively. The primary and secondary antibodies and dyes used for nuclear and cytoplasmic staining are listed in Table 2. The primary antibody specific for a particular viral protein was diluted 1,000-fold in blocking buffer (1× PBS with 3% BSA) and added to each well of the assay plate. The assay plates were incubated for 60 minutes at room temperature. The primary antibody was removed, and the cells were washed 3 times with 1× PBS. The secondary detection antibody was an anti-mouse (or rabbit) IgG conjugated with Dylight488 (Thermo Fisher Scientific, Waltham, MA). The secondary antibody was diluted 1,000-fold in blocking buffer and was added to each well in the assay plate. Assay plates were incubated for

60 minutes at room temperature. Nuclei were stained using Draq5 (Biostatus, Shepshed Leicestershire, UK) or 33342 Hoechst (ThermoFisher Scientific) for Vero and HFF-1 cell lines. Both dyes were diluted in 1× PBS. The cytoplasm of HFF-1 (EBOV assay) and Vero E6 (MERS assay) cells were counter-stained with CellMask^{TM} Deep Red (Thermo Fisher Scientific, Waltham, MA). Cell images were acquired using a Perkin Elmer Opera confocal plate reader (Perkin Elmer, Waltham, MA) using 10× air objective to collect five images per well. Virus-specific antigen was quantified by measuring fluorescence emission at a 488 nm wavelength and the stained nuclei were quantified by measuring fluorescence emission at a 640 nm wavelength. Acquired images were analyzed using Harmony and Acapella PE software. The Draq5 signal was used to generate a nuclei mask to define each nuclei in the image for quantification of cell number. The CellMask Deep Red dye was used to demarcate the Vero and HFF-1 cell borders for cell-number quantitation. The viral-antigen signal was compartmentalized within the cell mask. Cells that exhibited antigen signal higher than the selected threshold were counted as positive for viral infection. The ratio of virus positive cells to total number of analyzed cells was used to determine the percent infection for each well on the assay plates. Effect of compounds on the viral infection was assessed as percent inhibition of infection in comparison to control wells. The resultant cell number and percent infection were normalized for each assay plate. The Z´ values for all antiviral assays were >0.3. Analysis of dose response curve was performed using GeneData Screener software applying Levenberg-Marquardt algorithm (LMA) for curve fitting strategy. The curve-fitting process, including individual data point exclusion were pre-specified by default software settings. R^{2-}value quantified goodness of fit and fitting strategy was considered acceptable at $R^2 > 0.8$.

587 **Table 2. List of primary and secondary antibodies used in immune-staining assay**

	Antibodies for Immune Staining		
Virus	Primary Antibody	Secondary Antibody	Cell Staining
Ebola virus (EBOV) Marburg virus (MARV) Venezuelan equine encephalitis virus (VEEV) Chikungunya virus (CHIK) Lassa virus (LASV) Junín virus (JUNV)	mm 6D8 anti-GP mm 9G4 anti-GP mm 1A4A anti-E2 mm 2D21-1 anti-E2 mm L52-161-6 anti-GP -GQC03_BF11 anti-GP	DyLight 488 anti-mouse-IgG	Draq5 (Nuclei)
Middle East respiratory syndrome (MERS)	40069-RP02 rb - HCoV-EMC/2012 spike(S) protein	DyLight 488 anti-rabbit-IgG	Draq5 and 33342Hoechst, CellMask red (Cytoplasm)

588

589

590 **Marburg virus assay**

591 HeLa cells were seeded at 2,000 cells/well in a 384-well plate, and compounds were added to the
592 assay plates. Assay plates were transferred to the BSL-4 suite and infected with 1 pfu per cell
593 MARV, which resulted in 50% to 70% of the cells expressing virus antigen in a 48-h period.
594 Virus infection was quantified by immuno-staining using antibodies that recognized the viral
595 glycoproteins as described in Table 2.

596 **Sudan virus assay**

HeLa cells were seeded at 2,000 cells/well in a 384-well plate, and compounds were added to the assay plates. Assay plates were transferred to the BSL-4 suite and infected with 0.08 pfu SUDV per cell, which resulted in 50% to 70% of the cells expressing virus antigen in a 48-h period. Virus infection was quantified by immuno-staining using antibodies that recognized the viral glycoproteins as described in Table 2.

Junin virus assay

HeLa cells were seeded at 2,000 cells/well in a 384-well plate, and compounds were added to the assay plates. Assay plates were transferred to the BSL-4 suite and infected with 0.3 pfu per cell JUNV, which resulted in ~50% of the cells expressing virus antigen in a 48-h period. Virus infection was quantified by immuno-staining using antibodies that recognized the viral glycoproteins as described in Table 2.

Lassa fever virus assay

HeLa cells were seeded at 2,000 cells/well in a 384-well plate, and compounds were added to the assay plates. Assay plates were transferred to the BSL-4 suite and infected with 0.1 pfu per cell LASV, which resulted in >60% of the cells expressing virus antigen in a 48-h period. Virus infection was quantified by immuno-staining using antibodies that recognized the viral glycoproteins as described in Table 2.

Middle East respiratory syndrome virus assay

African Green Monkey (*Chlorocebus* sp) kidney epithelial cells (Vero E6) were seeded at 4,000 cells per well in a 384-well plate, and compounds were added to the assay plates. Assay plates were transferred to the BSL-4 suite and infected with 0.5 pfu per cell of MERS virus, which

resulted in >70% of the cells expressing virus antigen in a 48-h period. Virus infection was quantified by immuno-staining using antibodies that recognized the viral glycoproteins as described in Table 2.

Chikungunya virus assay

U2OS cells were seeded at 3,000 cells per well in a 384-well plate, and compounds were added to the assay plates. Assay plates were transferred to the BSL-4 suite and infected with 0.5 pfu per cell of CHIK, which resulted in >80% of the cells expressing virus antigen in a 48-h period. Virus infection was quantified by immuno-staining using antibodies that recognized the viral glycoproteins as described in Table 2.

Venezuelan equine encephalitis virus assay

HeLa cells were seeded at 4,000 cells per well in a 384-well plate, and compounds were added to the assay plates. Assay plates were transferred to the BSL-4 suite and infected with 0.1 pfu per cell VEEV, which resulted in >60% of the cells expressing virus antigen in a 20-h period. Virus infection was quantified by immuno-staining using antibodies that recognized the viral glycoproteins as described in table 2.

Cytotoxicity assays

HEp-2 (1.5×10^3 cells/well) and MT-4 (2×10^3 cells/well) cells were plated in 384-well plates and incubated with the appropriate medium containing 3-fold serially diluted compound ranging from 15 nM to 100,000 nM. PC-3 (2.5×10^3 cells/well), HepG2 (4×10^3 cells/well), hepatocytes (1×10^6 cells/well), quiescent PBMCs (1×10^6 cells/well), stimulated PBMCs (2×10^5 cells/well), and RPTEC (1×10^3 cells/well) cells were plated in 96-well plates and incubated

with the appropriate medium containing 3-fold serially diluted compound ranging from 15 nM to 100,000 nM. Cells were cultured for 4-5 days at 37°C. Following the incubation, the cells were allowed to equilibrate to 25°C, and cell viability was determined by adding Cell-Titer Glo viability reagent. The mixture was incubated for 10 minutes, and the luminescence signal was quantified using an Envision plate reader.

In vitro RSV RNA synthesis assay

RNA synthesis by the RSV polymerase was reconstituted in vitro using purified RSV L/P complexes and an RNA oligonucleotide template (Dharmacon), representing nucleotides 1-14 of the RSV leader promoter (3´-UGCGCUUUUUUACG-5´)[30-32]. RNA synthesis reactions were performed as described previously, except that the reaction mixture contained 250 µM rGTP, 10 µM rUTP, 10 µM rCTP, supplemented with 10 µCi [α^{32}P] CTP, and either included 10 µM rATP or no ATP. Under these conditions, the polymerase is able to initiate synthesis from the position 3 site of the promoter, but not the position 1 site. The NTP metabolite of GS-5734 was serially diluted in DMSO and included in each reaction mixture at concentrations of 10, 30, or 100 µM as specified in Fig 1f. RNA products were analyzed by electrophoresis on a 25% polyacrylamide gel, containing 7M urea, in tris-taurine-EDTA buffer, and radiolabelled RNA products were detected by autoradiography.

RSV A2 polymerase inhibition assay

Transcription reactions contained 25 µg of crude RSV RNP complexes in 30 µL of reaction buffer (50 mM TRIS-acetate [pH 8.0], 120 mM potassium acetate, 5% glycerol, 4.5 mM $MgCl_2$, 3 mM DTT, 2 mM EGTA, 50 µg/mL BSA, 2.5 U RNasin, 20 µM ATP, 100 µM GTP, 100 µM UTP, 100 µM CTP, and 1.5 µCi [α-^{32}P]ATP [3,000 Ci/mmol]). The radiolabeled nucleotide used

in the transcription assay was selected to match the nucleotide analog being evaluated for inhibition of RSV RNP transcription.

To determine whether nucleotide analogs inhibited RSV RNP transcription, compounds were added using a 6-step serial dilution in 5-fold increments. After a 90-minute incubation at 30°C, the RNP, reactions were stopped with 350 µL of Qiagen RLT lysis buffer, and the RNA was purified using a Qiagen RNeasy 96 kit. Purified RNA was denatured in RNA sample loading buffer at 65°C for 10 minutes and run on a 1.2% agarose/MOPS gel containing 2M formaldehyde. The agarose gel was dried, exposed to a Storm phosphorimaging screen, and developed using a Storm phosphorimager.

Inhibition of human RNA polymerase II

For a 25 µL reaction mixture, 7.5 µL 1× transcription buffer (20 mM HEPES [pH 7.2-7.5], 100 mM KCl, 0.2 mM EDTA, 0.5 mM DTT, 20% glycerol), 3 mM $MgCl_2$, 100 ng CMV-(+) control DNA, and a natural mixture of NTPs were pre-incubated with various concentrations (0 µM to 500 µM) of the inhibitor at 30°C for 5 minutes. The natural mixture of NTPs contained 5-25 µM (equal to *K*m) of the competing ^{33}P-labeled NTP and 400 µM of the other three NTPs. The reaction was started by addition of 3.5 µL of HeLa+Extract. After 1 h of incubation at 30°C, the polymerase reaction was stopped by addition of 10.6 µL Proteinase K mixture that contained final concentrations of 2.5 µg/µL Proteinase K, 5% SDS, and 25 mM EDTA. After incubation at 37°C for 3-12 h, 10 µL of the reaction mixture was mixed with 10 µL of the loading dye (98% formamide, 0.1% xylene cyanol and 0.1% bromophenol blue), heated at 75°C for 5 minutes, and loaded onto a 6% polyacrylamide gel (8 M urea). The gel was dried for 45 minutes at 70°C and

682 exposed to a phosphorimager screen. The full length product, 363 nucleotide runoff RNA, was
683 quantified using a Typhoon Trio Imager and Image Quant TL Software.

684 **Inhibition of human mitochondrial RNA polymerase**

685 Twenty nanomolar POLRMT was incubated with 20 nM template plasmid (pUC18-LSP)
686 containing POLRMT light-strand promoter region and transcription factors mtTFA (100 nM)
687 and mtTFB2 (20 nM) in buffer containing 10 mM HEPES (pH 7.5), 20 mM NaCl, 10 mM DTT,
688 0.1 mg/mL BSA, and 10 mM $MgCl_2$[33]. The reaction mixture was pre-incubated to 32°C, and the
689 reactions were initiated by addition of 2.5 μM of each of the natural NTPs and 1.5 μCi of ^{32}P-
690 GTP. After incubation for 30 minutes at 32°C, reactions were spotted on DE81 paper and
691 quantified.

692 **Molecular modeling**

693 A homology model of RSVA2 and EBOV polymerases were built using the HIV-RT X-ray
694 crystal structure (PDB:1RTD). (Schrödinger Release 2015-1: Prime, version 3.9, Schrödinger,
695 LLC, New York, NY, 2015, default settings with subsequent rigid body minimization and side
696 chain optimization. Loop insertions not in 1RTD of greater than 10 amino acids were not built).

697 **Quantitative real-time PCR for in vivo studies**

698 For quantitative assessment of viral RNA nonhuman primate plasma samples, whole blood was
699 collected using a K3 EDTA Greiner Vacuette tube (or equivalent) and sample centrifuged at
700 2500 (± 200) RCF for 10 ± 2 min. To inactivate virus, plasma was treated with 3 parts (300 μL)
701 TriReagent LS and samples were transferred to frozen storage (-60°C to -90°C), until removal
702 for RNA extraction. Carrier RNA and QuantiFast High Concentration Internal Control (Qiagen)

were spiked into the sample prior to extraction, conducted according to manufacturer's instructions. The viral RNA was eluted in AVE Buffer. Each extracted RNA sample was tested with the QuantiFast Internal Control RT-PCR RNA Assay (Qiagen) to evaluate the yield of the spiked-in QuantiFast High Concentration Internal Control. If the internal control amplified within manufacturer-designated ranges, further quantitative analysis of the viral target was performed. RT-PCR was conducted using an ABI 7500 Fast Dx using primers specific to EBOV glycoprotein. Samples were run in triplicate using a 5 µL template volume. For quantitative assessments, the average of the triplicate genomic equivalents (ge) per reaction were determined and multiplied by 800 to obtain ge/mL of plasma. Standard curves were generated using synthetic RNA. The limits of quantification for this assay are $8.0 \times 10^4 - 8.0 \times 10^{10}$ ge/mL of plasma. Acceptance criteria for positive template control (PTC), negative template control (NTC), negative extraction control (NEC), and positive extraction control (PEC) are SOP-specified. For qualitative asssessments, the limit of detection (LOD) was defined as Ct 38.07, based on method validation testing. An animal was considered to have tested positive for detection of EBOV RNA when a minimum of 2 of 3 replicates were designated as "positive" and PTC, NTC, and NEC controls meet specified method-acceptance criteria. A sample was designated as "positive" when the Ct value was <LOD Ct.

Pharmacokinetic evaluations

Three uninfected male rhesus monkeys (*Macaca maniculata*) were used for the pharmacokinetic study. GS-5734 was formulated in solution at 5 mg/mL with 12% sulfobutylether-β-cyclodextrin in water, pH 3.5-4.0, and 2 mL/kg was administered by slow bolus (approximately 1 min) for a final dose of 10 mg/kg. Blood samples for plasma and PBMC were collected from a femoral vein/artery and were taken from each monkey over a 24-h period. Plasma samples were obtained

at predose and at 0.083, 0.25, 0.5, 1, 2, 4, 8, and 24 h postdose. PBMC samples were obtained at 2, 4, 8, and 24 h. Blood samples for plasma were collected into chilled collection tubes containing sodium fluoride/ potassium oxalate (NaF/K-Ox) as the anticoagulant and were immediately placed on wet ice, followed by centrifugation to obtain plasma. Blood samples for PBMC isolation were collected at room temperature into CPT vacutainer tubes containing sodium heparin for isolation. Plasma and isolated PBMC samples were frozen immediately and stored at ≤60°C until analyzed.

For plasma analysis, an aliquot of 25 µL of each plasma sample was treated with 100 µL of 90% methanol and acetonitrile mixture (1:1, v:v) and 10% water with 20 nM 5-(2-aminopropyl)indole as an internal standard. One hundred microliters of samples were filtered through an Agilent Captiva 96 well 0.2 µm filter plate. Filtered samples were dried down completely for approximately 20 minutes and reconstituted with 1% acetonitrile and 99% water with 0.01% formic acid. An aliquot of 10 µL was injected for LC-MS/MS using a HTC Pal autosampler. Analytes were separated on a Phenomenex Synergi Hydro-RP 30A column (75 × 2.0 mm, 4.0 µm) using a Waters Acquity ultra performance LC (Waters Corporation, Milford, MA, USA), a flow rate of 0.26 mL/min, and a gradient from Mobile phase A containing 0.2% formic acid in 99% water and 1% acetonitrile to mobile phase B containing 0.2% formic acid in 95% acetonitrile and 5% water over 4.5 minutes. MS/MS analysis used a Waters Xevo TQ-S in positive multiple reaction monitoring mode using an electrospray probe. Plasma concentrations of GS-734, Ala-Met and Nuc were determined using an 8-point calibration curve spanning a concentration range of over 3 orders of magnitude. Quality control samples run at the beginning and end of the run to ensure accuracy and precision within 20%. Intracellular metabolites in PBMC were quantified by LC-MS/MS as described above for in vitro activation studies.

Radiolabeled tissue distribution

Six cynomolgus monkeys were administered a single dose of [^{14}C]GS-5734 at 10 mg/kg (25 μCi/kg) by IV administration (slow bolus). Tissues were collected from 3 animals at 4 and 168 h post dose. The tissues were excised, rinsed with saline, blotted dry, weighed, and placed on wet ice. Tissues (testes, epididymis, eyes and brain; following homogenization) and plasma were analyzed by liquid scintillation counting. Concentrations were converted to ng equivalents of GS-5734 per gram of sample.

In vivo efficacy

Rhesus monkeys (*Macaca mulatta*) were challenged on day 0 by intramuscular injection with a target dose of 1000 pfu of EBOV-Kikwit (Ebola virus H.sapiens-tc/COD/1995/Kikwit), which was derived from a clinical specimen obtained during an outbreak occurring in The Democratic Republic of the Congo (formerly Zaire) in 1995. Animals (3-6 years) were randomly assigned to experimental treatment groups, stratified by sex and balanced by body weight, using SAS® statistical software (Cary, North Carolina, USA). Study personnel responsible for assessing animal health (including euthanasia assessment) and administering treatments were experimentally blinded to group assignment of animals. Challenge virus was propagated from the clinical specimen using cultured cells (Vero or Vero E6) for a total of four passages. GS-5734 was formulated at Gilead Sciences in water with 12% sulfobutylether-β-cyclodextrin (SBE-β-CD), pH adjusted to 3.0 using HCl. Formulations were administered to anesthetized animals by bolus intravenous injection at a rate of approximately 1 min/dose in the right or left saphenous vein. The volume of all vehicle or GS-5734 injections was 2.0 mL/kg body weight. Animals

were anesthetized using IM injection of a solution containing ketamine (100 mg/mL) and acepromazine (10 mg/mL) at 0.1 mL/kg body weight.

Animals were observed at least twice daily to monitor for disease signs, and animals that survived to day 28 were deemed to be protected. Study personnel alleviated unnecessary suffering of infected animals by euthanizing clinically moribund animals. The criteria used as the basis for euthanasia of moribund animals were defined prior to study initiation and included magnitude of responsiveness, reduced body temperature, and/or specified alterations to serum chemistry parameters[34]. Serum chemistry was analyzed using a Vitros 350 Chemistry System (Ortho Clinical Diagnostics), and coagulation parameters were evaluated using a Sysmex CA-1500 coagulation analyzer (Siemens Healthcare Diagnostics). Hematology analysis was conducted using a Siemens Advia 120 Hematology System with multispecies software (Siemens Healthcare Diagnostics). On days in which GS-5734 or vehicle dosing were scheduled with blood sample collection for clinical pathology or viremia analysis, blood samples were collected immediately prior to dose administration.

Animal care

Pharmacokinetic and radiolabeled tissue distribution studies in uninfected cynomolgus and rhesus macques were conducted at Covance, Inc. (Madison, WI). Protocols were reviewed by an Institutional Animal Care and Use Committee (IACUC) at Covance. Efficacy experiments involving EBOV were performed in ABSL-4 at USAMRIID. Research was conducted under an Institutional Animal Care and Use Committee approved protocol in compliance with the Animal Welfare Act, PHS Policy, and other federal statutes and regulations relating to animals and experiments involving animals. The facilities where this research was conducted are accredited

by the Association for Assessment and Accreditation of Laboratory Animal Care, International and strictly adhere to principles stated in the Guide for the Care and Use of Laboratory Animals, National Research Council, 2011 (National Academies Press, Washington, DC.).

Statistics

Combined vehicle group from Part 1 and 2 (N = 6 animals total) was used as control group in all statistical comparisons. The impact of GS-5734 treatment on the survival rates was estimated using Kaplan-Meier method and analyzed by log-rank analysis using Dunnett-Hsu procedure to adjust for multiple comparisons. The effect on systemic viral RNA levels was assessed by the analysis of variance (ANOVA) comparing each GS-5734 treatment group with vehicle group using Dunnett's test to adjust for multiple comparisons. Wilcoxon rank-sum test without adjustment for multiple comparisons was used to compare the effects of GS-5734 treatment on hematology, coagulation and clinical chemistry parameters. All data met the statistical assumptions of the test performed.

Method References

25 Uebelhoer, L. S. *et al.* High-throughput, luciferase-based reverse genetics systems for identifying inhibitors of Marburg and Ebola viruses. *Antiviral Res.* **106**, 86-94, doi:10.1016/j.antiviral.2014.03.018 (2014).

26 Towner, J. S. *et al.* Generation of eGFP expressing recombinant Zaire ebolavirus for analysis of early pathogenesis events and high-throughput antiviral drug screening. *Virology* **332**, 20-27 (2005).

27 Shao, R. & Guo, X. Human microvascular endothelial cells immortalized with human telomerase catalytic protein: a model for the study of in vitro angiogenesis. *Biochem. Biophys. Res. Commun.* **321**, 788-794, doi:10.1016/j.bbrc.2004.07.033 (2004).

28 Mason, S. W. *et al.* Polyadenylation-dependent screening assay for respiratory syncytial virus RNA transcriptase activity and identification of an inhibitor. *Nucleic Acids Res.* **32**, 4758-4767, doi:10.1093/nar/gkh809 (2004).

29 Durand-Gasselin, L. *et al.* Nucleotide analogue prodrug tenofovir disoproxil enhances lymphoid cell loading following oral administration in monkeys. *Mol. Pharm.* **6**, 1145-1151, doi:10.1021/mp900036s (2009).

30 Noton, S. L., Deflube, L. R., Tremaglio, C. Z. & Fearns, R. The respiratory syncytial virus polymerase has multiple RNA synthesis activities at the promoter. *PLoS Pathogens* **8**, e1002980, doi:10.1371/journal.ppat.1002980 (2012).

31 Noton, S. L. *et al.* Respiratory syncytial virus inhibitor AZ-27 differentially inhibits different polymerase activities at the promoter. *J. Virol.* **89**, 7786-7798, doi:10.1128/JVI.00530-15 (2015).

32 Tremaglio, C. Z., Noton, S. L., Deflube, L. R. & Fearns, R. Respiratory syncytial virus polymerase can initiate transcription from position 3 of the leader promoter. *J. Virol.* **87**, 3196-3207, doi:10.1128/JVI.02862-12 (2013).

33 Lodeiro, M. F. *et al.* Identification of multiple rate-limiting steps during the human mitochondrial transcription cycle in vitro. *J. Biol. Chem.* **285**, 16387-16402, doi:10.1074/jbc.M109.092676 (2010).

34 Warren, T. K. *et al.* Euthanasia assessment in ebola virus infected nonhuman primates. *Viruses* **6**, 4666-4682, doi:10.3390/v6114666 (2014).

Extended Data Fig Legends

Extended Data Figure 1: a, Putative mechanism for the intracellular activation of GS-5734. Following cellular permeation the ester is cleaved by hydrolase activity followed by chemically catalyzed release of phenol to yield the negatively charged Ala-Met. Amidase cleavage results in release of the NMP that is converted to the pharmacologically active NTP by successive nucleotide kinase mediated phosphorylation steps. Nucleotidase and phosphotase activity dephosphorylates the nucleotide metabolites to the poorly phosphorylated Nuc. **b,** Intracellular metabolite profile in human macrophages. Following a 2-h pulse incubation (black bar at top of y-axis) of 1 μM GS-5734 with human monocyte-derived macrophages from three different donors (mean ± s.d.). GS-5734 is rapidly metabolized and not detected in cells. Transient exposure to the intermediate metabolite Ala-Met is observed followed by persistent Nuc and nucleotide analog exposure. The pharmacologically active NTP is formed quickly achieving a Cmax at 4 h and persisted with a half-life of 16 ± 1 h in the three donors. Intracellular concentration estimated based on an intracellular volume of 1 pL/cell. **c,** Efficiency of GS-5734 activation in human and rhesus cells in vitro. Intracellular NTP concentrations formed in human and rhesus PBMC, monocytes, and monocyte-derived macrophages during a 2-h incubation with 1 μM GS-5734 (results are the average of two (PBMC and monocyte) to six (macrophage) independent experiments done in cells from different donors). Intracellular concentrations estimated based on a cell volume of 0.2 pL/cell for PBMC and monocytes and 1 pL/cell for macrophage. GS-5734 more efficiently delivers the pharmacologically active triphosphate analog into human cells than rhesus. Triphosphate levels in human cells were approximately 5-fold higher than rhesus. Higher levels in human cells reflect more efficient ester hydrolysis, the first step in intracellular activation (data not shown). **d,** Intracellular NTP levels required for

858 inhibition of Ebola virus replication in cell culture. The diastereomeric mixture at phosphorous
859 containing GS-5734 was incubated continuously for 72 h at 1 μM and levels of intracellular NTP
860 determined (results are the average of duplicate incubations done in each cell type; two
861 independent studies were done in HMVEC isolated from different donors). The corresponding
862 EVD EC50 values for the diastereomeric mixture were 100, 184, and 121 nM in human
863 macrophages, Hela, and HMVEC, respectively, suggesting that an average intracellular NTP
864 concentration of approximately 5 μM is required for 50% inhibition in vitro.

865

866 **Extended Data Figure 2: Virus yield assay.** Huh-7 cells seeded in 96-well plates were
867 infected with wild-type EBOV (Makona) for 1 h at 0.1 plaque forming unit (pfu) per cell. The
868 virus inoculum was removed and replaced with 100 μL per well of media containing the
869 appropriate dilution of compound. At 3 days post-infection, supernatants were collected, and the
870 amount of virus was quantified by endpoint dilution assay. The endpoint dilution assay was
871 conducted by preparing serial dilutions of the assay media and adding these dilutions to fresh
872 Vero cell monolayers in 96-well plates to determine the tissue culture infectious dose that caused
873 50% infection (TCID50). To measure levels of viral RNA from infected cells, total RNA was
874 extracted using MagMAX™-96 Total RNA Isolation Kit (Invitrogen, Carlsbad, CA) and
875 quantified using a quantitative reverse transcription polymerase chain reaction (qRT-PCR) assay
876 with primers and probes specific for the EBOV nucleoprotein gene.

877

878 **Extended Data Figure 3:** Homology model of respiratory syncytial virus (RSV) A2 (Cyan) and
879 EBOV (coral) polymerase based on HIV-RT (PDB:1RTD) with NTP (green).

Extended Data Figure 4: Clinical signs of disease in individual rhesus monkeys exposed to Ebola virus. Animals were observed multiple times each day and were subjectively assigned a clinical disease score ranging from 0 to 5 based on responsiveness, posture, and activity. Maximum daily scores were converted to color code, with darker colors indicative of more severe disease signs. The schematic was truncated to emphasize clinical scores during the acute disease phase, and none of the animals exhibited clinical disease signs outside of the times that are shown.

Extended Data Table Titles and Legends

Extended Data Table 1: In vitro cytotoxicity of GS-5734 and Nuc in human cell lines and primary cells.

* All CC_{50} values represent the mean ± s.d. of at least 2 independent experiments. Puromycin was included in experiments as a positive-control for cytotoxicity

Extended Data Table 2: Individual plasma viral RNA [log_{10}(copies/mL)]

–, unscheduled sampling; D, day; DET, detectable, but below the lower limit of quantitation (8.0 × 10^4 copies/mL); ND, not detected.

Extended Data Table 3: Summary and statistical analysis of plasma viral RNA

NA, not applicable due to no survivors in vehicle group.

* P-values are from ANOVA comparing each GS-5734 treatment Group with Vehicle Group using Dunnett's test to adjust for multiple comparisons. EBOV RNA values reported as "<LLOD" were substituted as 10^3 RNA copies/mL and values reported as ">LLOD, <LLOQ" were substituted as LLOQ of 8.0×10^4 RNA copies/mL for computation purpose.

Statistically significant P-values ($P < 0.05$) are highlighted in bold.

Extended Data Table 4: Statistical summary of selected clinical pathology parameters

ALP, alkaline phosphatase; ALT, alanine aminotransferase; APTT, activated partial thromboplastin time; AST, aspartate aminotransferase; BUN, blood urea nitrogen; CRK, creatine kinase; CRP, C-reactive protein; D, day; GGT, gamma glutamyl transferase; LDH, lactate dehydrogenase; PT, prothrombin time; TT, thrombin time.

* Wilcoxon rank-sum test without adjustment for multiple comparisons using combined Group 1+4 as control group for the analysis. Statistically significant P-values ($P < 0.05$) are highlighted in bold.

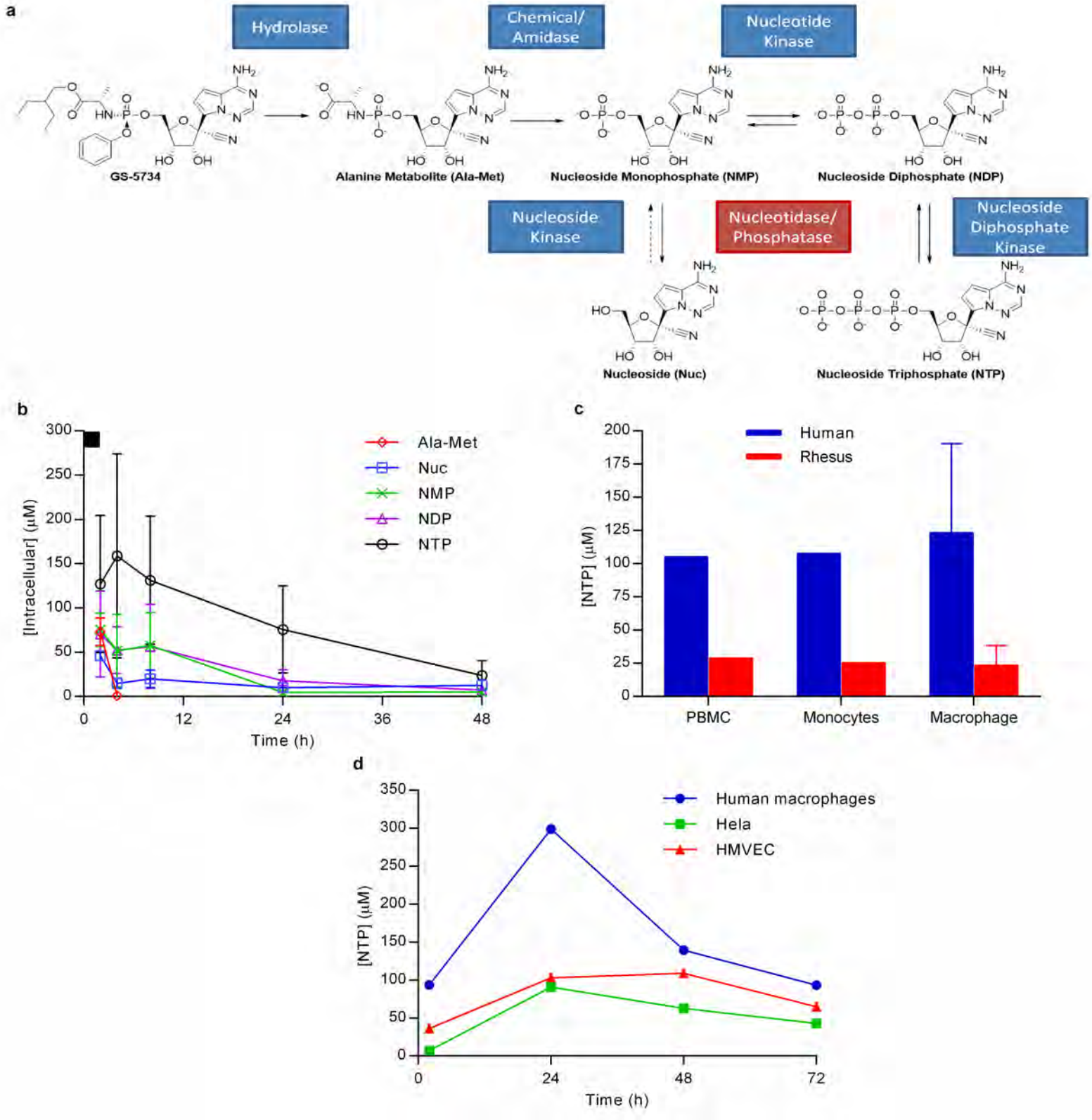
a
Hydrolase
Chemical/
Amidase
Nucleotide
Kinase
GS-5734
Alanine Metabolite (Ala-Met)
Nucleoside Monophosphate (NMP)
Nucleoside Diphosphate (NDP)
Nucleoside
Kinase
Nucleotidase/
Phosphatase
Nucleoside
Diphosphate
Kinase
Nucleoside (Nuc)
Nucleoside Triphosphate (NTP)
b
[Intracellular] (μM)
Time (h)
Ala-Met
Nuc
NMP
NDP
NTP
c
[NTP] (μM)
Human
Rhesus
PBMC
Monocytes
Macrophage
d
[NTP] (μM)
Time (h)
Human macrophages
Hela
HMVEC

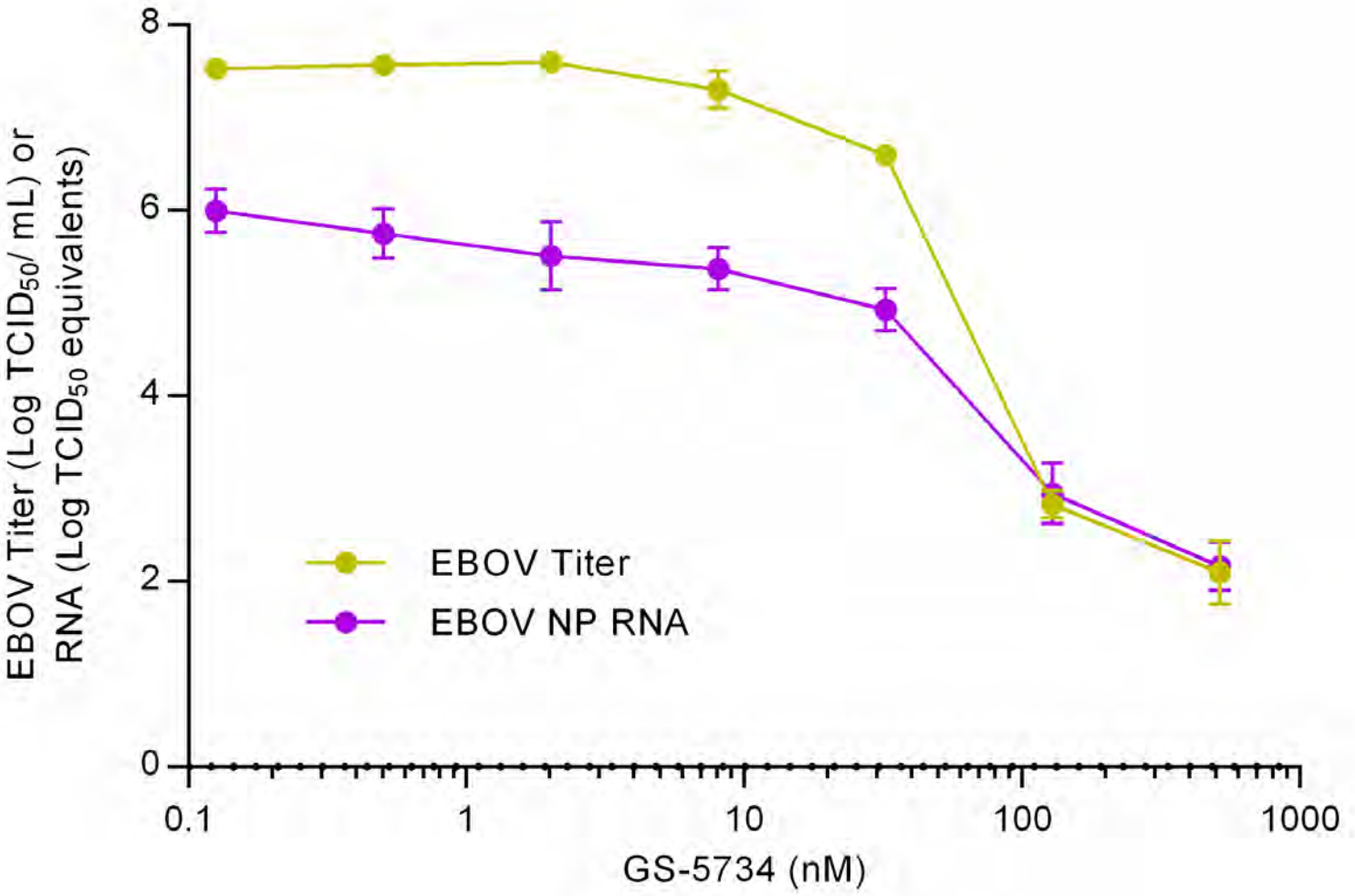

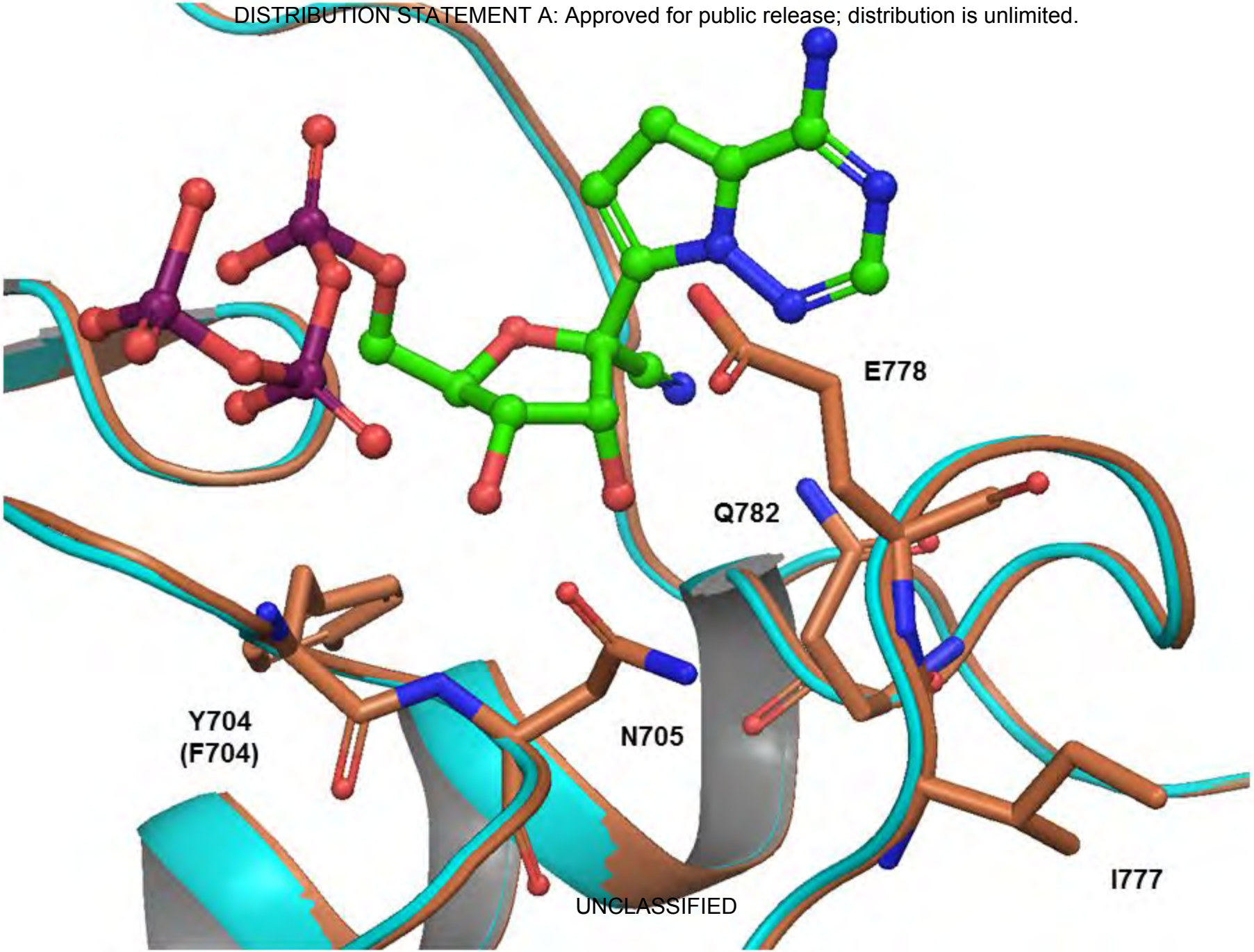

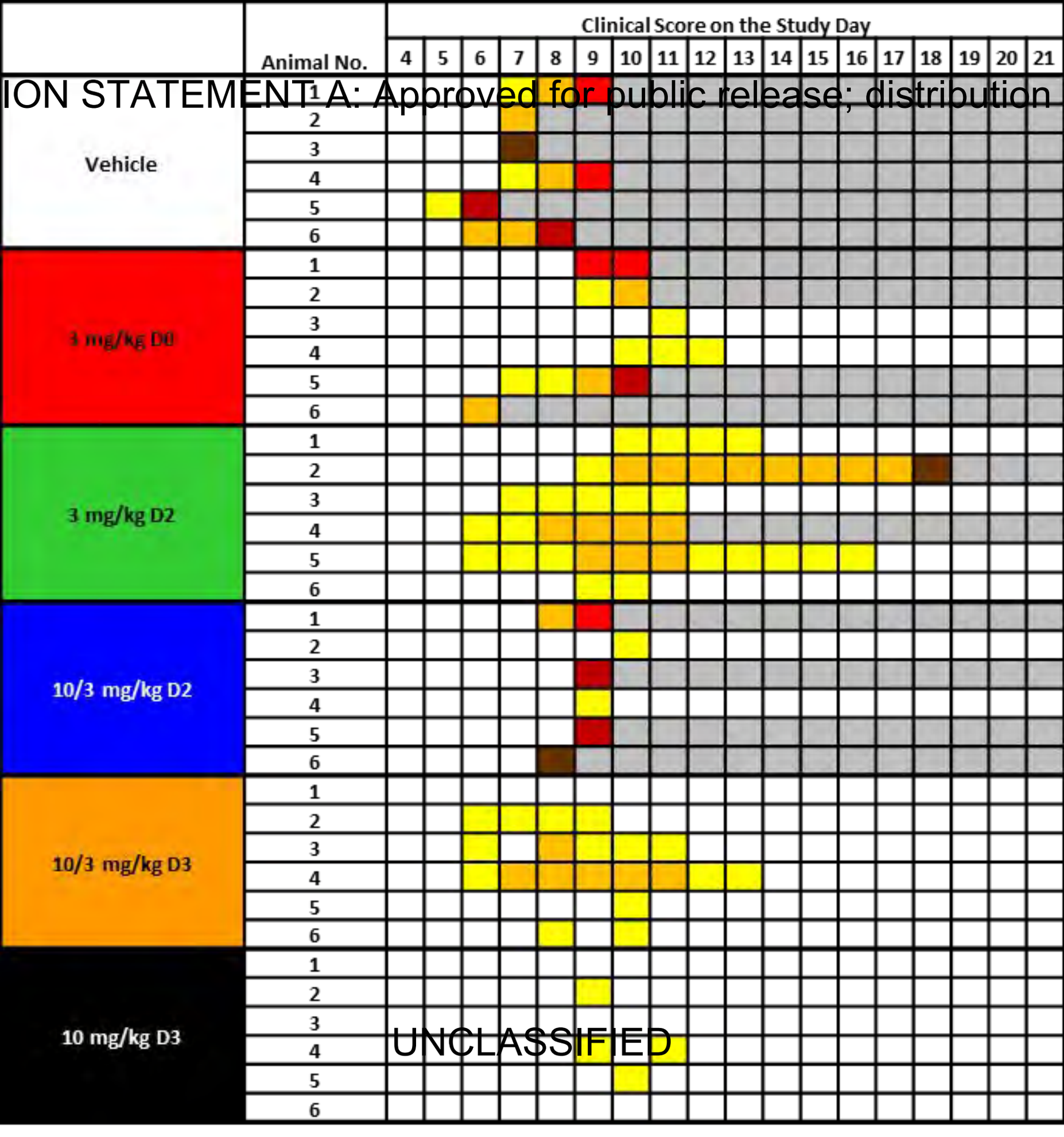

	CC_{50} (μM)*		
	GS-5734	Nuc	Puromycin
Human cell lines			
HEp-2	6.0 ± 1.5	> 100	0.53 ± 0.10
HepG2	3.7 ± 0.2	> 100	0.73 ± 0.01
PC-3	8.9 ± 1.6	> 100	0.52 ± 0.11
MT-4	1.7 ± 0.4	69.3 ± 25.7	0.12 ± 0.03
Human primary cells			
Hepatocytes	2.5 ± 0.6	> 100	1.5 ± 0.6
Renal proximal tubular epithelial cells (RPTEC)	12.9 ± 6.2	> 100	1.1 ± 0.3
Quiescent PBMCs	> 20	> 100	6.8 ± 1.4
Stimulated PBMCs	14.8 ± 5.8	> 100	1.6 ± 0.2

Treatment Description	Animal #	Study Day 0	2	3	4	5	6	7	8	9	10	12	14	18	21/22	28/29
Vehicle																
	1	ND	ND	ND	6.6	9.0	–	10.0	–	9.5						
	2	ND	ND	ND	5.9	8.9	–	9.8								
	3	ND	ND	6.5	8.2	8.5	–	8.6								
	4	ND	ND	DET	6.6	8.4	–	8.4	–	8.1						
	5	ND	ND	5.8	8.8	10.0	10.3									
	6	ND	ND	5.4	7.4	9.4	–	9.2	8.7							
GS-5734 3 mg/kg D0																
	1	ND	ND	ND	DET	6.0	–	7.3	–	7.4	7.3					
	2	ND	ND	ND	ND	4.9	–	6.8	–	9.9						
	3	ND	ND	ND	DET	5.5	–	6.5	–	5.8	–	DET	ND	–	ND	ND
	4	ND	ND	ND	ND	4.9	–	5.8	–	5.6	–	DET	ND	–	ND	ND
	5	ND	ND	ND	DET	5.7	–	9.1	–	9.1	8.6					
	6	ND	ND	DET	7.2	9.3	–									
GS-5734 3 mg/kg D2																
	1	ND	ND	ND	DET	6.0	–	6.6	–	6.8	–	6.9	6.0	–	ND	ND
	2	ND	ND	ND	6.4	7.6	–	7.1	–	6.8	–	DET	ND	ND		
	3	ND	ND	ND	DET	6.6	–	7.5	–	8.2	–	5.2	ND	–	ND	ND
	4	ND	ND	ND	5.1	7.0	–	7.4	–	6.6	–					
	5	ND	ND	4.9	6.9	8.1	–	8.1	–	6.6	–	5.2	ND	–	ND	ND
	6	ND	ND	ND	DET	5.5	–	6.7	–	5.9	–	ND	ND	–	ND	ND
GS-5734 10/3 mg/kg D2																
	1	ND	DET	5.2	5.8	7.9	–	8.2	–	8.0						
	2	ND	ND	ND	ND	DET	–	DET	–	ND	–	ND	ND	–	ND	ND
	3	ND	ND	ND	DET	6.1	–	7.8	–	7.5						
	4	ND	ND	ND	4.9	5.5	–	6.1	–	DET	–	ND	ND	–	ND	ND
	5	ND	ND	ND	ND	DET	–	8.2	–	8.2						
	6	ND	ND	ND	5.3	7.1	–	6.9	8.1							
GS-5734 10/3 mg/kg D3																
	1	ND	ND	DET	5.4	6.5	–	6.5	–	5.0	–	ND	ND	–	ND	ND
	2	ND	ND	5.3	6.2	7.1	–	6.8	–	6.0	–	ND	ND	–	ND	ND
	3	ND	ND	DET	5.1	6.9	–	7.0	–	7.0	–	6.7	ND	–	ND	ND
	4	ND	ND	ND	DET	7.0	–	8.1	–	8.3	–	6.2	DET	–	ND	ND
	5	ND	ND	ND	ND	DET	–	ND	–	5.5	–	ND	ND	–	ND	ND
	6	ND	ND	DET	5.8	6.6	–	6.2	–	6.8	–	ND	ND	–	ND	ND
GS-5734 10 mg/kg D3																
	1	ND	ND	DET	5.7	6.1	–	6.0	–	DET	–	ND	ND	–	ND	ND
	2	ND	ND	ND	DET	DET	–	DET	–	5.6	–	ND	ND	–	ND	ND
	3	ND	ND	ND	6.7	DET	–	ND	–	ND	–	ND	ND	–	ND	ND
	4	ND	ND	ND	ND	DET	–	ND	–	ND	–	ND	ND	–	ND	ND
	5	ND	ND	ND	ND	ND	–	ND	–	ND	–	ND	ND	–	ND	ND
	6	ND	ND	DET	5.6	6.9	–	5.5	–	5.9	–	ND	ND	–	ND	ND

	Plasma Viral RNA, mean log_{10} copies/mL (P value*)				
Day	Vehicle	GS-5734 3 mg/kg D0	GS-5734 3 mg/kg D2	GS-5734 10/3 mg/kg D2	GS-5734 10/3 mg/kg D3	GS-5734 10 mg/kg D3
3	4.77	3.32 (**0.019**)	3.32 (**0.020**)	3.36 (**0.023**)	4.33 (0.454)	3.63 (0.062)
4	7.24	4.66 (**0.001**)	5.52 (**0.024**)	4.49 (**0.001**)	5.06 (**0.005**)	4.81 (**0.002**)
5	9.05	6.04 (**<0.001**)	6.82 (**0.002**)	6.07 (**<0.001**)	6.52 (**0.001**)	5.12 (**<0.001**)
7	9.19	7.09 (**0.013**)	7.24 (**0.015**)	7.00 (**0.007**)	6.28 (**0.001**)	4.24 (**<0.001**)
9	8.76	7.55 (0.351)	6.82 (0.132)	6.30 (0.065)	6.42 (0.072)	4.22 (**0.001**)
12	–	4.90 (NA)	5.05 (NA)	3.00 (NA)	4.14 (NA)	3.00 (NA)

	Mean Change from Baseline, Day 7 (P value compared with Group 1+4*)				
Parameter	Vehicle Day 0	GS-5734 3 mg/kg D0	GS-5734 3 mg/kg D2	GS-5734 10/3 mg/kg D2	GS-5734 10/3 mg/kg D3	GS-5734 10 mg/kg D3
Platelet count (10^3/ µL)	-279	-118 (**0.012**)	-202 (0.055)	-155 (0.055)	-98 (**0.014**)	-65 (**0.008**)
PT (sec)	5.0	1.3 (**0.01**)	3.2 (0.27)	1.6 (0.06)	2.5 (**0.02**)	1.7 (**0.01**)
APTT (sec)	47.7	12.6 (**0.012**)	19.3 (**0.014**)	14.3 (**0.008**)	15.2 (**0.008**)	9.8 (**0.008**)
Fibrinogen (mg/dL)	2.5	-4.7 (**0.012**)	-5.5 (**0.008**)	-5.0 (**0.014**)	-5.0 (**0.014**)	-4.4 (**0.008**)
TT (sec)	50.2	-1.4 (**0.012**)	2.6 (**0.008**)	1.4 (**0.008**)	3.6 (**0.008**)	-1.5 (**0.008**)
Antithrombin (%)	-39.6	-6.1 (**0.012**)	-10.3 (**0.008**)	-7.9 (**0.008**)	5.6 (**0.008**)	3.1 (**0.008**)
D-dimer (mg/dL)	1.15	0.13 (**0.012**)	-0.09 (**0.008**)	0.11 (**0.008**)	-0.12 (**0.005**)	0.02 (**0.007**)
ALT (U/L)	340	14 (**0.012**)	24 (**0.008**)	116 (0.083)	28 (**0.008**)	32 (**0.008**)
AST (U/L)	1425	273 (**0.014**)	206 (**0.014**)	90 (**0.020**)	157 (**0.014**)	36 (**0.014**)
ALP (U/L)	1238	-69 (**0.012**)	-74 (**0.008**)	7 (**0.008**)	8 (**0.008**)	-66 (**0.008**)
CRK (U/L)	5420	1277 (**0.020**)	1002 (**0.014**)	841 (**0.014**)	682 (**0.014**)	96 (**0.014**)
GGT (U/L)	146	-12 (**0.012**)	-13 (**0.008**)	-2 (**0.008**)	1 (**0.008**)	-12 (**0.008**)
LDH (U/L)	8391	1006 (**0.020**)	2263 (**0.014**)	2358 (**0.014**)	2439 (**0.014**)	352 (**0.014**)
Bilirubin (mg/dL)	1.3	0 (0.071)	0 (**0.048**)	0 (**0.048**)	0 (**0.048**)	0 (**0.048**)
BUN (mg/dL)	60	0 (**0.021**)	1 (**0.028**)	2 (**0.036**)	5 (0.055)	1 (**0.021**)
Creatinine (mg/dL)	1.80	0.12 (**0.015**)	0.27 (**0.017**)	0.18 (**0.014**)	0.27 (**0.014**)	0.43 (0.066)
Lipase (U/L)	205	17 (0.14)	34 (0.12)	-17 (0.055)	36 (0.12)	-12 (**0.036**)
Triglycerides (mg/dL)	538	-7 (**0.012**)	52 (**0.008**)	63 (**0.008**)	420 (0.083)	-6 (**0.008**)
CRP (mg/dL)	48.6	48.8 (0.83)	43.8 (1.0)	41.2 (0.31)	35.3 (0.24)	13.2 (**0.008**)
Albumin (g/dL)	-1.5	-0.8 (**0.012**)	-1.2 (0.170)	-0.8 (**0.036**)	-0.8 (**0.022**)	-0.7 (**0.008**)
Total protein (mg/dL)	-1.1	-0.5 (**0.034**)	-0.9 (0.27)	-0.6 (0.17)	-0.4 (**0.035**)	-0.4 (**0.008**)
Chloride (mEq/dL)	-14	-3 (**0.011**)	-5 (**0.008**)	-6 (**0.013**)	-6 (0.067)	0 (**0.008**)
Phosphate (mEq/dL)	0.2	-2.1 (**0.036**)	-2.5 (**0.021**)	-1.5 (0.12)	-1.0 (0.65)	-0.3 (0.93)
Sodium (mg/dL)	-17	-8 (**0.019**)	-10 (**0.042**)	-9 (0.054)	-7 (**0.042**)	-5 (**0.014**)

Table of Contents

I. General Information

All organic compounds were synthesized at Gilead Sciences, Inc (Foster City, CA). unless otherwise noted. Commercially available solvents and reagents were used as received without further purification. 2,3,5-Tri-*O*-benzyl-D-ribono-1,4-lactone (**1**) was purchased from Carbosynth (Berkshire, UK). 7-iodopyrrolo[2,1-*f*][1,2,4]triazin-4-amine (**2**) was prepared as previously described by Clarke, M. O. *et al*[35]. (*S*)-2-ethylbutyl 2-aminopropanoate hydrochloride (**8**) was prepared as previously described by Meppen, M. *et al*[36]. The radiolabeled analogue [^{14}C]GS-5734 (specific activity 58.0 mCi/mmol) was obtained from Moravek Biochemicals (Brea, CA) and was prepared in a similar manner described for GS-5734 using [^{14}C]TMSCN. Nuclear magnetic resonance (NMR) spectra were recorded on a Varian Mercury Plus 400 MHz at room temperature, with tetramethylsilane as an internal standard. Proton nuclear magnetic resonance spectra are reported in parts per million (ppm) on the δ scale and are referenced from the residual protium in the NMR solvent (chloroform-d_1: δ 7.26, methanol-d_4: δ 3.31, water-d_2: δ 4.79, DMSO-d_6: δ 2.50). Data is reported as follows: chemical shift [multiplicity (s = singlet, d = doublet, t = triplet, q = quartet, p = pentet, sep = septet, m = multiplet, br = broad, app = apparent), coupling constants (*J*) in Hertz, integration. Carbon-13 nuclear magnetic resonance spectra are reported in parts per million on the δ scale and are referenced from the carbon resonances of the solvent (chloroform-d_1: δ 77.16, methanol-d_4: δ 49.15, DMSO-d_6: δ 39.52). Data is reported as follows: chemical shift. No special nomenclature is used for equivalent carbons. Phosphorus-31 nuclear magnetic resonance spectra are reported in parts per million on the δ scale. Data is reported as follows: chemical shift [multiplicity (s = singlet, d = doublet, t = triplet), coupling constants (*J*) in Hertz. Analytical thin–layer chromatography was performed using Merck KGaA Silica gel 60 F_{254} glassplates with UV visualization. Preparative normal phase silica gel chromatography was carried out using a Teledyne ISCO CombiFlash Companion instrument with silica gel cartridges. Purities of the final compounds were determined by high-performance liquid chromatography (HPLC) and were greater than 95% unless otherwise noted. HPLC conditions to assess purity were as follows: Agilent 1100 Series HPLC, Phenominex Gemini 5 μm C18 110Å, 50 × 4.6 mm column; 2-98% gradient of 0.1% trifluoroacetic acid in water and 0.1% trifluoroacetic acid in acetonitrile; flow rate, 2 mL/min; acquisition time, 6 min; wavelength, UV 214 and 254 nm. Analytical ion-

exchange HPLC of the nucleoside triphosphate (**NTP**) was carried out as follows: Agilent 1100 Series HPLC, Thermo Scientific CNAPac™ PA-100 BioLC™ 4 × 250 mm column; 0-100% gradient of 0.5 M triethylammonium bicarbonate buffer in water; flow rate, 1 mL/min; acquisition time, 8 min; wavelength, UV 214 and 254 nm. High-resolution mass spectrometry (HRMS) was performed on an Agilent model 6230 Accurate Mass Time of Flight Mass Spectrometer featuring Agilent Jet Stream Thermal Focusing Technology, with an Agilent 1200 Rapid Resolution HPLC. HRMS chromatography was performed using an Agilent Zorbax Eclipse Plus C18 RRHD 1.8 μm, 2.1 × 50 mm column at 30 °C, with a 10-90% gradient of 0.05% trifluoroacetic acid in water and 0.05% trifluoroacetic acid in acetonitrile. **NTP** HRMS chromatography was performed using an Agilent Poroshell 120 PFP, 3.0, 50 mm, 2.7 μm LC column. Data processing was performed via Agilent MassHunter B.07 Qualitative Analysis. The reference masses used during the run were 118.086255 and 922.009798.

II. Preparation of Small Molecule Compounds

Nuc and **GS-5734** were prepared according to Scheme S1. Alternative methods for the synthesis of **Nuc** and GS-5734 mixture of phosphorus diastereoisomers have been described previously by Mackman, R. L. *et al*[37] and Metobo, S. E. *et al*[38]. (*S*)-2-ethylbutyl 2-(((*S*)-(4-nitrophenoxy)(phenoxy)phosphoryl)-amino)propanoate (**6**) was prepared according to Scheme S2. The nucleoside triphosphate (**NTP**) was prepared according to Scheme S3.

Scheme S1. Preparation of **Nuc** and **GS-5734**.

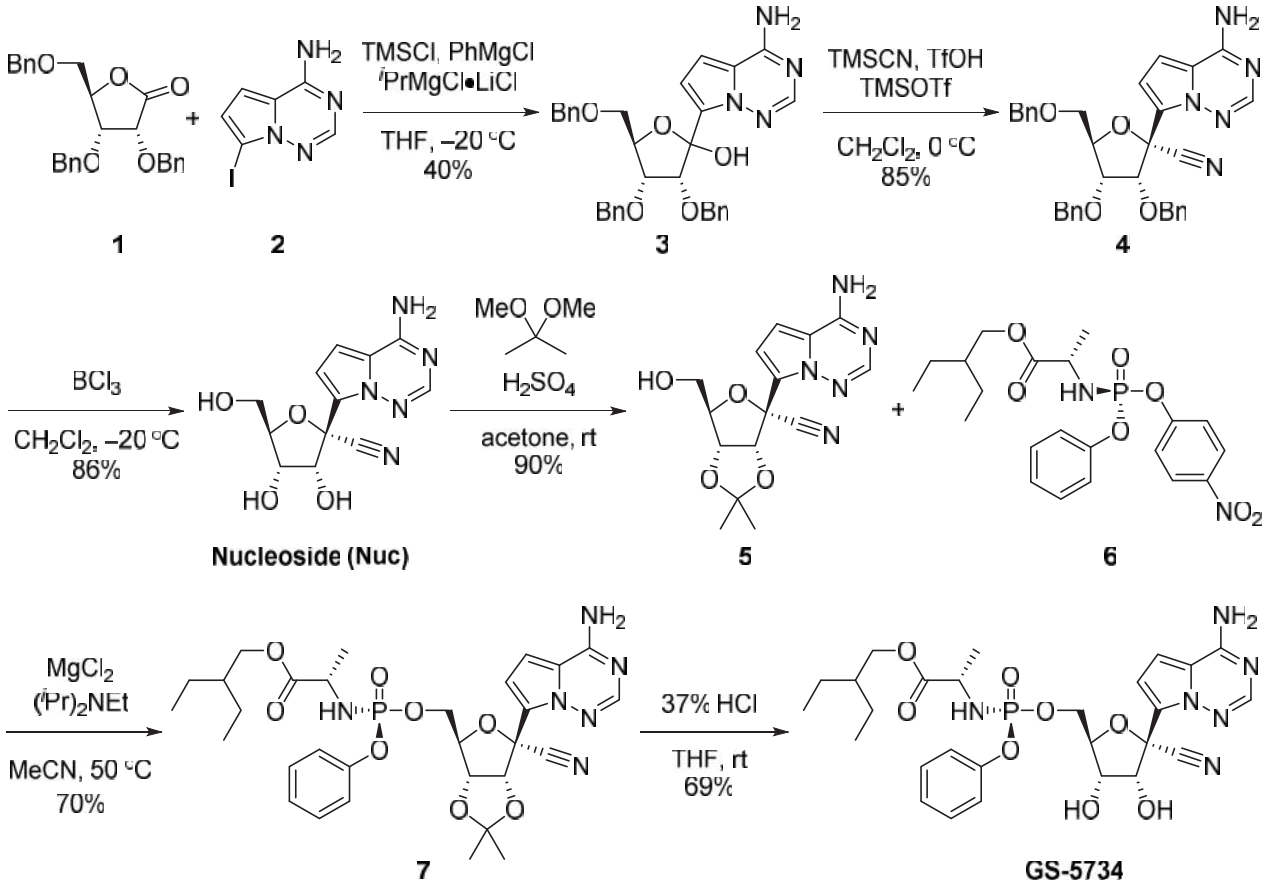

Scheme S2. Preparation of (*S*)-2-ethylbutyl 2-(((*S*)-(4-nitrophenoxy)(phenoxy)phosphoryl)-amino)propanoate (**6**).

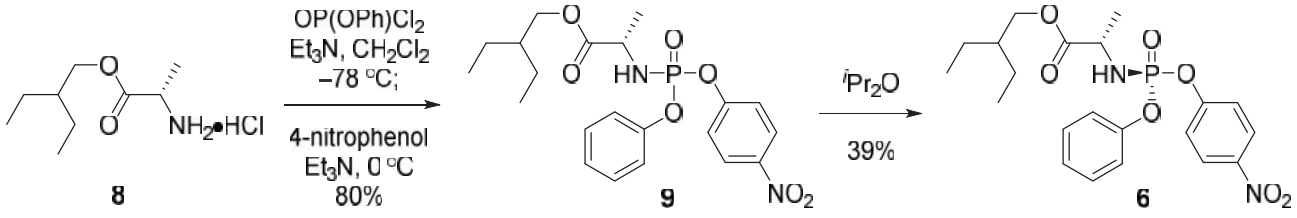

Scheme S3. Preparation of nucleoside triphosphate (**NTP**).

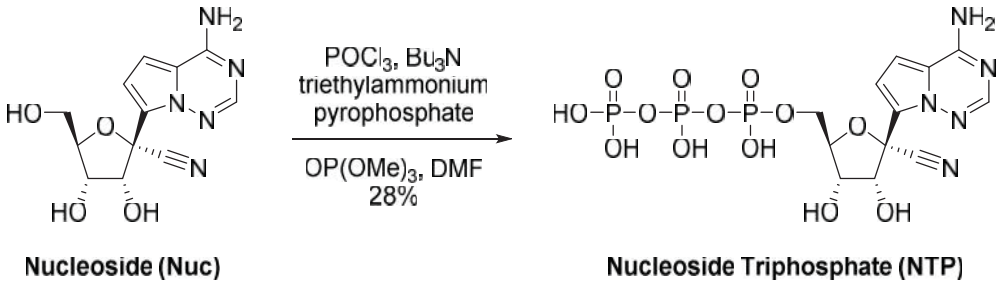

III. Experimental Procedures and Product Characterization

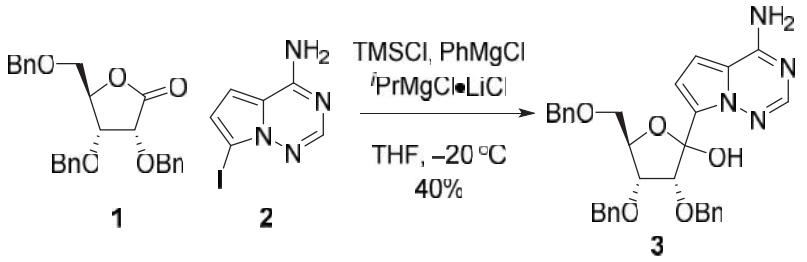

(3*R*,4*R*,5*R*)-2-(4-aminopyrrolo[2,1-*f*][1,2,4]triazin-7-yl)-3,4-bis(benzyloxy)-5-((benzyloxy)methyl)tetrahydrofuran-2-ol (3):

A solution of 7-iodopyrrolo[2,1-*f*][1,2,4]triazin-4-amine (**2**, 6.21 g, 23.9 mmol, 1 equiv) was suspended in tetrahydrofuran (150 mL) under an argon atmosphere. TMSCl (6.07 mL, 23.9 mmol, 2.00 equiv) was added and the resulting mixture was stirred for 10 min at room temperature. The solution was cooled to approximately 0 °C, and PhMgCl (2 M in tetrahydrofuran, 23.9 mL, 47.8 mmol, 2.00 equiv) was added slowly. The reaction mixture was stirred for approximately 20 min, and ^{i}PrMgCl (1 M in tetrahydrofuran, 25.1 mL, 25.1 mmol, 1.00 equiv) was then added while maintaining an internal reaction temperature below 5 °C. After 15 min, the reaction mixture was cooled to approximately –20 °C and a solution of 2,3,5-tri-*O*-benzyl-D-ribono-1,4-lactone (**1**, 10.0 g, 23.9 mmol, 1.00 equiv) in tetrahydrofuran (30 mL) was added slowly while maintaining an internal reaction temperature of approximately –20 °C. After 1 h, the reaction mixture was allowed to warm to 0 °C, and then quenched with methanol (20 mL) followed by acetic acid (20 mL) and water (20 mL). The resulting mixture was allowed to

warm to room temperature and was then concentrated under reduced pressure. The resulting concentrate was partitioned between ethyl acetate (250 mL) and aqueous hydrochloric acid solution (1 M, 250 mL). The organic layer was separated and then washed with 10% aqueous sodium bicarbonate solution (250 mL) and brine (250 mL), dried over anhydrous sodium sulfate, and concentrated under reduced pressure. The crude residue was subjected to silica gel chromatography eluting with 0- 10% methanol in ethyl acetate to afford the mixture of isomers **3** (13.2 g, 41.5%) as an off-white solid. ^{1}H-NMR (400 MHz, DMSO-d_6): δ 8.06 (br s, 2H), 7.99 (s, 1H), 7.37 – 7.22 (m, 11H), 7.19 – 7.10 (m, 3H), 7.03 – 6.97 (m, 2H), 6.95 (d, J = 4.8 Hz, 1H), 5.39 (d, J = 5.9 Hz, 1H), 5.05 (d, J = 5.2 Hz, 1H), 4.61 – 4.54 (m, 2H), 4.52 – 4.42 (m, 4H), 4.06 – 3.98 (m, 1H), 3.93 (dd, J = 5.9, 4.4 Hz, 1H), 3.69 (dd, J = 10.1, 3.4 Hz, 1H), 3.47 (dd, J = 10.0, 6.4 Hz, 1H); ^{13}C-NMR (100 MHz, DMSO-d_6): δ 187.98, 155.88, 148.96, 138.63, 138.43, 138.14, 128.67, 128.14, 128.12, 127.82, 127.54, 127.44, 127.26, 127.21, 127.09, 118.60, 117.51, 103.15, 102.30, 81.91, 80.92, 72.50, 72.33, 71.74, 71.44, 69.42; HRMS (m/z): $[M]^+$ calcd for $C_{32}H_{32}N_4O_5$, 552.2373; found, 552.2382; HPLC: t_R = 3.293 min.

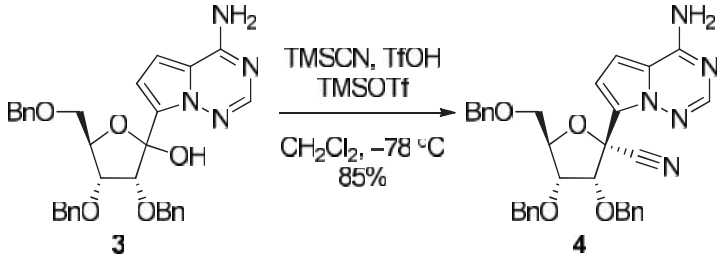

(2*R*,3*R*,4*R*,5*R*)-2-(4-aminopyrrolo[2,1-*f*][1,2,4]triazin-7-yl)-3,4-bis(benzyloxy)-5-((benzyloxy)methyl)tetrahydrofuran-2-carbonitrile (4):

To a solution of (3*R*,4*R*,5*R*)-2-(4-aminopyrrolo[2,1-*f*][1,2,4]triazin-7-yl)-3,4-bis(benzyloxy)-5-((benzyloxy)methyl)tetrahydrofuran-2-ol (**3**, 57.9 g, 105 mmol, 1 equiv) in dichloromethane (100 mL) pre-cooled to –78 °C was added trifluoromethanesulfonic acid (18.3 mL, 206 mmol, 2.00 equiv). After the reaction was stirred for 10 min, TMSOTf (38.9 mL, 216 mmol, 2.10 equiv) was slowly added and the resulting mixture was stirred for 30 min at –78 °C. TMSCN (56.5 mL, 451 mmol, 4.00 equiv) was then added slowly and the mixture was stirred for 2 h. Triethylamine (50 mL) was added and the reaction mixture was allowed to warm to room temperature. Solid

sodium bicarbonate (80 g) was then added followed by the slow addition of water (300 mL) and the resulting mixture was stirred for 10 min. The layers were then separated and the aqueous layer was extracted with dichloromethane. The combined organic extracts were washed with brine, dried over anhydrous sodium sulfate and concentrated under reduced pressure. The crude residue was subjected to silica gel chromatography eluting with 40- 100% ethyl acetate in hexanes to afford the product **4** (58.9 g, 85%) as an off-white solid. ^{1}H-NMR (400 MHz, DMSO-d_6): δ 7.99 – 7.82 (m, 3H), 7.37 – 7.23 (m, 15H), 6.88 (d, J = 4.5 Hz, 1H), 6.76 (d, J = 4.5 Hz, 1H), 4.91 (d, J = 5.0 Hz, 1H), 4.85 (d, J = 11.7 Hz, 1H), 4.77 (d, J = 11.7 Hz, 1H), 4.60 – 4.45 (m, 4H), 4.40 (q, J = 4.6 Hz, 1H), 4.12 (t, J = 5.4 Hz, 1H), 3.69 (dd, J = 11.1, 3.7 Hz, 1H), 3.59 (dd, J = 11.1, 4.7 Hz, 1H); ^{13}C-NMR (100 MHz, DMSO-d_6): δ 155.54, 147.86, 138.08, 137.94, 137.32, 128.17, 128.14, 128.11, 127.93, 127.72, 127.52, 127.40, 122.63, 116.78, 116.73, 110.48, 100.81, 81.90, 79.25, 77.61, 76.26, 72.30, 72.27, 71.45, 68.79; HRMS (m/z): $[M]^+$ calcd for $C_{33}H_{31}N_5O_4$, 561.2376; found, 561.2394; HPLC: t_R = 3.581 min.

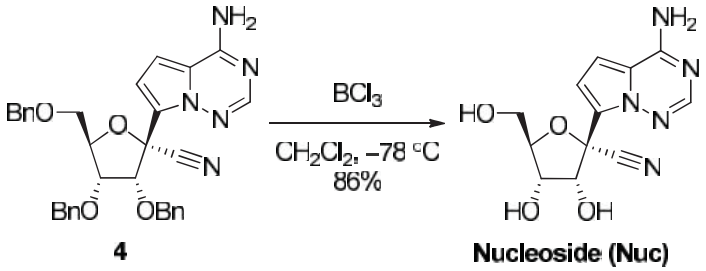

4 **Nucleoside (Nuc)**

(2*R*,3*R*,4*S*,5*R*)-2-(4-aminopyrrolo[2,1-*f*][1,2,4]triazin-7-yl)-3,4-dihydroxy-5-(hydroxymethyl)tetrahydrofuran-2-carbonitrile (Nuc):

Boron trichloride (1 M, 35.0 mL, 35.0 mmol, 3.80 equiv) was slowly added to a solution of (2*R*,3*R*,4*R*,5*R*)-2-(4-aminopyrrolo[2,1-*f*][1,2,4]triazin-7-yl)-3,4-bis(benzyloxy)-5-((benzyloxy)methyl)tetrahydrofuran-2-carbonitrile (**4**, 5.11 g, 9.10 mmol, 1 equiv) in anhydrous dichloromethane (50 mL) at –78 °C under an argon atmosphere. The reaction mixture was allowed to warm to –40 °C and was stirred for 2 h. The reaction mixture was cooled to –78 °C and methanol (10 mL) was added dropwise. A solution of triethylamine (13 mL) in methanol (20 mL) was added dropwise and the reaction mixture was allowed to warm to room temperature. The resulting mixture was concentrated under reduced pressure. The solid residue

was slurried with hexanes (50 mL) and the supernatant was then decanted (3×). The remaining solid residue was suspended into methanol (50 mL) and was heated to 45 °C. Water (50 mL) was added, and the resulting mixture was concentrated at 45 °C under reduced pressure to remove the volatiles to a final volume of approximately 35 mL water. The mixture was allowed to cool to room temperature and the fine white solids were collected by vacuum filtration and dried in an oven at 70 °C overnight to afford the product **Nuc** (2.27 g, 86%). ^{1}H-NMR (400 MHz, water-d_2): δ 8.10 (s, 1H), 7.37 (d, J = 5.1 Hz, 1H), 7.14 (d, J = 4.8 Hz, 1H), 4.94 (d, J = 5.4 Hz, 1H), 4.42 (app q, J = 4.2 Hz, 1H), 4.35 (t, J = 5.1 Hz, 1H), 3.86 (dd, J = 12.8, 3.2 Hz, 1H), 3.79 (dd, J = 12.8, 4.7 Hz, 1H); ^{13}C-NMR (100 MHz, DMSO-d_6): δ 155.62, 147.87, 123.87, 117.34, 116.52, 110.77, 100.79, 85.42, 78.56, 74.24, 70.07, 60.94; HRMS (m/z): $[M]^+$ calcd for $C_{12}H_{13}N_5O_4$, 291.0968; found, 291.0967; HPLC: t_R = 0.350 min.

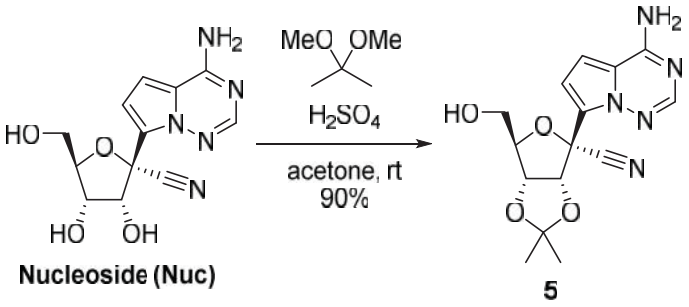

(3a*R*,4*R*,6*R*,6a*R*)-4-(4-aminopyrrolo[2,1-*f*][1,2,4]triazin-7-yl)-6-(hydroxymethyl)-2,2-dimethyltetrahydrofuro[3,4-*d*][1,3]dioxole-4-carbonitrile (5):

Sulfuric acid (18 M, 1.4 mL, 26 mmol, 1.3 equiv) was added dropwise to a suspension of **Nuc** (5.8 g, 20 mmol, 1 equiv) and 2,2-dimethoxypropane (12 mL, 95 mmol, 4.8 equiv) in acetone (145 mL) at room temperature. The reaction mixture was stirred for 30 min, and was warmed to 45 °C. After 30 min, the reaction was allowed to cool to room temperature, and solid sodium bicarbonate (5.8 g) and water (5.8 mL) were sequentially added. The mixture was stirred for 15 min and then concentrated under reduced pressure. The residue was dissolved into ethyl acetate (150 mL) and water (50 mL). The organic layer was separated and the water layer was extracted with ethyl acetate (2 × 50 mL). The combined organic extracts were dried over anhydrous sodium sulfate and then concentrated under reduced pressure to afford product **5** (6.54 g, 99%),

which was used directly in the next step without further purification. Analytically pure samples of **5** could be obtained through silica gel chromatography eluting with ethyl acetate. ^{1}H-NMR (400 MHz, DMSO-d_6): δ 8.03 – 7.84 (m, 3H), 6.90 (app q, J = 4.6 Hz, 2H), 5.37 (d, J = 6.6 Hz, 1H), 5.01 (t, J = 5.7 Hz, 1H), 4.89 (dd, J = 6.6, 3.1 Hz, 1H), 4.31 (td, J = 5.2, 3.0 Hz, 1H), 3.59 – 3.45 (m, 2H), 1.63 (s, 3H), 1.37 (s, 3H); ^{13}C-NMR (100 MHz, DMSO-d_6): δ 156.00, 148.58, 122.92, 117.37, 116.67, 115.83, 111.01, 101.28, 85.83, 84.33, 81.97, 80.37, 61.31, 26.30, 25.55; HRMS (m/z): $[M]^+$ calcd for $C_{15}H_{17}N_5O_4$, 331.1281; found, 331.1279; HPLC: t_R = 1.906 min.

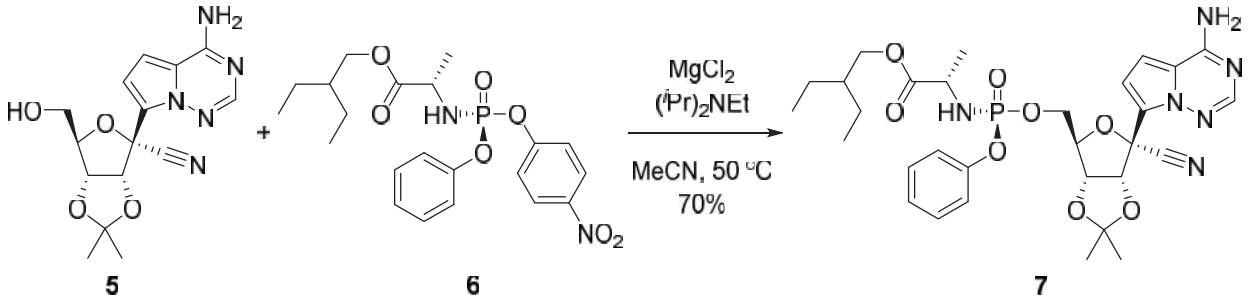

5 **6** **7**

(*S*)-2-ethylbutyl 2-(((*S*)-(((3a*R*,4*R*,6*R*,6a*R*)-6-(4-aminopyrrolo[2,1-*f*][1,2,4]triazin-7-yl)-6-cyano-2,2-dimethyltetrahydrofuro[3,4-*d*][1,3]dioxol-4-yl)methoxy)(phenoxy)phosphoryl)amino)propanoate (7):

Acetonitrile (16 mL) was added to a mixture of (2*S*)-2-ethylbutyl 2-(((4-nitrophenoxy)(phenoxy)phosphoryl)amino)propanoate (**6**, 1.79 g, 3.98 mmol, 1.20 equiv), (3a*R*,4*R*,6*R*,6a*R*)-4-(4-aminopyrrolo[2,1-*f*][1,2,4]triazin-7-yl)-6-(hydroxymethyl)-2,2-dimethyltetrahydrofuro[3,4-*d*][1,3]dioxole-4-carbonitrile (**5**, 1.10 g, 3.32 mmol, 1 equiv), and magnesium chloride (316 mg, 3.32 mmol, 1.00 equiv) at room temperature. The solution was heated to 50 °C for 10 min, and *N*,*N*-diisopropylethylamine (1.45 mL, 8.30 mmol, 2.50 equiv) was added. After 20 min, the reaction mixture was allowed to cool to room temperature, and then diluted with ethyl acetate (100 mL). The organic layer was washed with 5% aqueous citric acid solution (40 mL), saturated aqueous ammonium chloride solution (40 mL), 5% aqueous potassium carbonate solution (2 × 40 mL), and brine (40 mL). The organic layer was dried over anhydrous sodium sulfate and concentrated under reduced pressure. The crude residue was subjected to silica gel chromatography eluting with 0- 100% ethyl acetate in hexanes to afford the

product **7** (1.5 g, 70%). ^{1}H-NMR (400 MHz, methanol-d_4): δ 7.86 (s, 1H), 7.30 – 7.23 (m, 2H), 7.17 – 7.10 (m, 3H), 6.89 (q, J = 4.6 Hz, 2H), 5.34 (d, J = 6.6 Hz, 1H), 4.99 (dd, J = 6.6, 3.5 Hz, 1H), 4.60 – 4.53 (m, 1H), 4.36 – 4.24 (m, 2H), 4.02 (dd, J = 10.9, 5.8 Hz, 1H), 3.92 (dd, J = 10.9, 5.7 Hz, 1H), 3.84 (dq, J = 9.7, 7.1 Hz, 1H), 1.70 (s, 3H), 1.50 – 1.42 (m, 1H), 1.40 (s, 3H), 1.36 – 1.23 (m, 7H), 0.86 (t, J = 7.4 Hz, 6H); ^{13}C-NMR (100 MHz, methanol-d_4): δ 174.92, 174.87, 157.21, 152.08, 152.01, 148.46, 130.66, 130.65, 126.08, 126.07, 124.56, 121.35, 121.30, 118.31, 117.78, 117.01, 112.34, 102.43, 85.68, 84.90, 84.82, 83.07, 82.57, 68.09, 66.96, 51.46, 41.69, 26.52, 25.55, 24.22, 24.20, 20.46, 20.39, 11.34, 11.31; ^{31}P-NMR (162 MHz, methanol-d_4): δ 3.38 (s); HRMS (*m*/*z*): $[M]^+$ calcd for $C_{30}H_{39}N_6O_8P$, 642.2567; found, 642.2584; HPLC: t_R = 3.349 min.

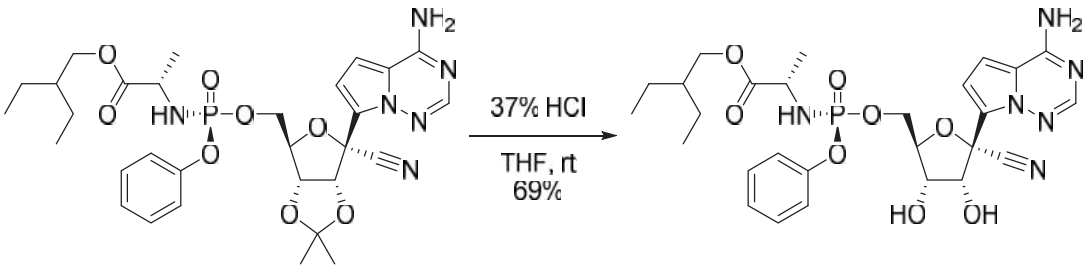

7 **GS-5734**

(*S*)-2-ethylbutyl 2-(((*S*)-(((2*R*,3*S*,4*R*,5*R*)-5-(4-aminopyrrolo[2,1-*f*][1,2,4]triazin-7-yl)-5-cyano-3,4-dihydroxytetrahydrofuran-2-yl)methoxy)(phenoxy)phosphoryl)amino)propanoate (GS-5734):

To a stirred solution of (*S*)-2-ethylbutyl 2-(((*S*)-(((3a*R*,4*R*,6*R*,6a*R*)-6-(4-aminopyrrolo[2,1-*f*][1,2,4]triazin-7-yl)-6-cyano-2,2-dimethyltetrahydrofuro[3,4-*d*][1,3]dioxol-4-yl)methoxy)(phenoxy)phosphoryl)amino)propanoate (**7**, 12.9 g, 20.0 mmol, 1 equiv) in tetrahydrofuran (100 mL) was added 37% aqueous hydrochloric acid solution (20 mL) slowly at 0 °C. The reaction mixture was allowed to warm to room temperature. After 5 h, the reaction mixture was diluted with water (100 mL) and adjusted to pH=8 by the addition of saturated aqueous sodium bicarbonate solution (200 mL). The resulting mixture was extracted with ethyl acetate (100 mL), and the organic extract was then washed with brine (50 mL), dried over anhydrous sodium sulfate and concentrated under reduced pressure. The crude residue was

subjected to silica gel chromatography eluting with 0- 100% ethyl acetate in hexanes to afford **GS-5734** (8.3 g, 69%). ^{1}H-NMR (400 MHz, methanol-d_4): δ 7.86 (s, 1H), 7.33 – 7.26 (m, 2H), 7.21 – 7.12 (m, 3H), 6.91 (d, J = 4.6 Hz, 1H), 6.87 (d, J = 4.6 Hz, 1H), 4.79 (d, J = 5.4 Hz, 1H), 4.43 – 4.34 (m, 2H), 4.28 (ddd, J = 10.3, 5.9, 4.2 Hz, 1H), 4.17 (t, J = 5.6 Hz, 1H), 4.02 (dd, J = 10.9, 5.8 Hz, 1H), 3.96 – 3.85 (m, 2H), 1.49 – 1.41 (m, 1H), 1.35 – 1.27 (m, 8H), 0.85 (t, J = 7.4 Hz, 6H). ^{13}C-NMR (100 MHz, methanol-d_4): δ 174.98, 174.92, 157.18, 152.14, 152.07, 148.27, 130.68, 126.04, 125.51, 121.33, 121.28, 117.90, 117.58, 112.29, 102.60, 84.31, 84.22, 81.26, 75.63, 71.63, 68.10, 67.17, 67.12, 51.46, 41.65, 24.19, 20.56, 20.50, 11.33, 11.28.; ^{31}P-NMR (162 MHz, methanol-d_4): δ 3.66 (s); HRMS (m/z): $[M]^+$ calcd for $C_{27}H_{35}N_6O_8P$, 602.2254; found, 602.2274; HPLC: t_R = 2.911 min.

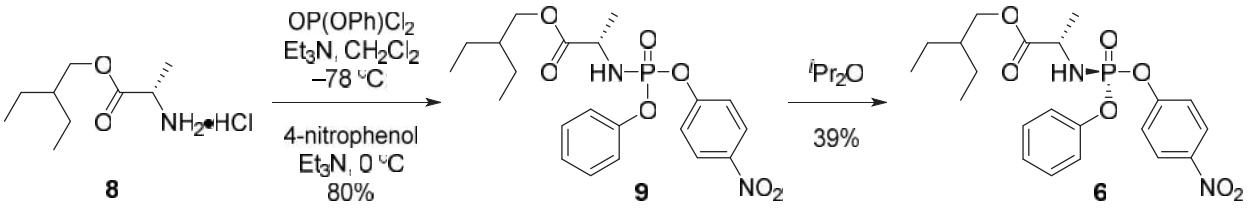

(*S*)-2-ethylbutyl 2-(((*S*)-(4-nitrophenoxy)(phenoxy)phosphoryl)amino)propanoate (6):

(*S*)-2-ethylbutyl 2-aminopropanoate hydrochloride (**8**, 26.0 g, 124 mmol, 1.10 equiv) was suspended in dichloromethane (200 mL) and the resulting mixture was cooled to –78 °C. Phenyl dichlorophosphate (18.5 mL, 124 mmol, 1.10 equiv) was then added followed by the slow addition of triethylamine (17.2 mL, 124 mmol, 1.10 equiv). The resulting mixture was allowed to warm to room temperature and stirred for 3 h. The mixture was then cooled to 0 °C and 4-nitrophenol (15.5 g, 112 mmol, 1 equiv) was added followed by the slow addition of triethylamine (17.2 mL, 124 mmol, 1.10 equiv). The resulting mixture was allowed to warm to room temperature and stirred for 3 h. The reaction mixture was then concentrated under reduced pressure and the crude residue was subjected to silica gel chromatography eluting with 0- 30% ethyl acetate in hexanes to afford **9** (33 g, 66%) as a colorless semi-solid. ^{1}H-NMR (400 MHz, chloroform-d_1): δ 8.22 (d, J = 9.0 Hz, 2H), 7.37 (dt, J = 13.7, 7.8 Hz, 4H), 7.28 – 7.16 (m, 3H), 4.21 – 4.10 (m, 1H), 4.10 – 3.99 (m, 2H), 3.95 – 3.85 (m, 1H), 1.55 – 1.45 (m, 1H), 1.45 – 1.14

(m, 7H), 0.87 (t, J = 7.4 Hz, 6H); ^{13}C-NMR (100 MHz, chloroform-d_1): δ 173.27, 173.24, 173.18, 173.16, 155.68, 155.63, 155.62, 155.57, 150.39, 150.33, 150.27, 129.97, 129.95, 129.95, 125.70, 125.67, 125.60, 120.94, 120.92, 120.89, 120.87, 120.23, 120.19, 120.18, 120.14, 67.89, 67.87, 50.63, 50.61, 40.33, 40.32, 23.26, 23.24, 21.17, 21.13, 21.08, 11.03, 11.01; ^{31}P-NMR (162 MHz, chloroform-d_1): δ –3.04 (s), –3.10 (s); HRMS (m/z): $[M]^+$ calcd for $C_{21}H_{27}N_2O_7P$, 450.1556; found, 450.1571; HPLC: t_R = 4.258 min.

(2*S*)-2-ethylbutyl 2-(((4-nitrophenoxy)(phenoxy)phosphoryl)amino)propanoate (**9**, 10.5 g, 23.3 mmol, 1 equiv) was suspended in diisopropyl ether (42 mL) and gently stirred. After 22 h, the white solids were collected by vacuum filtration and dried to afford product **6** (4.10 g, 39%) as a single diastereoisomer. ^{1}H-NMR (400 MHz, DMSO-d_6): δ 8.34 – 8.26 (m, 2H), 7.54 – 7.47 (m, 2H), 7.44 – 7.37 (m, 2H), 7.27 – 7.19 (m, 3H), 6.68 (dd, J = 13.6, 10.0 Hz, 1H), 4.07 – 3.94 (m, 1H), 3.92 (d, J = 5.7 Hz, 2H), 1.40 (app p, J = 6.2 Hz, 1H), 1.30 – 1.19 (m, 7H), 0.79 (t, J = 7.4 Hz, 6H); ^{13}C-NMR (100 MHz, DMSO-d_6): δ 172.78, 172.73, 155.58, 155.52, 150.18, 150.11, 144.06, 129.80, 125.74, 125.15, 121.06, 121.00, 120.19, 120.15, 66.19, 50.00, 39.65, 22.50, 22.48, 19.68, 19.61, 10.73, 10.71. ^{31}P-NMR (162 MHz, DMSO-d_6): δ –1.25 (s); HRMS (m/z): $[M]^+$ calcd for $C_{21}H_{27}N_2O_7P$, 450.1556; found, 450.1571; HPLC: t_R = 4.258 min.

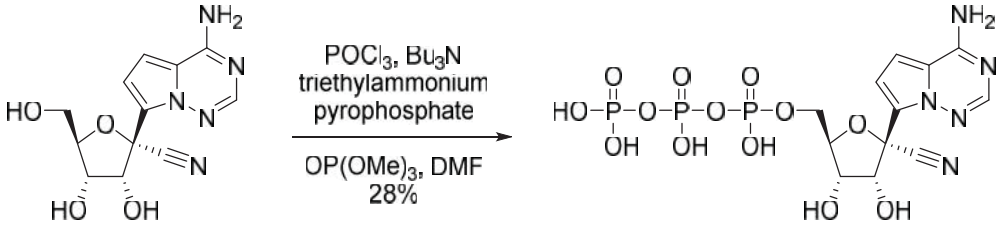

((2*R*,3*S*,4*R*,5*R*)-5-(4-aminopyrrolo[2,1-*f*][1,2,4]triazin-7-yl)-5-cyano-3,4-dihydroxytetrahydrofuran-2-yl)methyl tetrahydrogen triphosphate (NTP):

To a solution of **Nuc** (1.00 g, 3.43 mmol, 1 equiv) in $OP(OMe)_3$ (15 mL) at 0 °C was added $POCl_3$ (827 mg, 5.39 mmol, 1.57 equiv). The reaction mixture was stirred at 0 °C for 4 h, and solution of pyrophosphate tributylamine salts (3.00 g, 5.47 mmol, 1.59 equiv) in acetonitrile (10 mL) was added followed by the addition of tributylamine (3.11 g, 16.8 mmol, 4.89 equiv). The

reaction mixture was stirred at 0 °C for 30 min, and then quenched by the addition of triethylammonium bicarbonate buffer (1 M, 40 mL). The resulting mixture was stirred at room temperature for 30 min, and then triethylamine (4 mL) was added. The mixture was stirred an additional 30 min, and concentrated under reduced pressure and co-evaporated with water (2×). The residue was dissolved in water (40 mL) and the solution was subjected to ion-exchange column chromatography (Column: Thermo Scientific, DNAP PA-100, 4 × 250 mm; eluting with water, then 5-35% 1 M triethylammonium bicarbonate buffer in water). The product fractions were combined, concentrated under reduced pressure and co-evaporated with water. The residue was dissolved in water (40 mL) and was resubjected to ion-exchange column chromatography (Column: Thermo Scientific, DNAP PA-100, 4 × 250 mm; eluting with water, then 5-35% 1 M triethylammonium bicarbonate buffer in water). The product fractions were combined and concentrated under reduced pressure to afford the product **NTP** triethylamonium salt (770 mg, 24%, 1.8 equiv triethylamonium) as an off-white solid. ^{1}H-NMR (400 MHz, water-d_2, signals for triethylammonium denoted by *): δ 7.93 (br s, 1H), 7.11 – 7.03 (m, 1H), 6.95 – 6.84 (m, 1H), 5.07 – 4.98 (m, 1H), 4.65 – 4.57 (m, 1H), 4.57 – 4.50 (m, 1H), 4.31 – 4.15 (m, 1H), 4.13 – 4.00 (m, 1H), 3.16 – 3.00 (m, 6H*), 1.30 – 1.13 (m, 9H*); ^{13}C-NMR (100 MHz, water-d_2, signals for triethylammonium denoted by *): δ 155.49, 147.21, 122.98, 117.11, 116.45, 111.08, 102.22, 85.32, 76.16, 74.75, 70.14, 64.64, 46.36*, 8.32*; ^{31}P-NMR (162 MHz, D_2O): δ –5.56 (d, J = 19.4 Hz), –10.96 (d, J = 19.2 Hz), –21.45 (t, J = 19.4 Hz); HRMS (m/z): $[M]^+$ calcd for $C_{12}H_{16}N_5O_{13}P_3$, 530.9957; found, 530.9957; ion-exchange HPLC: t_R = 5.422 min.

IV. NMR Spectra

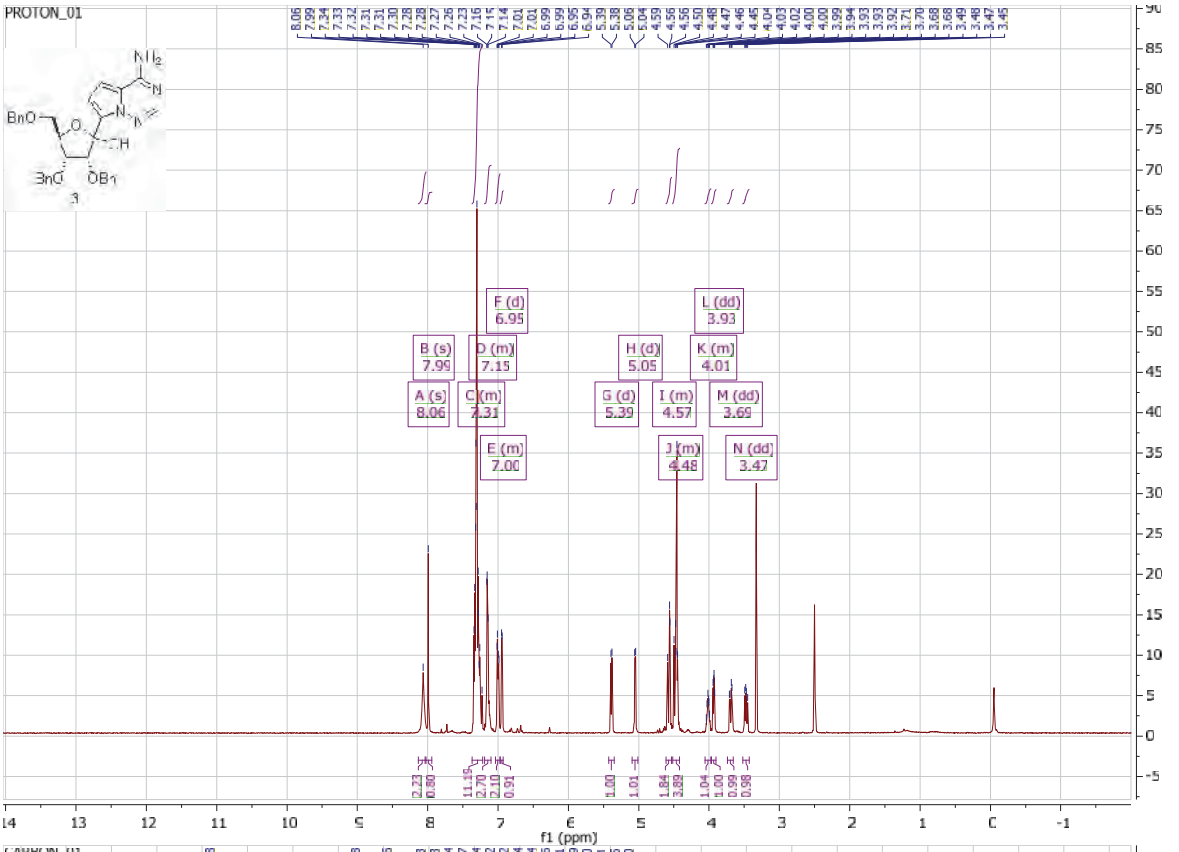
PROTON_01
F (d) 6.95
L (dd) 3.93
B (s) 7.99
D (m) 7.15
H (d) 5.05
K (m) 4.01
A (s) 8.06
C (m) 7.31
G (d) 5.39
I (m) 4.57
M (dd) 3.69
E (m) 7.00
J (m) 4.48
N (dd) 3.47
f1 (ppm)

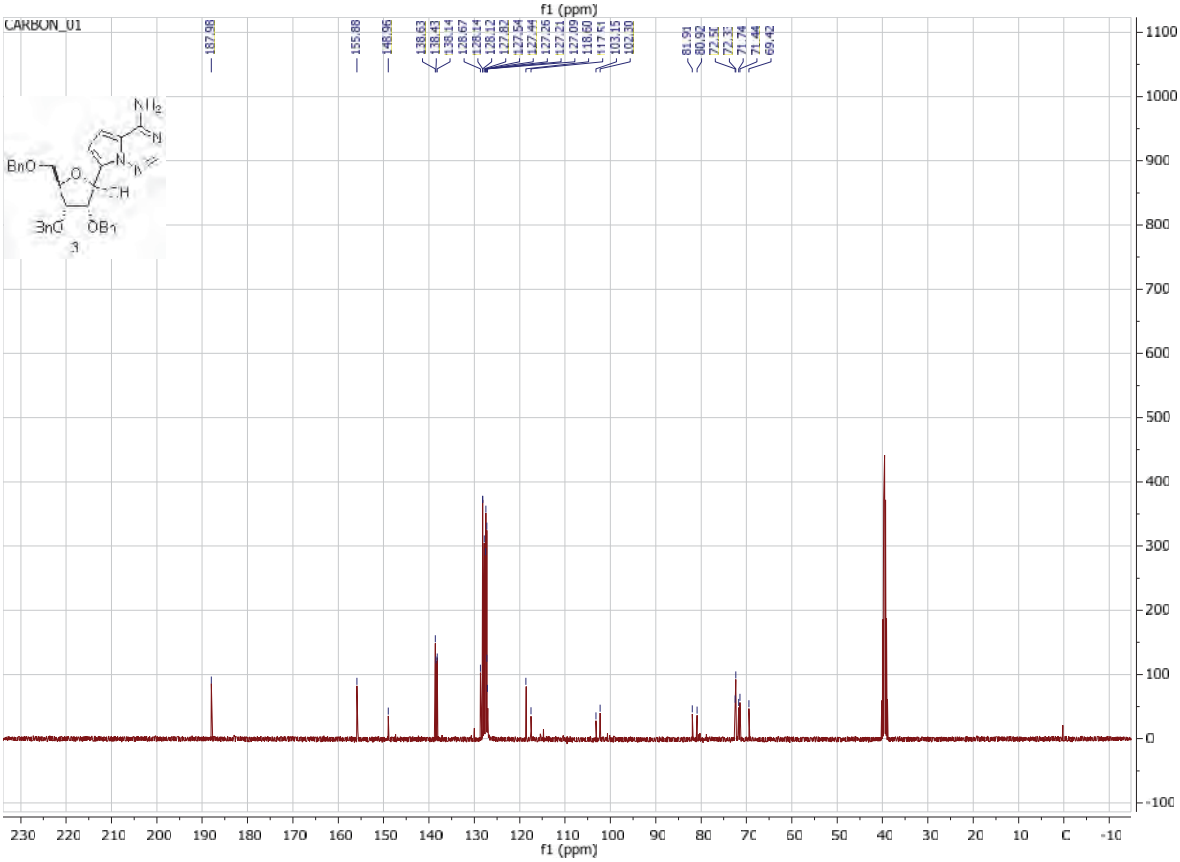
CARBON_01
f1 (ppm)

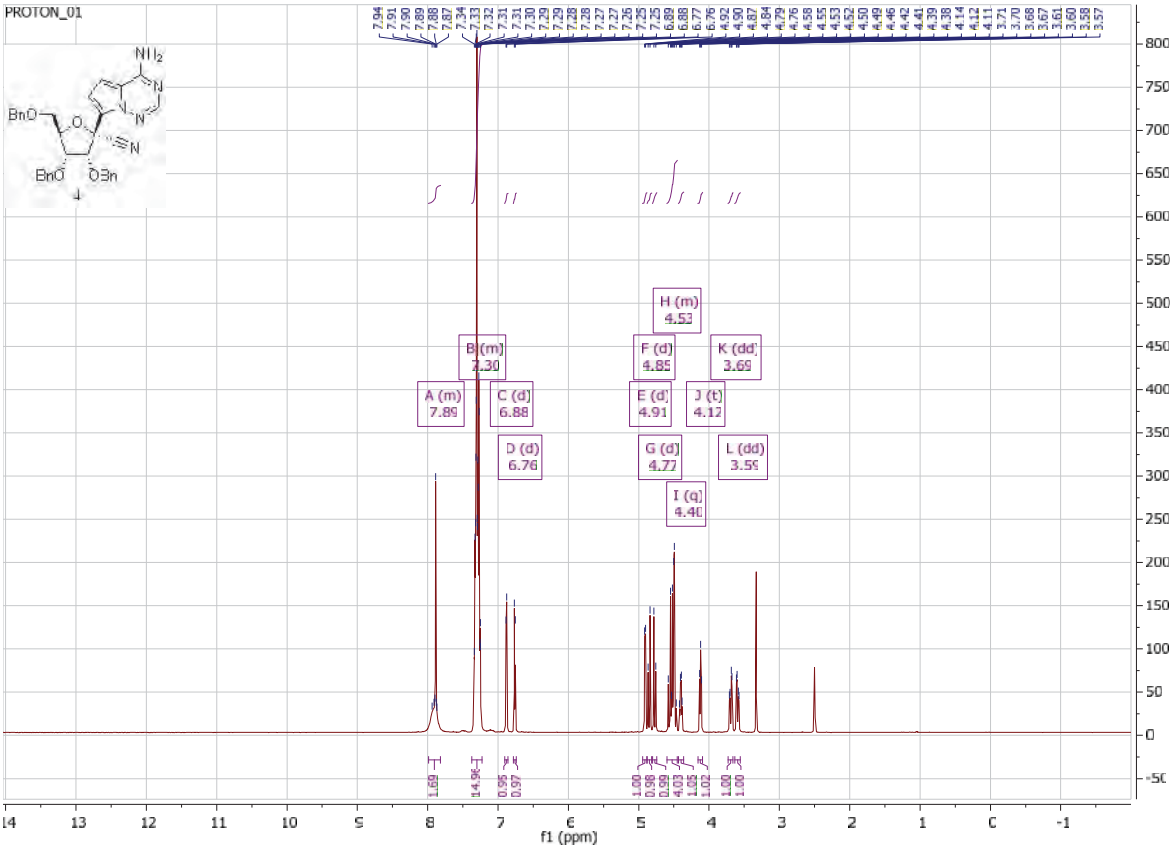
PROTON_01
A (m) 7.89
B (m) 7.30
C (d) 6.88
D (d) 6.76
E (d) 4.91
F (d) 4.85
G (d) 4.77
H (m) 4.53
I (q) 4.48
J (t) 4.12
K (dd) 3.69
L (dd) 3.59
f1 (ppm)

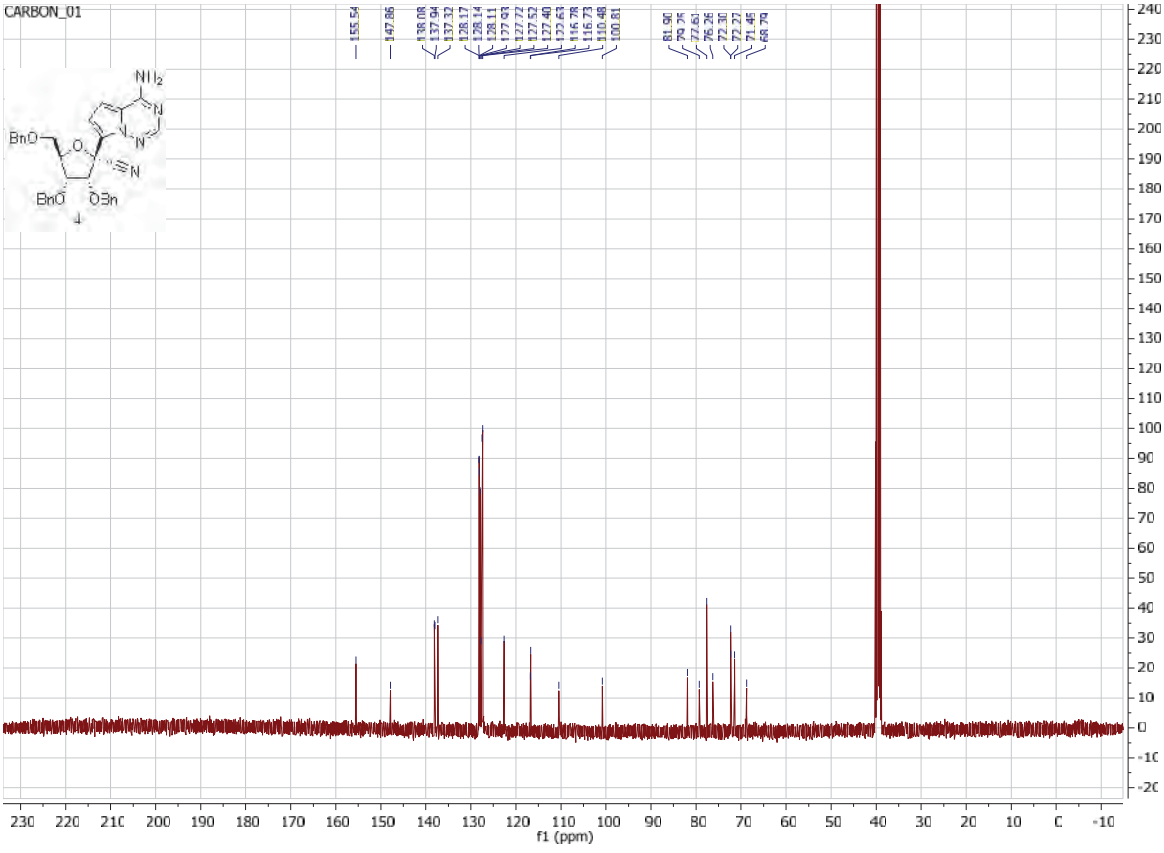
CARBON_01
f1 (ppm)

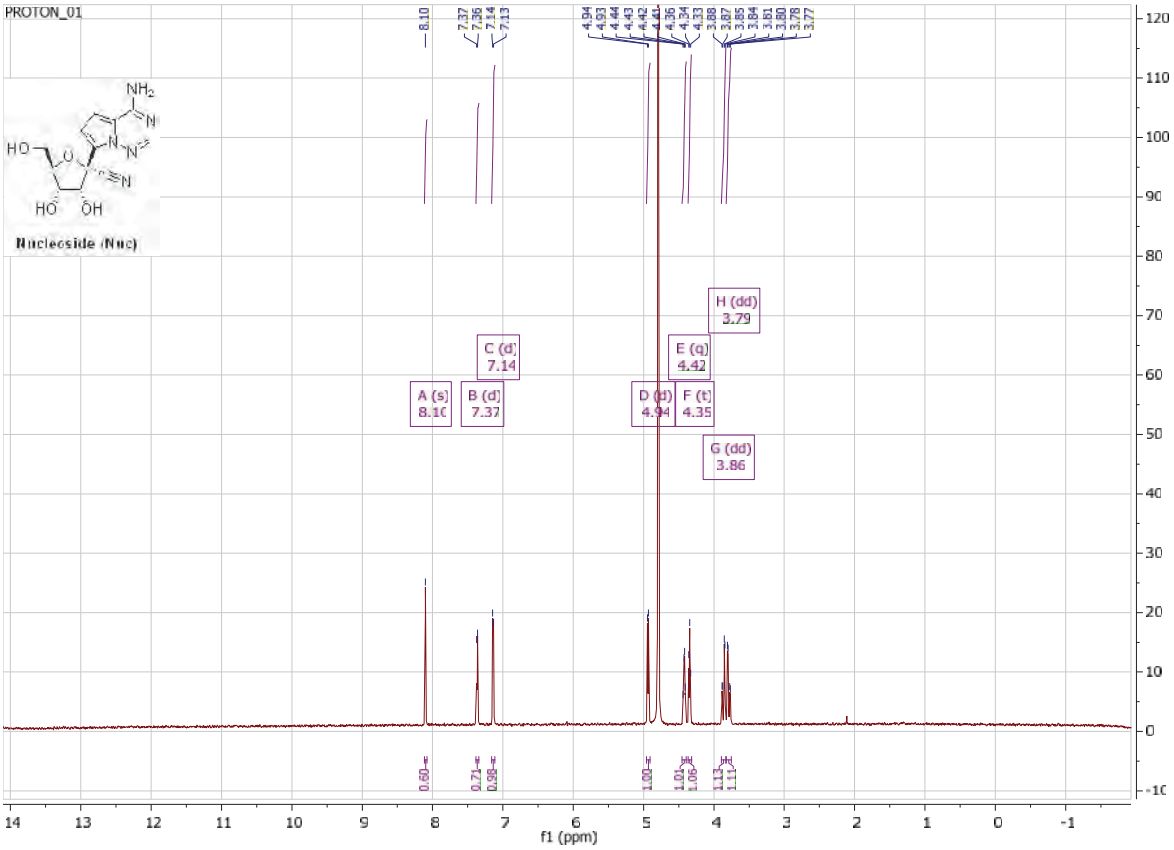
PROTON_01
Nucleoside (Nuc)
A (s) 8.10
B (d) 7.37
C (d) 7.14
D (d) 4.94
E (q) 4.42
F (t) 4.35
G (dd) 3.86
H (dd) 3.79
f1 (ppm)

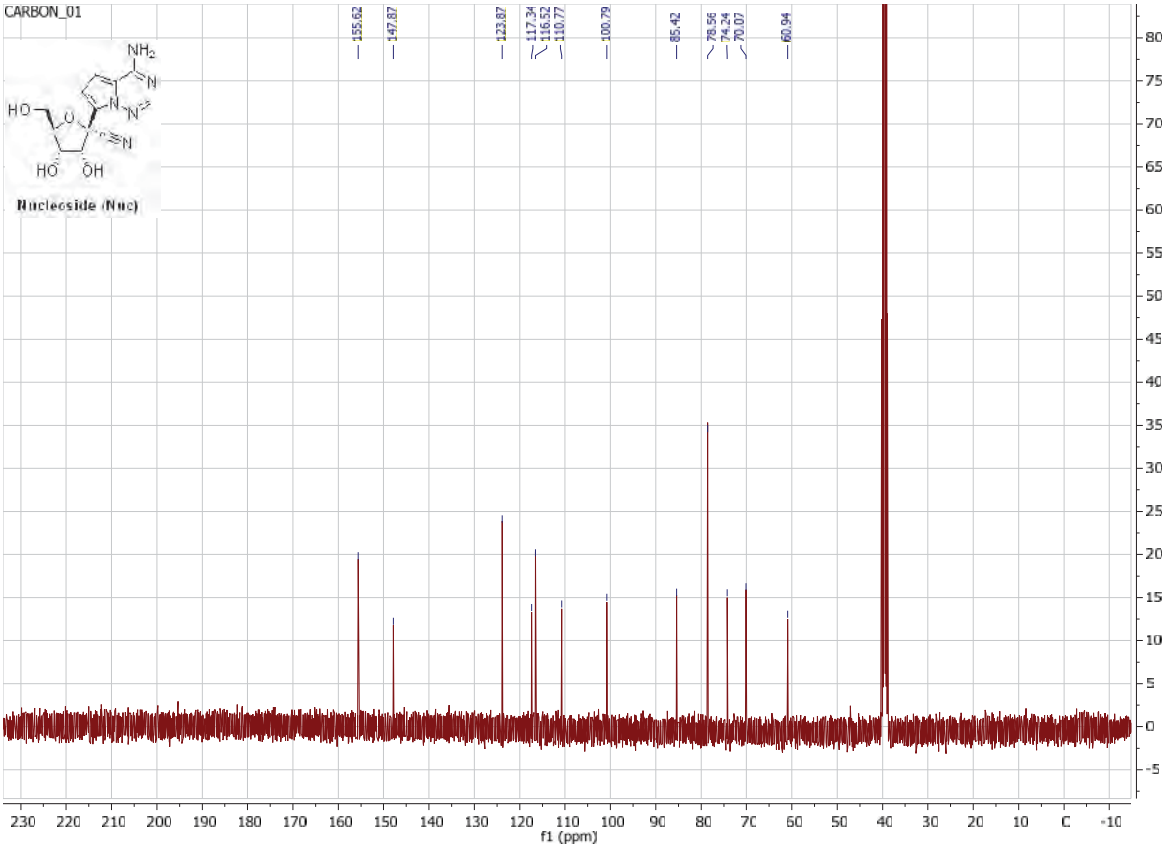
CARBON_01
Nucleoside (Nuc)
155.62
147.87
123.87
117.34
116.52
110.77
100.79
85.42
78.56
74.24
70.07
60.94
f1 (ppm)

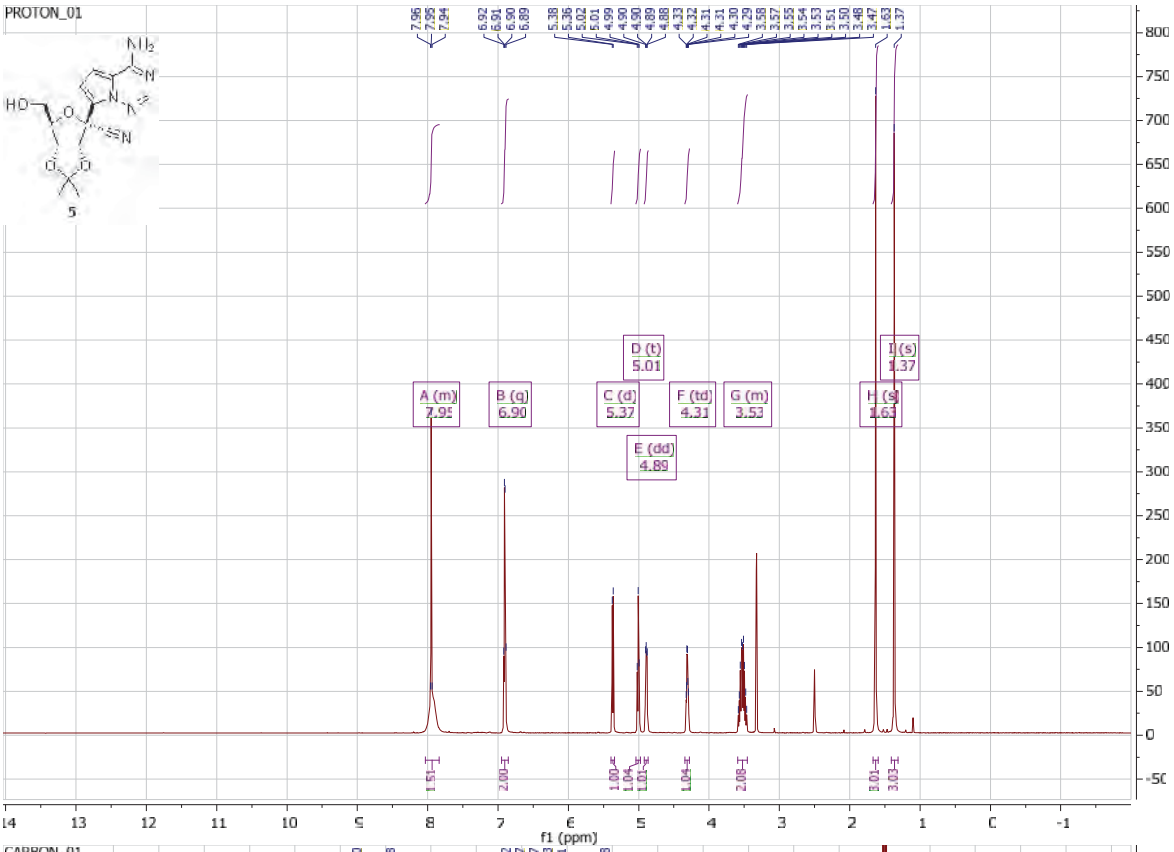
PROTON_01
A (m) 7.95
B (q) 6.90
C (d) 5.37
D (t) 5.01
E (dd) 4.89
F (td) 4.31
G (m) 3.53
H (s) 1.63
I (s) 1.37
f1 (ppm)

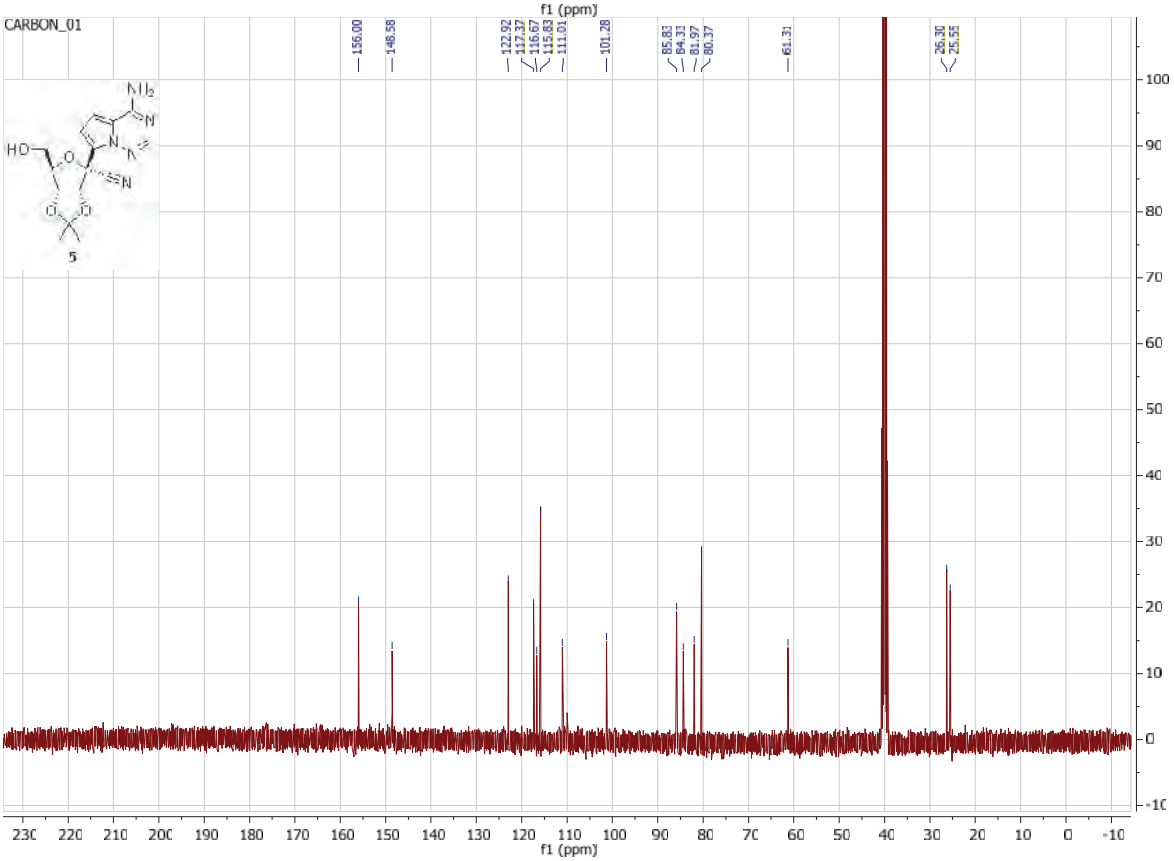
CARBON_01
156.00
148.58
122.92
117.37
116.67
115.83
111.01
101.28
85.81
84.33
81.97
80.37
61.31
26.30
25.55
f1 (ppm)

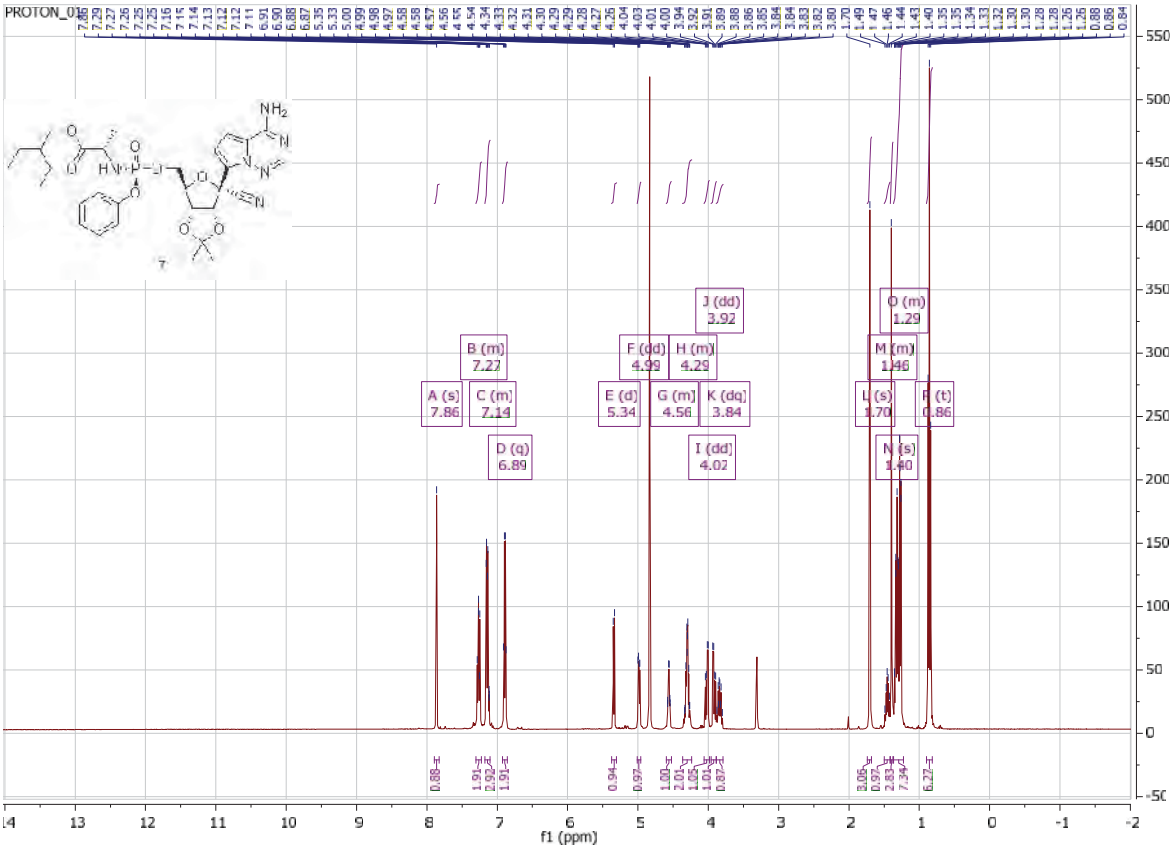
PROTON_01
A (s) 7.86
B (m) 7.27
C (m) 7.14
D (q) 6.89
E (d) 5.34
F (dd) 4.99
G (m) 4.56
H (m) 4.29
I (dd) 4.02
J (dd) 3.92
K (dq) 3.84
L (s) 1.70
M (m) 1.46
N (s) 1.40
O (m) 1.29
P (t) 0.86
f1 (ppm)

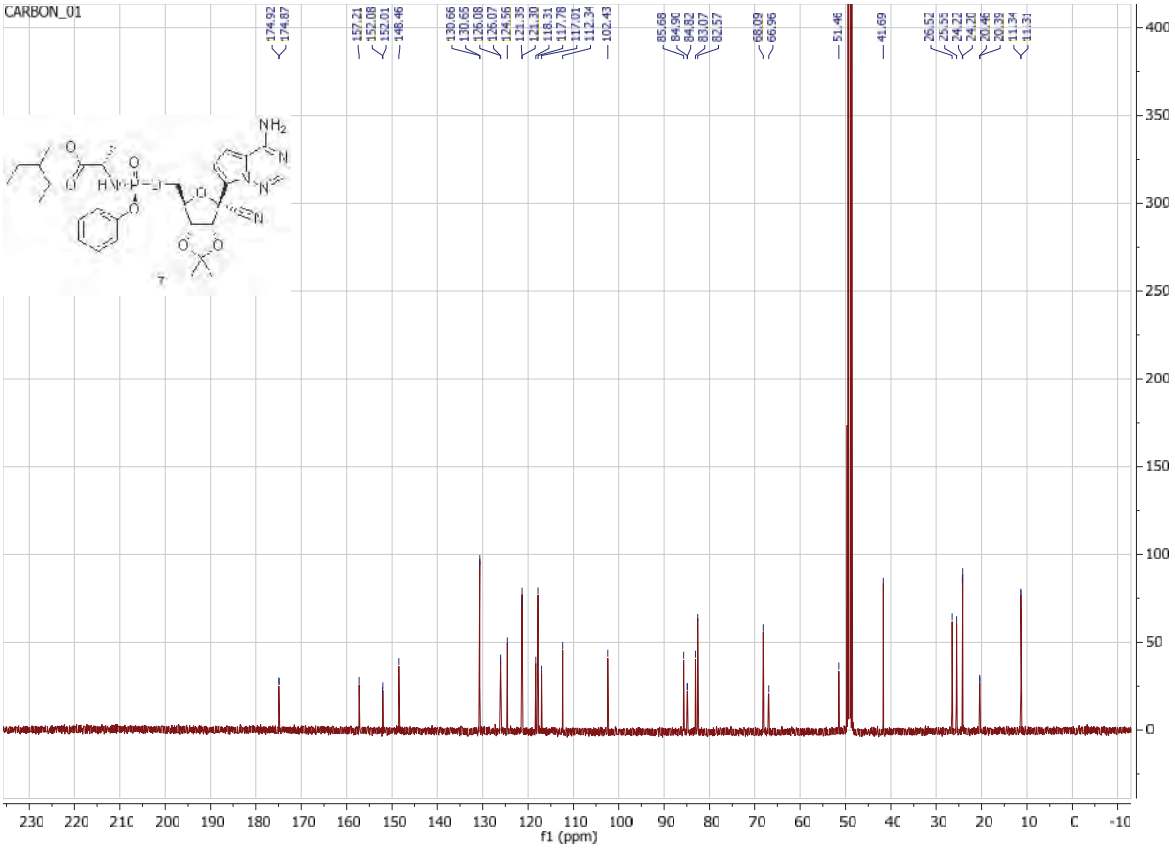
CARBON_01
f1 (ppm)

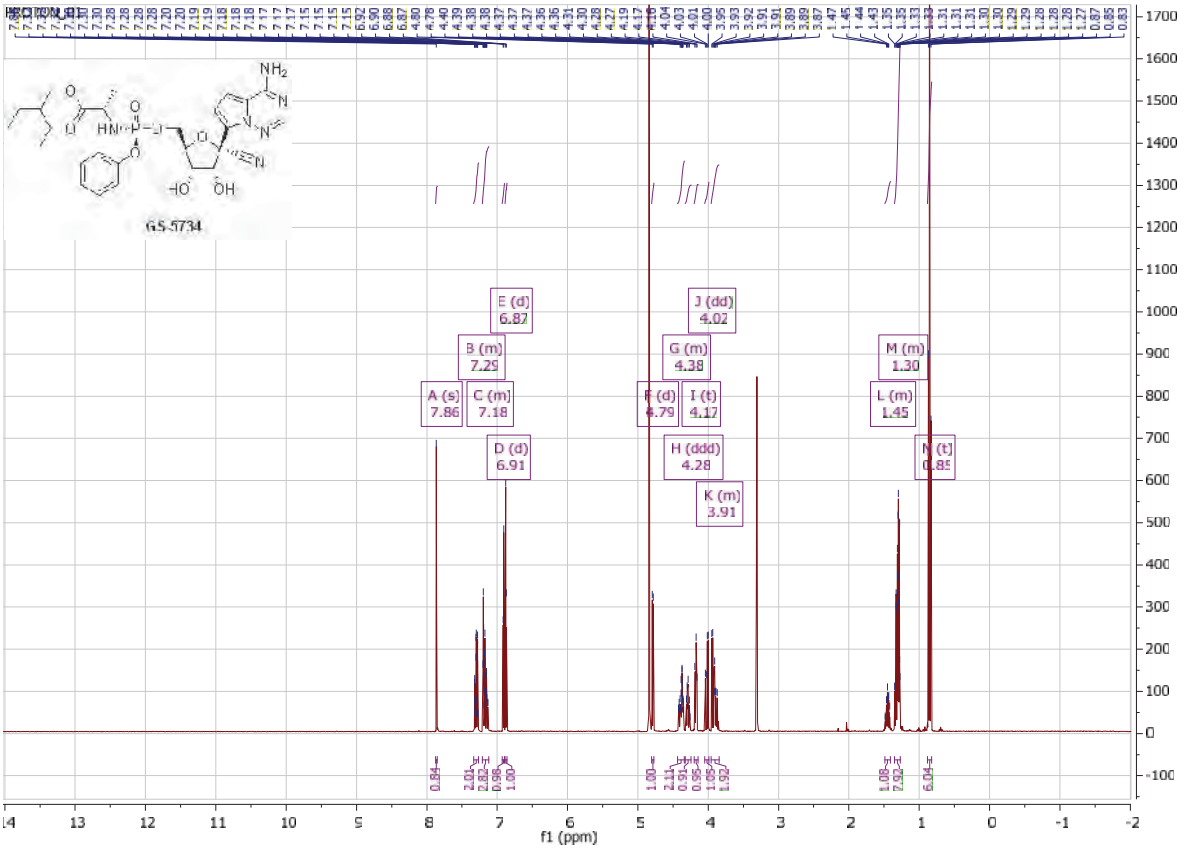
GS-5734
E (d) 6.87
J (dd) 4.02
B (m) 7.29
G (m) 4.38
M (m) 1.30
A (s) 7.86
C (m) 7.18
F (d) 4.79
I (t) 4.17
L (m) 1.45
D (d) 6.91
H (ddd) 4.28
K (m) 3.91
f1 (ppm)

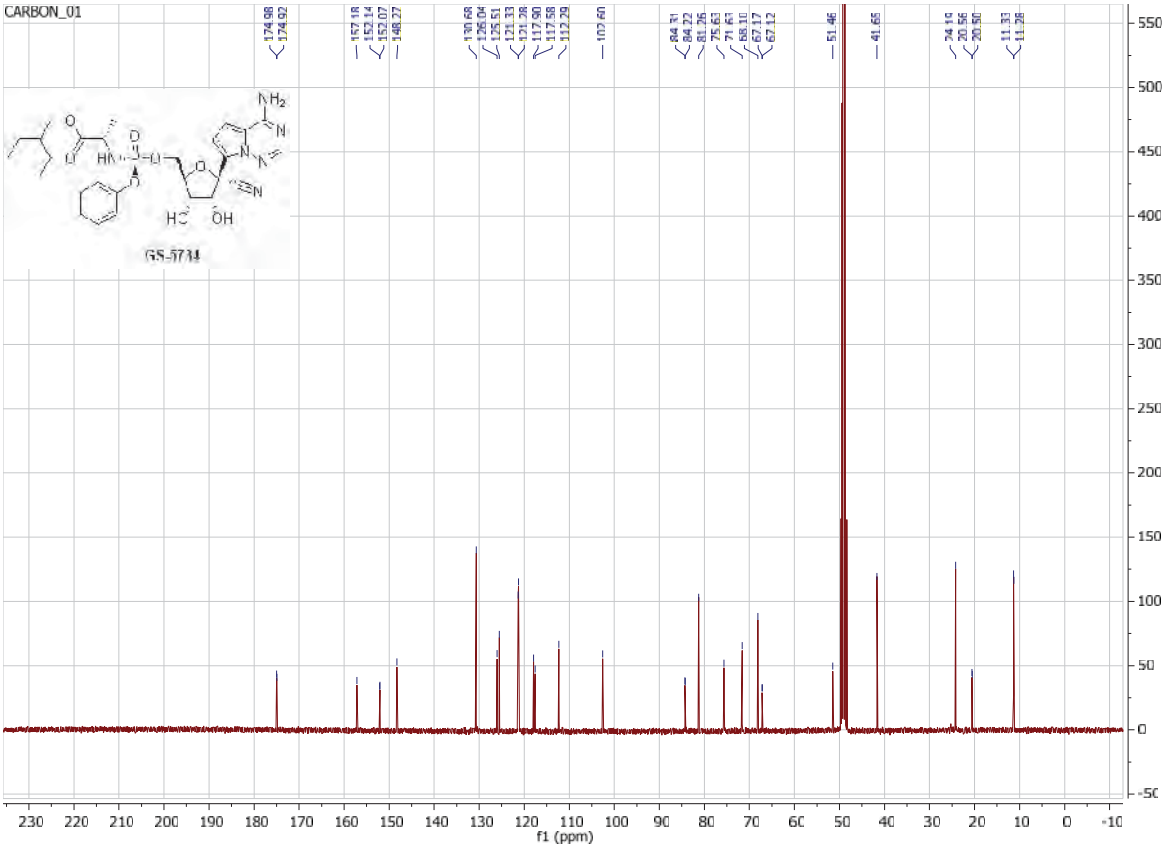
CARBON_01
GS-5734
f1 (ppm)

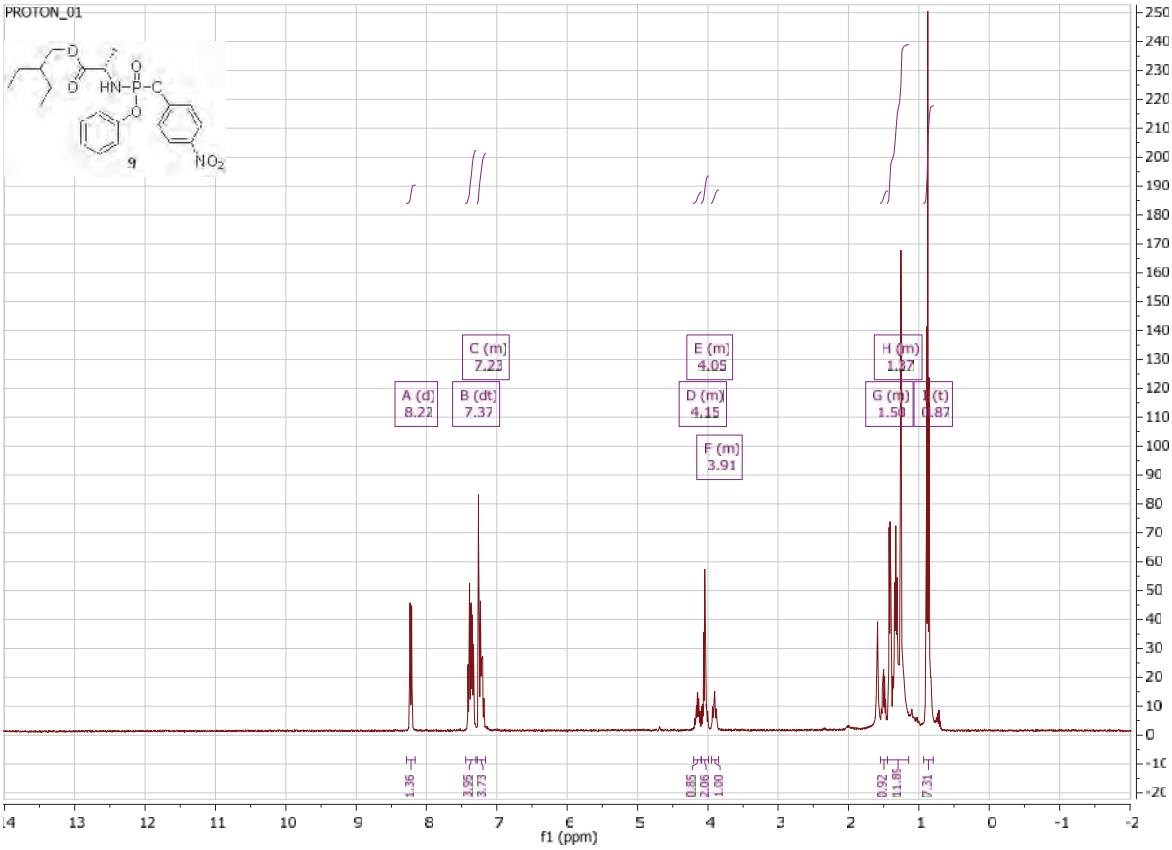
PROTON_01
A (d) 8.22
B (dt) 7.37
C (m) 7.23
D (m) 4.15
E (m) 4.05
F (m) 3.91
G (m) 1.58
H (m) 1.27
I (t) 0.87
f1 (ppm)

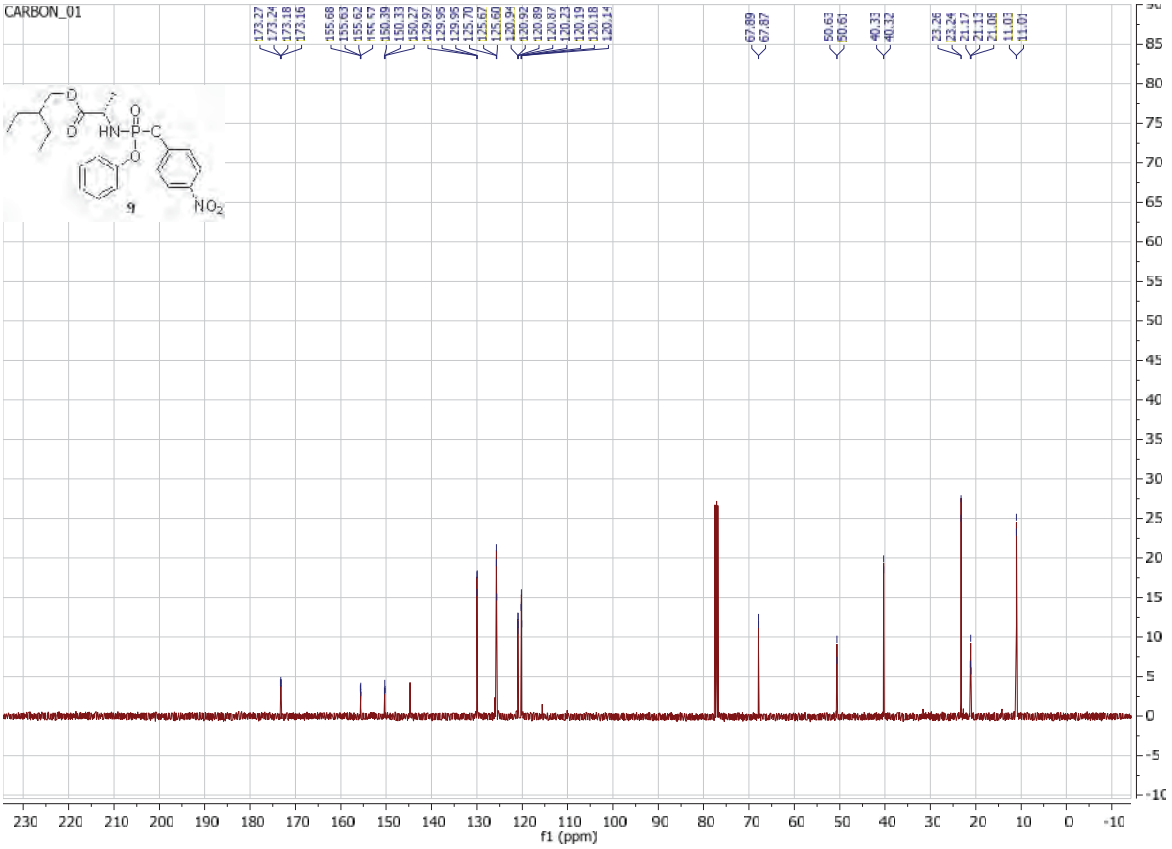
CARBON_01
f1 (ppm)

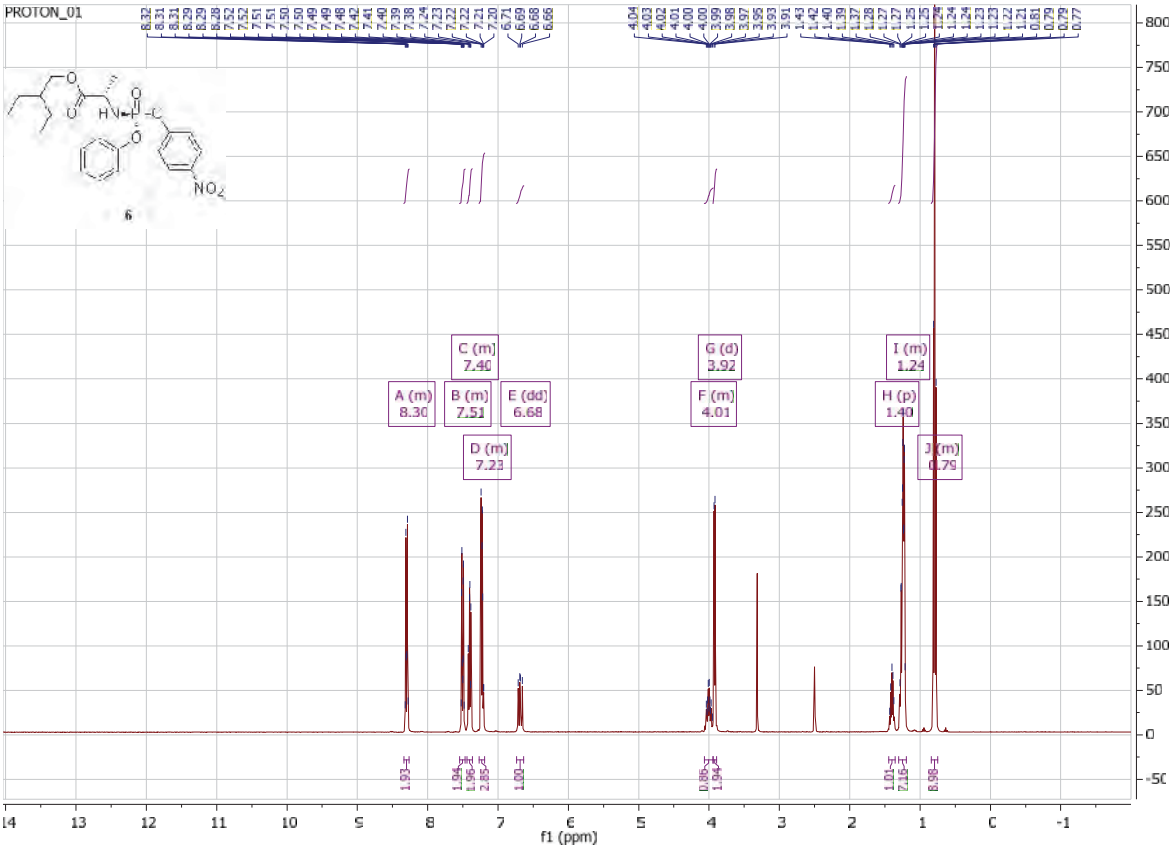
PROTON_01
A (m) 8.30
B (m) 7.51
C (m) 7.40
D (m) 7.23
E (dd) 6.68
F (m) 4.01
G (d) 3.92
H (p) 1.40
I (m) 1.24
J (m) 0.79
f1 (ppm)

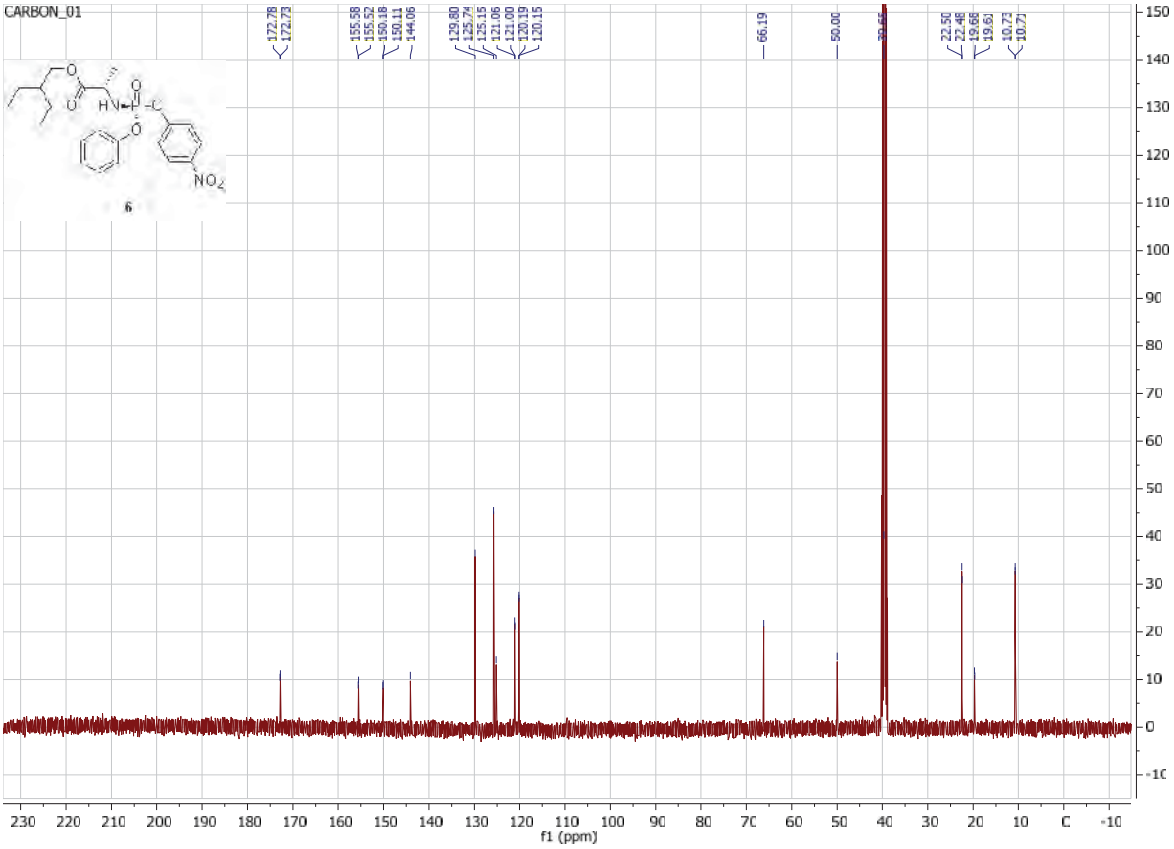
CARBON_01
f1 (ppm)

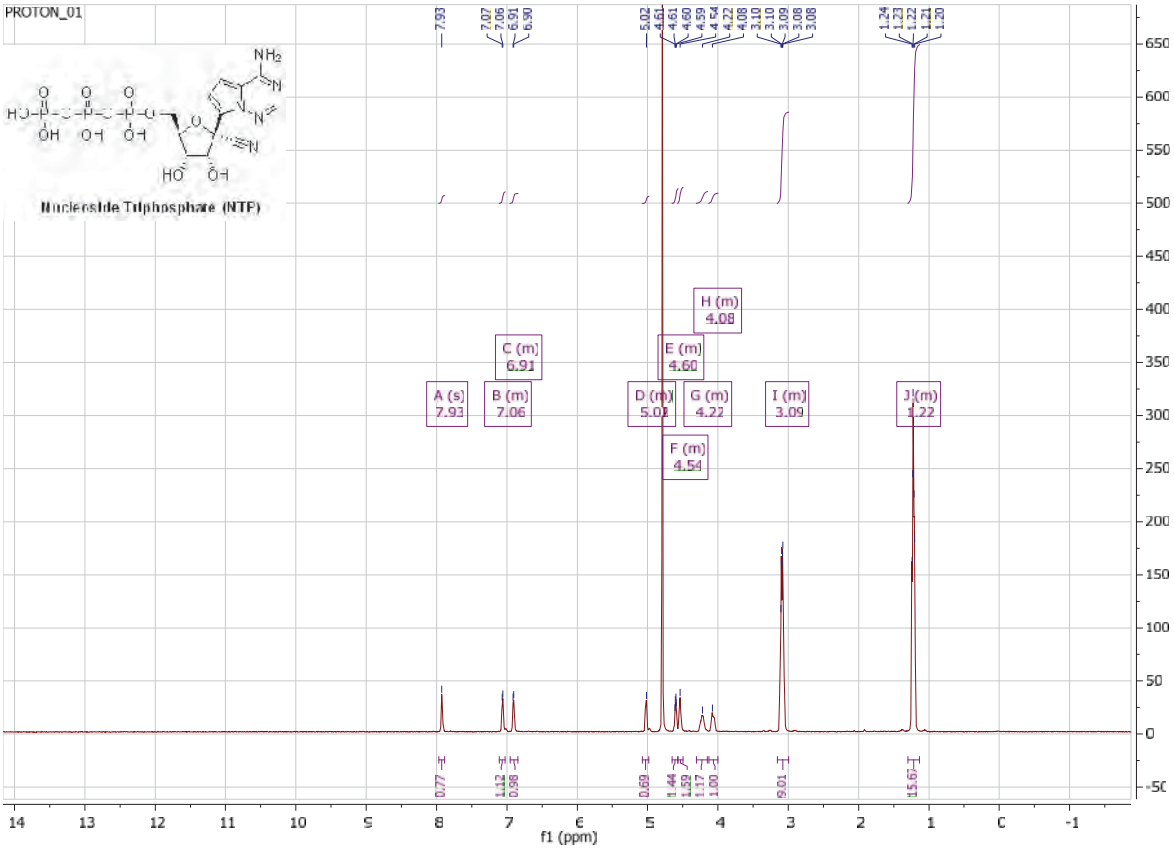
PROTON_01
Nucleoside Triphosphate (NTP)
A (s) 7.93
B (m) 7.06
C (m) 6.91
D (m) 5.02
E (m) 4.60
F (m) 4.54
G (m) 4.22
H (m) 4.08
I (m) 3.09
J (m) 1.22
f1 (ppm)

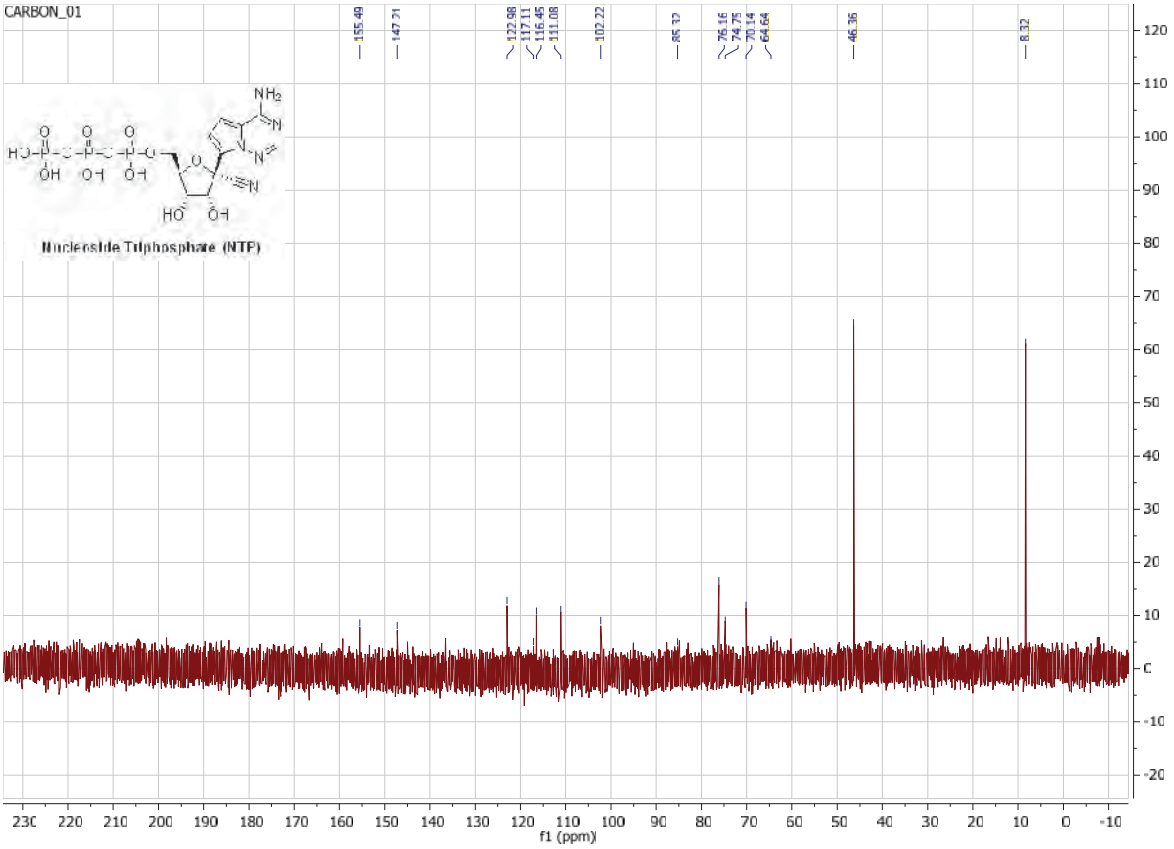
CARBON_01
Nucleoside Triphosphate (NTP)
f1 (ppm)

V. References

35. Clarke, M. O. *et al.* Pyrrolo[1,2-*f*][1,2,4]triazines useful for treating respiratory syncytial virus infections. *US Patent 2014064412*. Filed 06 Nov 2014.

36. Meppen, M. *et al.* Cyclic phosphoramidates as prodrugs of 2′-*C*-methylcytidine. *Eur. J. Med. Chem.* **44**, 3765-3770 (2009).

37. Mackman, R. L., Parrish, J. P., Ray, A. S. & Theodore, D. A. Methods and compounds for treating respiratory syncytial virus infections. *US Patent 2011045102*. Filed 22 Jul 2011.

38. Metobo, S. E. *et al.* Practical synthesis of 1′-substituted Tubercidin C-nucleoside analogues. *Tetrahedron Lett.* **53**, 484-486 (2012).